NOVEL BINDING PARTNERS OF Mu-OPIOID RECEPTOR AND THEIR REGULATORY ROLES

A DISSERTATION

SUBMITTED TO THE FACULTY OF THE GRADUATE SCHOOL

OF THE UNIVERSITY OF MINNESOTA

BY

XIN GE

IN PARTIAL FULFILLMENT OF THE REQUIREMENTS

FOR THE DEGREE OF

DOCTOR OF PHILOSOPHY

PING-YEE LAW

FACULTY ADVISOR

December 2009

ACKNOWLEDGMENTS

I would like to acknowledge the guidance of my adviser, Dr. Ping-Yee Law. He believed in me and allowed me to learn in my own way, even when we disagreed. I would like to thank the members of my committee: Drs. Tim Walseth, Ramakrishnan, Douglas Yee for their helpful comments and thought-provoking questions.

I would like to thank my family for their emotional and financial support. They made the graduate school experience more productive and enjoyable.

I also would like to acknowledge the people in the laboratory of Dr. Ping-Yee Law Without them, I would have to spend more time to grope the methods.

Finally, I would like to sincerely thank Dr. Horace Loh for his leadership, both in the laboratory and department.

Part I: Abstract

G-protein-coupled receptors (GPCRs) represent a super-family of proteins in the human genome (>900), which include at least one third of current drug targets. Associated proteins of GPCRs consist of the down-stream signaling pathway, which convert the external stimulus to the final signal of cellular function change. Some useful methods have been used to explore the sophisticated network of GPCR-associated proteins, such as yeast-two hybridization and GST fusion protein pull-down assay. However, in both methods, only one or two domains of the receptor were used to construct a fusion protein for identifying scaffolding proteins. This cannot reflect the conditions in which an agonist/antagonist mediates the opioid receptors' conformational change that leads to protein recruitment. To identify the binding partners of MOR, a member of GPCR rhodopsin subfamily that clarified to be important in regulating drug tolerance and addiction, we purified MOR complexes from $(His)_6$-tagged MOR stably expressing neuroblastma neuro2A (N2A) cells. Combine with Mass Spectrometry and LC MS/MS (Liquid chromatography-electrospray ionization tandem mass spectrometry), some novel MOR binding partners were found. Two of them are studied further about their important roles in regulating MOR functions.

Ribophorin I (RPNI), a component of the oligosaccharidetransferase complex, could directly interact with MOR. RPNI can be shown to participate in MOR export by the intracellular retention of the receptor after siRNA knocking-down of endogenous RPNI. Over-expression of RPNI rescued the surface expression of the MOR ^{344}KFCTR^{348} deletion mutant (C2) independent of

calnexin. Furthermore, RPNI regulation of MOR trafficking is dependent on the glycosylation state of the receptor, as reflected in the inability of over-expression of RPNI to affect the trafficking of the N-glycosylation deficient mutants, or GPCR such as k-opioid receptor that has minimal glycosylation sites. Hence, this novel RPNI chaperone activity is a consequence of N-glycosylation-dependent direct interaction with MOR.

G protein-regulated inducer of neurite outgrowth 1 (GRIN1) can influence MOR lipid raft location by tethering the receptor with the heterotrimeric G protein α-subunit. GST fusion pull-down and receptor mutational analyses indicated the ^{267}GSKEK^{271} sequence within the MOR 3rd intracellular loop was involved in interacting with the GRIN1 sequence distinct from that participated in the Gα binding. The uncoupling of Gα from MOR with PTX reduced the amount of GRIN1 co-immunoprecipitated with MOR while the amount of GRIN1 coimmunoprecipitated with Gα was unchanged. Furthermore, over-expression of GRIN1 significantly enhanced the amount of MOR in lipid raft and the receptor signaling magnitude as measured by Src kinase activation. Such increase in MOR signaling was demonstrated further by determining the GRIN1-dependent neurite outgrowth. In contrast to minimal neurite outgrowth induced by etorphine in control cells, over-expression of GRIN1 and the increase in GRIN1-MOR interaction resulted in the increase in etorphine- and not-morphine-induced neurite outgrowth in the neuroblastoma N2A cell that was PTX sensitive. Knocking-down of endogenous GRIN1 by siRNA attenuated the agonist-induced neurite outgrowth. Disrupting lipid raft by MβCD also blocked neurite outgrowth.

Hence, by serving as a tether between Gα and MOR, GRIN1 stabilizes the receptor within the lipid rafts and potentiates the receptor signaling in the neurite outgrowth process.

Table of Contents

Figures list

Part II: Introduction

The formation of a signaling complex, or receptosome, has been shown to affect G protein-coupled receptors (GPCRs) signal transduction processes (1-3). The proteins that are associated with GPCRs may play at least four distinct roles in the receptor signaling. First, a GPCR-associated protein may directly regulate receptor signaling (e.g., Gi/o, RGS) (4-6). Second, a GPCR-associated protein may control receptor signaling by mediating receptor localization and/or trafficking (e.g., ARF, GASP) (7,8). Third, a GPCR-associated protein may modulate receptor function by regulating the receptor's conformation and pharmacological role (e.g. as chaperone) (9). Finally, a GPCR-associated protein may act as a scaffold, physically linking the receptor to various effectors (e.g. arrestin) (10,11). These four roles are not mutually exclusive. Each GPCR-associated protein may play one, two, three, or all four of these roles. Hence, identifying the binding partners of GPCR is essential in understanding GPCR signaling mechanism.

Being a member of the GPCR superfamily and rhodopsin subfamily, opioid receptors (μ, δ, κ) have the putative structures of seven transmembrane domains and an extracellular N terminus with multiple glycosylation sites (12-14). They play critical roles in drug tolerance and dependence in the nervous system via coupling to members of the Gi/Go proteins (4). Their activation results in adenylyl cyclase inhibition and/or the regulation of other effector systems (15,16). Recently, some components of the opioid receptor scaffolding complex have been identified by a yeast-two hybrid system and GST fusion protein pull-down assay. For example, the δ-opioid receptor (DOR) has been shown to interact with sorting nexin1 (SNX1) and the

G protein-coupled receptor-associated sorting protein (GASP), which preferentially modulates lysosome sorting of DOR (8,17). The intermediate filament-binding protein of actin, periplakin, potentially competes with G proteins for opioid receptors and restricts agonist-mediated G protein activation (18). Filament A, a protein known to couple membrane proteins to actin, was shown to interact with the carboxyl tail domain of MOR and regulate MOR trafficking (19). PKCI, a protein kinase C-interacting protein that specifically binds to the C terminus of human MOR, has been shown to block agonist-induced inhibition of adenylyl cyclase and suppress MOR desensitization partially at the G protein level and completely at the adenylyl cyclase level (20). Phospholipase D2 (PLD2), a phospholipid-specific phosphodiesterase in plasma membranes, also was found to be associated with rat MOR and affect receptor trafficking (21). Recently, a truncated form (38-117) of GEC1 was found to specifically interact with the C-tail of the human kappa opioid receptor (hKOR) and be important for trafficking hKOR in the biosynthesis pathway (22).

When opioid receptor synthesis occurs, the completed core oligosaccharide is transferred from the dolichylpyrophosphate carrier to a growing, newly synthesized polypeptide chain, which is coupled through an N-glycosidic bond to the side chain of an asparagine residue. The oligosaccharyltransferase responsible for this transfer is a complex enzyme with its active site in the ER lumen (23). During the translocation into the ER lumen, polypeptides on membrane-bound polysomes may be cotranslationally modified by N-glycosylation (24). In this process, the OST catalyzes the transfer of high mannose oligosaccharides, which are preassembled on lipid-anchored dolicholpyro-phosphate moieties to an asparagine residue within an Asn-X-

Ser/Thr consensus motif of nascent polypeptide chains facing the lumen of the ER (25). Immediately after coupling to the polypeptide chain, terminal glucose and mannose residues are removed by ER glucosidases and mannosidases (26). When the glycoprotein moves to the Golgi complex, the glycan chains undergo further trimming of mannoses. N-glycosylation has been found to be an important factor in the regulation of protein folding, stability, sorting and secretion (27). For opioid receptors, this *N*-glycosylation is a rate-limiting step in their translocation to the cell membrane (28). However, the detailed mechanism of the opioid receptors biosynthesis is still elusive. A truncated form (38-117) of GEC1 was found to specifically interact with the C-tail of the human kappa opioid receptor (hKOR) and be important for trafficking hKOR in the biosynthesis pathway (22). Whether proteins similar to GEC1 participate in MOR maturation process remains unknown.

At the same time, G-protein-coupled receptors (GPCRs) use heterotrimeric guanine nucleotide binding proteins (G proteins) as signaling intermediates between activated receptors and their intracellular effectors. GPCR signaling complex consists minimally of three protein components: a receptor, a G protein and a signalling effector. During the course of receptor signaling, these components at one time must physically interact with each other for signals to propagate. Lipid rafts, microdomains located within the plasma membrane, cluster receptors and components of receptor signaling cascades. Selective partitioning of proteins into lipid rafts often influences lipid transport, membrane trafficking and signal transduction. In these manners, lipid rafts can serve as signaling platforms for receptors and effectors (29). Proteins known to interact with lipid rafts, and to have activities influenced by such interaction, include GPCRs (e.g.

the β2-adrenergic receptor, β2AR), tyrosine kinase receptors (e.g. EGF receptors and nerve growth factor receptors), GTPases (e.g. H-Ras and α-subunits of heterotrimeric G proteins) and non-receptor tyrosine kinases (e.g. Src and Src family kinases), as well as MEK and ERK(30-36). The function of lipid rafts in organizing and mediating GPCRs' signal transduction was reported for many receptor classes and subtypes(37,38). Physical interaction between opioid receptor and G protein in lipid raft represents the high-affinity state of agonist binding(39,40), suggesting that the localization of receptor and G protein in lipid rafts may facilitate their coupling and subsequently influence agonist binding to receptors. In addition, raft domains differentially affect different opioid receptors' agonist binding and the coupling of G proteins to opioid receptors can determine distinct signaling pathways. For example, human κ-opioid receptors (KOR) expressed in Chinese hamster ovary cells (CHO cells) is located in lipid rafts and its localization in the microdomains and cholesterol depletion of these cells have no effect on the association between KOR and G protein (41), indicating receptor and G protein occupy different membrane compartments. By contrast, lipid raft was demonstrated to be crucial for agonist-selected signal transduction of μ-opioid receptors (MOR), which resulted from differential change of the receptor- G protein coupling in lipid raft (42).

It is highlighted in recent studies that the influence of lipid rafts on signaling proteins is dynamic in both directions(43-45). This means that proteins are able to mediate their signaling environment (e.g., post-modification like palmitoylation/depalmitoylation or myristoylation/de myristoylation could affect signaling proteins' stay in lipid rafts, and different affinity of signaling proteins for

lipid rafts could affect themselves and their associated proteins to be hold in or expelled out of lipid rafts), thereby modifying the properties and organization of signaling proteins in lipid rafts (46,47). Finally, signaling amplitude can be amplified or diminished in these signaling microdomains. Collectively, the varieties of interactions between lipid rafts and proteins reflect the complexity of their relationship and the multitude of possible regulatory processes involved in GPCR-associated signal transduction(43,48).

To address these issues, yeast-two hybrid system and GST fusion protein pull-down assay were used to identify some components of GPCRs' scaffolding complex (22,49). But as to these methods, only one or two domains of the receptor were used to construct a fusion protein for identifying scaffolding proteins. They cannot reflect agonist/antagonist-mediated conformational change responsible for protein recruitment. To identify the binding partners of MOR, a member of GPCR rhodopsin subfamily, we purified MOR complexes from neuroblastma neuro2A (N2A) cells stably expressing $(His)_6$-tagged MOR . Ribophorin I (RPNI), a member of the oligosaccharide transferase family that was assumed to be responsible for N-glycosylation of newly synthesized proteins and G protein-regulated inducer of neurite outgrowth 1(GRIN1) have been found to be directly associated with MOR.

Furthermore, our results showed that RPNI was a critical mediator of the MOR transport from the endoplasmic reticulum (ER) to the cell membrane. Our data demonstrate that, in addition to N-glycosylation, RPNI acts as a novel key regulator in the transport of nascent receptors, thus affecting MOR function.

On the other hand, GRIN1 was initially found specifically expressed in brain and interacted selectively with activated α-subunits of the Gi subfamily ($G_i\alpha$, $G_o\alpha$, and $G_z\alpha$). GRIN1 colocalizes with $G_o\alpha$ at the growth cone of neuronal cells and promotes neurite extension in Neuro2a cells (50). It was reported that the interaction between GRIN1 and activated $G_o\alpha$ induces activation of Cdc42, which led to morphological changes in neuronal cells (51). However, GRIN1 does not contain domains homologous to known signaling motifs. To illustrate whether GRIN1 could affect MOR-activation signaling pathway to induce neurite outgrowth, confocal microscopy and lipid raft fraction extraction experiment were performed. Our data showed that overexpression of GRIN1 could significantly immobilize MOR within lipid raft and induce neurite outgrowth in the presence of etorphine. Our data suggested that GRIN1 might have distinct function besides its interaction with activated $G_i\alpha$.

Part III: Methods

Expression of (His)6-MOR in the N2A Cells

The rat MOR tagged with the (His)6-epitope at N-terminus was subcloned in pCDNAmp vector. N2A cells were cultured in Dulbecco's modified Eagle's medium (DMEM) supplemented with 100 units/ml penicillin, 100 μg/ml streptomycin, and 10% fetal calf serum (DMEM growth medium) in a 10% CO2 incubator. These N2A cells then were transfected with 10 μg of the (His)6-MOR plasmids. The colonies surviving the antibiotic Geneticin (G418) selection (1 mg/ml) were isolated. The cell clone that expressed MOR at the level of 0.8 pmole/mg protein was used in receptor complex purification.

Cell Culture and Transient Transfection

N2A cells were maintained in DMEM containing 10% fetal bovine serum and penicillin/streptomycin. Cells were plated on 100-mm dishes (for immunoprecipitation studies) or 6-well plates (for flow cytometry studies) at a density of 250,000 cells/ml, and grown to 80% confluency. Transfections were performed using the Superfect transfection reagent (QiaGen, Valencia CA). Transfection medium was replaced with medium containing fresh serum 12-18 hours after transfection, and cells were harvested 24-48 hours later.

Purification of Receptor Complex

Sixty 150mm dishes of stably expressing (His)6-MOR N2A cells and 150mm dishes of control N2A cells were lysed with 1% Triton X-100 at 4°C for 2 hours. Lysate was

collected and centrifuged at 10,000x g for 15 minutes at 4°C. Supernatant was collected and purified by Ni2+ resin columns (Invitrogen Carlsbad, CA). Then the columns were washed ten times with wash buffer and eluted with elution buffer provided by the kit (Invitrogen Carlsbad, CA). Eluates were concentrated with Amicon concentration cells (Amicon Beverly, MA). Protein was separated by SDS-PAGE and silver-stained, and the presence of MOR was identified by Western analysis.

Proteolytic Digestion

Silver-stained gel bands were excised, dried and destained by incubating in 15 mM K3Fe(CN)6 and 50 mM Na2S2O3 at 24°C for 15 minutes, and then washed with 100 mM NH4HCO3. Destained gels were dried and rehydrated in 50 mM NH4HCO3 and 5 mM CaCl2 solution with 0.01 mg/ml sequence-grade modified porcine trypsin (Promega, Madison, WI) and incubated at 37°C overnight. Trypsinized fragments were collected by sonicating the gel pieces in 50 µl of 25 mM NH4HCO3 and again after adding 50 µl of 50% acetonitrile. The supernatant was collected and sonicated repeatedly in 50 µl of 5% formic acid and again after adding 50 µl of 50% acetonitrile. The supernatant was pooled. DTT was added to a final concentration of 1 mM, and the sample was dried and frozen at -80°C for MALDI-TOF or LC MS/MS.

LC MS/MS Spectrometry

Prior to LC MS/MS analysis, the sample was reconstituted with load buffer and the entire sample was injected. LC MS/MS methods were as described in (52). LC MS/MS results were analyzed by ProteinPilotTM Software 2.0, software revision

number 50861 (Applied Biosystems Inc, ABI, (53). The search engine uses biological modification invoked through the search effort (i.e., semi- and non-trypsin peptides are included in the search) as the search parameters. Protein Database was NCBI's nr mouse subset database from musculus_NCBInr_CTM_20061212, and was appended to a contaminants database (107,806 proteins total).

Immunoprecipitation and Western-blot Analysis

Confluent cells were washed in phosphate-buffered saline (PBS) at 4°C and lyzed for 30 minutes in solubilization buffer (1% Triton X-100, 150 mM NaCl, 1 mM EGTA, pH 7.4) containing mammalian protease inhibitor cocktail (Sigma-Aldrich, St. Louis, MO), at 4°C. Lysate was centrifuged for 30 minutes at 10,000 x g, and the supernatant was collected and assayed for protein by the BCA method (Pierce, Rockford, IL). A total of 500 µg of protein was pre-cleared with Protein G Sepharose beads (Sigma-Aldrich) and incubated with 1 µg mouse anti-HA antibodies for 2-3 hours followed by incubation with 30 µl Protein G Sepharose for 3 hours, all at 4°C. Sepharose beads were pelleted by brief centrifugation at 10,000 x g, at 4°C, and washed three times with solubilization buffer. Proteins were eluted by re-suspending in two volumes of 2X SDS-sample buffer (10mM Tris, 15 mM SDS, 20 mM DTT, 20% glycerol, 0.02% bromphenol blue, pH 6.8) followed by incubation at 65°C for 30 minutes. Proteins were resolved by SDS-PAGE, transferred to Immobilon-P membranes (Millipore, Bedford, MA), and immunoblotted with anti-FLAG M2 (Sigma-Aldrich) primary antibodies and detected by anti-mouse AP-linked secondary antibodies (Bio-Rad) in

Tris-buffered saline containing 5% powdered milk and 0.1% Tween-20, unless indicated otherwise.

In Vitro Translation

Each construct was translated in vitro using the TnT Coupled Transcription/Translation System (Promega) following the company's protocol. This protocol simplifies in vitro translation by starting with cDNA. The addition of RNA polymerase to the translation mixture eliminated the separate synthesis of RNA from DNA. In brief, the TnT buffer, rabbit reticulocyte lysate, RNA polymerase, amino acid mixture, and RNase inhibitor were added to a 0.5 ml microcentrifuge tube placed on ice. 1 μg of plasmid DNA was added to the tube and briefly spun to mix reaction components to the bottom of tube. The reaction was then incubated at 30°C for 90 min.

Gel-overlay Assay

Protein samples were separated by SDS-PAGE gel and transferred to Immobilon-P membranes (Millipore, Bedford, MA), incubated with in vitro translation product of FLAG-RPNI for 1 hr at room temperature. The membrane was washed for five minutes three times at room temperature with TTBS and immunoblotted with anti-FLAG primary antibodies (Sigma Aldrich). The association of the in vitro translated product was detected with anti-mouse AP-linked secondary antibodies (Bio-Rad) diluted in Tris-buffered saline containing 5% powdered milk and 0.1% Tween-20.

Construct siRNA of RPNI

The GenScript's siRNA design center siRNA Target Finder and siRNA Construct Builder (http://www.genscript.com/rnai. html) was used to design siRNA sequence for RPNI with following nucleotide sequences: Sense1:GATCCCGTTGTTCTCGTAA TGTACTTTGTTGATATCCGCAAAGTACATTACGAGAACAATTTTTTCCAAA; Antisense1:AGCTTTTGGAAAAAATTGTTCTCGTAATGTACTTTGCGGATATC AACAAAGTACATTACGAGAACAACGG;Sense2:GATCCCATCTTCAGTGCAT ACTGGTCATTGATATCCGTGACCAGTATGCACTGAAGATTTTTTTCCAAA;A ntisense2:AGCTTTTGGAAAAAAATCTTCAGTGCATACTGGTCACGGATATCA ATGACCAGTATGCACTGAAGATGG;Sense3:GATCCCGTATTGACAGTCTCAT CAAAGTTTGATATCCGACTTTGATGAGACTGTCAATATTTTTTCCAAA;Antis ense3:AGCTTTTGGAAAAAATATTGACAGTCTCATCAAAGTCGGATATCAAA CTTTGATGAGACTGTCAATACGG.

Confocal Microscopy

Cells transfected with GFP-tagged vector, GFP-tagged RPNI, and GFP-tagged RPNI siRNA were grown in 6-well culture plates on glass coverslips to 60% -75% confluency and fixed in 3.7% paraformaldehyde for 30 minutes. Adherent cells were treated with lysis buffer (0.1% Triton-X100, 150mM NaCl, 1mM EGTA, pH7.4) for 20 minutes. Then cells were incubated with mouse anti-HA antibody (1:1000) for 1 hour, followed by washing with PBS. Cells then were incubated with goat anti-mouse Alexa 594 (1:1000). All antibody incubations were performed in PBS with 10% BSA. Cells were dried briefly and mounted onto glass slides using Vectashield (Vector Labs,

Burlingame, CA). HA-tagged MOR was visualized by immunofluorescence, using BD CARVII™ Confocal Imager with a Leica DMIRE2 fluorescence microscope.

Fluorescence Flow Cytometry

Cells were grown in 12-well culture plates to 80%-85% confluency. Before the addition of antibodies, cells were rinsed twice with serum-free DMEM. Then the cells were incubated at 4 °C for 60 minutes in serum-free DMEM with anti-HA antibody (1:500). Afterward, the cells were washed twice with serum-free DMEM and incubated with Alexa633-labeled goat anti-mouse IgG secondary antibody (1:400) at 4 °C for 1 additional hour. Then the cells were washed and fixed with 3.7% formaldehyde before quantifying the receptor immunoreactivity with fluorescence flow cytometry (FACScan, BD Biosciences). Fluorescence intensity of 10,000 cells was collected for each sample. Cell Quest software (BD Biosciences) was used to calculate the mean fluorescence intensity of the cell population. In our study, two-color flow cytometry was used. A stained non-transfected sample (Mock) was processed with the cytometer to adjust the voltages on FSC and SSC detectors for viewing the populations of interest. The R1 region was adjusted around the population. The fluorescent detector voltages were adjusted to place the unstained events in the lower left quadrant. After that, each sample was installed and data were required. Only the cells that transfected with GFP were used to obtain the data on MOR fluorescence. All FACS analyses were conducted three times with triplicate samples in each experiment.

Pull-down Assay of GST-MOR 3rd Intracellular Loop with In Vitro Translation Product of GRIN1

The cDNA sequences of MOR 2nd intracellular loop (MORIL2), MOR 3rd intracellular loop (MORIL3), MOR C-tail (MORCT) was obtained from cDNA of rat MOR plasmids by PCR using the following primers:

MORIL2: sense:GGATCCCTCTGCACCATGAGCGTGGAC;

antisense:GGATCCTCAGCAGACGTTGACGATTTTGGC;

MORIL3: sense: GGATCCTACGGCCTGATGATCTTACGA;

antisense:GGATCCTCACACGACCACCAGCACCATCCG;

MORCT: sense:GGATCCGATGAAAACTTCAAGCGATGC;

antisense:GGATCCTTAGGGCAATGGAGCAGTTTC

The cDNA sequences of the GST fusion proteins of MORIL2, MORIL3 and MORCT were cloned into the pGXT2 vector within BamH1 restriction site, transformed into E. coli BL21-CodonPlus (DE3)-RP (Stratagene, La Jolla, CA). GST, MORIL2, MORIL3, or MORCT proteins were adsorbed onto glutathione-agarose beads (Sigma-Aldrich Co) and washed three times with phosphate buffered saline for pull-down analysis. In vitro translation product of GRIN1 was incubated with GST or GST-MOR 2nd, GST-MOR 3rd intracellular loop and GST-MOR C-tail fusion protein pre-loaded glutathione-agarose beads on an end-to-end rocker for 1 hour at 4°C. After that, beads were washed three times with ice-cold GST wash buffer containing 1mM complete cocktail (Roche) and SDS-PAGE was performed with samples eluted by 10mM reduced glutathione (50mM Tris-HCL, 5% glycerol, pH 8.0). Immunoblotting was performed with mouse anti-HA antibody (Covance) for HA-GRIN1. The loading

amount of GST or GST-MOR 2nd, GST-MOR 3rd intracellular loop and GST-MOR C-tail fusion protein was demonstrated by coomassie blue staining.

Construct GST-i33 mutant and GST-i35 mutant of MOR

The GST fusion proteins of MOR i33 mutant (MORi33), MOR i35 mutant (MORi35) were constructed by cloning the PCR products of MORi33 or MORi35 mutants into the BamH1/EcoRI site of the pGXT2 vector. These PCR products were generated using the rMOR cDNA cloned in pRCcmv and the following primers:

MORi33sense:GGATCCTACGGCCTGATGATCTTACGA

antisense:GGATCCTTAGGGCAATGGAGCAGTTTC

MORi35sense:GGATCCTACGGCCTGATGATCTTACGA

antisense:CAGATTCCTGTCCTTTTC

The plasmids were transformed into E. coli BL21-CodonPlus (DE3)-RP (Stratagene, La Jolla, CA) and the production of fusion proteins was induced by addition of 2 mM ITPG.

Lentivirus-mediated Expession of GRIN1 siRNA.

Constructs of GRIN1 siRNA was cloned into pcDNA-6.2GW/miR vector with siRNA sequence for GRIN1 designed by Invitrogen's RNAi design center and BLOCK-iT™ RNAi Designer (https: //rnaidesigner .invitrogen.com /rnaiexpress):

Sense1:TGCTGAACAAAGTCGTTCCAGAGTTGGTTTTGGCCACTGACTGACC AACTCTGACGACTTTGTT;Antisense1:CCTGAACAAAGTCGTCAGAGTTGGTC AGTCAGTGGCCAAAACCAACTCTGGAACGACTTTGTTC;Sense2:TGCTGAAC

ACAGGATTTCTGATCTCTGTTTTGGCCACTGACTGACAGAGATCAAATCCT
GTGTT;Antisense2:CCTGAACACAGGATTTGATCTCTGTCAGTCAGTGGCCAA
AACAGAGATCAGAAATCCTGTGTTC;Sense3:TGCTGTACTGAGGATACAAG
CTCTGTGTTTTGGCCACTGACTGACACAGAGCTTATCCTCAGTA;Antisense3:
CCTGTACTGAGGATAAGCTCTGTGTCAGTCAGTGGCCAAAACACAGAGCTT
GTATCCTCAGTAC;Sense4:TGCTGCAAAGACGGAGTTTCCACCTTGTTTTGG
CCACTGACTGACAAGGTGGACTCCGTCTTTG;Antisense4:CCTGCAAAGACG
GAGTCCACCTTGTCAGTCAGTGGCCAAAACAAGGTGGAAACTCCGTCTTTG
C.Lentivirus-mediated GRIN1 siRNA was made according to the protocal (http://tools.invitrogen.com /content /sfs /manuals / blockit_miRNA lentiviral _man .pdf).

Rat brain slice preparation

Experimental details are performed as described in (54). Briefly, All animal use was approved by the University of Minnesota Animal Use and Care Committee. Male Sprague Dawley rats, postnatal day 28 (P28) to P35, were killed by decapitation, and the brains were rapidly removed into ice-cold dissection buffer (2.6 mM KCl, 3 mM $MgCl_2$, 1 mM $CaCl_2$, 1.23 mM NaH_2PO_4, 10 mM dextrose, 212.7 mM sucrose, and 26 mM $NaHCO_3$). The components having high endogenous MOR expression such as lateral parabrachial nucleus, laminae, striatum, hippocampi, presubiculum and parasubiculum, amygdaloid nuclei, thalamic nuclei, locus coeruleus, etc, were removed and unrolled. Mini slices (400 μm) were prepared and transferred to a holding chamber containing artificial CSF (ACSF) (in mM: 124 mM NaCl, 5 KCl, 1.25

NaH_2PO_4, 10 dextrose, 1.5 $MgCl_2$, 2.5 $CaCl_2$, and 26 $NaHCO_3$) bubbled with 95% O_2/5% CO_2 maintained at 32°C. The slices were recovered for a minimum of 90 min before overnight incubation of PTX or lentivirus-mediated GRIN1siRNA for 48-hour following PTX treatment.

Rat brain slice Subcellular fractionation.

Rat brain slices' homogenates (H) were prepared using glass homogenizers from treated and control untreated hippocampal minislices in homogenization buffer (HB) [10 mM Tris base, pH 7.6, 320 mM sucrose, 150 mM NaCl, 5 mM EDTA, 5 mM EGTA, 1 mM benzamidine, 1 mM 4-(2-aminoethyl)benzenesulfonyl fluoride, 2 µg/ml leupeptin, 2 µg/ml pepstatin, and 50 mM NaF]. The homogenates were centrifuged at 1,000 x *g* to remove nuclei and large debris (P1). Supernatant was collected (S1). Pellet with crude membranes (P1) were homogenized and centrifuged again at 10,000 x *g*. Supernatant was collected as S2 and pull together with S1 and subjected to lipid raft fraction. Final pellets were sonicated in resuspension buffer (RB) (10 mM Tris, pH 8, 1 mM EDTA, and 1% SDS).

Construct siRNA of GRIN1

Construct of GRIN1 siRNA was cloned into GFP-tagged pRNAT H1.1 vector with siRNA sequence for GRIN1 designed by GenScript's siRNA design center siRNA Target Finder and siRNA Construct Builder (http://www.genscript.com/rnai. html):

Sense1:GATCCCGTTTCTGAGGTCATGAGATCCATTGATATCCGTGGATCTCA

TGACCTCAGAAATTTTTTCCAAA;*Antisense1*:AGCTTTTGGAAAAAATTTCTG

AGGTCATGAGATCCACGGATATCAATGGATCTCATGACCTCAGAAACGG;*S*

ense2:GATCCCGTTGCTGGAAACATACCTTCTGTTGATATCCGCAGAAGGTA TGTTTCCAGCAATTTTTTCCAAA;*Antisense2*:AGCTTTTGGAAAAAATTGCTG GAAACATACCTTCTGCGGATATCAACAGAAGGTATGTTTCCAGCAACGG;*Se nse3*:GATCCCGTCTGACGCTCCAAATGCTTCTTTGATATCCGAGAAGCATTT GGAGCGTCAGATTTTTTCCAAA;*Antisense3*:AGCTTTTGGAAAAAATCTGACG CTCCAAATGCTTCTCGGATATCAAAGAAGCATTTGGAGCGTCAGACGG;*Sen se4*:GATCCCGTTTGCTGGAACATGGCATGTCTTGATATCCGGACATGCCATG TTCCAGCAAATTTTTTCCAAA;*Antisense4*:AGCTTTTGGAAAAAATTTGCTGG AACATGGCATGTCCGGATATCAAGACATGCCATGTTCCAGCAAACGG.

Live cell imaging by confocal microscopy

Cells transfected with GFP-GRIN1 were grown in 10 mm culture plates with a glass coverslip at bottom to 30% - 40% confluency and treated with 100 nM etorphine or with 100 nM morphine as indicated for 10 minutes. After that, cells were washed with fresh medium three times and incubated in fresh medium without FBS at 37°C for 48 hours. GFP-tagged GRIN1 were visualized by immunofluorescence using a BD CARVII^{TM} Confocal Imager and a Leica DMIRE2 fluorescence microscope. Fluorescence images were taken at time "0" after medium was changed, and at different time points during agonist incubation as indicated. For statistic analysis, images from more than twenty fields in each sample were measured and calculated. The percentages of cells possessed neurite-outgrowth vs total cells were analyzed with Prism 4, Version 4.0 by GraphPad Software, Inc.

Immunoprecipitation of GRIN1 with adenovirus-mediated expression of G protein α-subunit

The construction of PTX-resistant adeno-Gαi2-Leu, adeno-Gαi3-Leu, and adeno-Gαo-Leu were described previously (55). N2A cells stably-expressing MOR with hemagglutinin (HA) tagged at the N terminus in 100 mm dishes were infected with PTX-resistant adeno-Gαi2-Leu, adeno-Gαi3-Leu, or adeno-Gαo-Leu viruses using Superfect transfection reagent (QIAGEN) as described previously (55). 24 h later, cells were transfected with HA-GRIN 1 using Superfect transfection reagent according to manufacturer's instruction. On the next day, 100 ng/ml PTX was added and the cells were incubated overnight. Then the cells were treated with 100 nM etorphine for 10 min or with saline. Cells were then lyzed in lysis buffer (50 mM sodium phosphate (pH 7.2), 100 mM NaCl, 1 mM DTT and 0.5% C12E10 supplemented with Complete Protease Inhibitors (Roche Applied Science)). After centrifugation at 12,000 ×g for 20 min, the supernatant was immunoprecipitated with rabbit polyclonal antibodies against Gαi2, Gαi3(56), or Gαo (Thermo Fisher Scientific, Fremont, CA) antibody and rProtein G agarose beads (Invitrogen, CA) at 4 °C overnight. Then the beads were washed 5 times with cell lysis buffer and were extracted with SDS-PAGE sample buffer. The eluted proteins were resolved by SDS-PAGE and were analyzed by western blot analysis with anti-HA antibody. For control, the cells were not infected with adeno-Gαi2-Leu, adeno-Gαi3-Leu, or adeno-Gαo-Leu viruses but transfected with HA-GRIN 1 to exclude the nonspecific binding. Use Image Quant for quantification analysis.

Lipid Raft Extract Preparation

N2A Cells stably expressing HA-MOR in 150 mm plates were grown and transfected with vector, GRIN1, GRIN1 siRNA respectively. To prepare rafts (57), 1.5 ml of raft buffer (500 mM sodium carbonate, pH 7.5, at 4°C) was added after the medium was aspirated and cells were scraped from the plates. An equal volume (1.5 ml) of modified Barth's solution (MBS) buffer PH 6.8 containing 80% sucrose was added and the combined supernatants were placed in the bottom of a centrifuge tube. 3 ml step gradient of 5% and 35% sucrose in raft buffer was layered on top of the lysate. Gradients were centrifuged for 18 hours at 12,000 ×g using a SW-41 rotor in a Beckman ultracentrifuge. After centrifugation, 1ml fractions of the gradients were collected. Total proteins in each fraction were precipitated by 5% TCA and washed three times with cold acetone (4°C), then dissolved in Laemmli buffer and separated on a 10% SDS-polyacrylamide gel. Afterward, the separated proteins were transferred to Immobilon-P membrane (Millipore, Bedford, MA), and the membrane was blocked in a blocking solution of 10% dry milk and 1% Tween 20 in Tris-buffered saline. Western analyses were carried with mouse anti-HA (1:2000), mouse monoclonal anti-transferrrin (1: 1000) or rabbit anti-T116 (1:100) respectively. Primary antibody was probed with alkaline phosphatase-conjugated secondary antibodies (1:5000). Proteins bands were detected by the addition of the ECF substrate and fluorescence of the bands was determined with Storm 860 (GE Healthcare). Band intensities were quantified and analyzed using ImageQuant (GE Healthcare). To normalize the Western analyses from separate runs, the relative percentage of the proteins in each fraction was obtained by

dividing each individual gradient fraction versus the sum of the pixels from all fractions.

Part IV: Results

Chapter 1:

Identification of RPNI direct binding to MOR

In order to identify components of MOR signaling complexes, $(His)_6$-MOR stably expressed in N2A cells was partially purified with a Ni^{2+} resin column and the proteins within the receptor complex were separated as described in Materials and Methods. Silver-staining of the gels revealed multiple protein bands including $(His)_6$-MOR identified subsequently with western analysis, which migrated as a diffused band with molecular weight between 65-70 KDa (Fig 1.1A). Several protein bands were excised and analyzed using MALDI-TOF mass spectrometry as described. One of the proteins with significant mascot probability score (>65) was tentatively identified to be ribophorin I (RPNI). The protein band around 85 KD was demonstrated conclusively as being RPNI with the LC MS/MS spectrometry analysis. Five distinct peptides were identified from MS/MS spectra with >90% confidence (representing 9% sequence coverage) and 3 peptides were identified with <90% confidence. Total coverage (all peptides) was 13.6% by amino acid sequence (Table 1.1). Equivalent protein candidates reported were gi|74207369, gi|55715894, gi|48474583 and gi|31543605. They all refer to the sequence of RPNI. The distribution of the 5 peptides within the RPNI amino acid sequence was summarized in Figure 1.2A. To confirm whether MOR interacts with RPNI and whether this interaction occurs in intact cells, we carried out coimmunoprecipitation studies with lysate from N2A cells transiently transfected with MOR and RPNI. Expression of full length RPNI tagged at the N-terminus with the

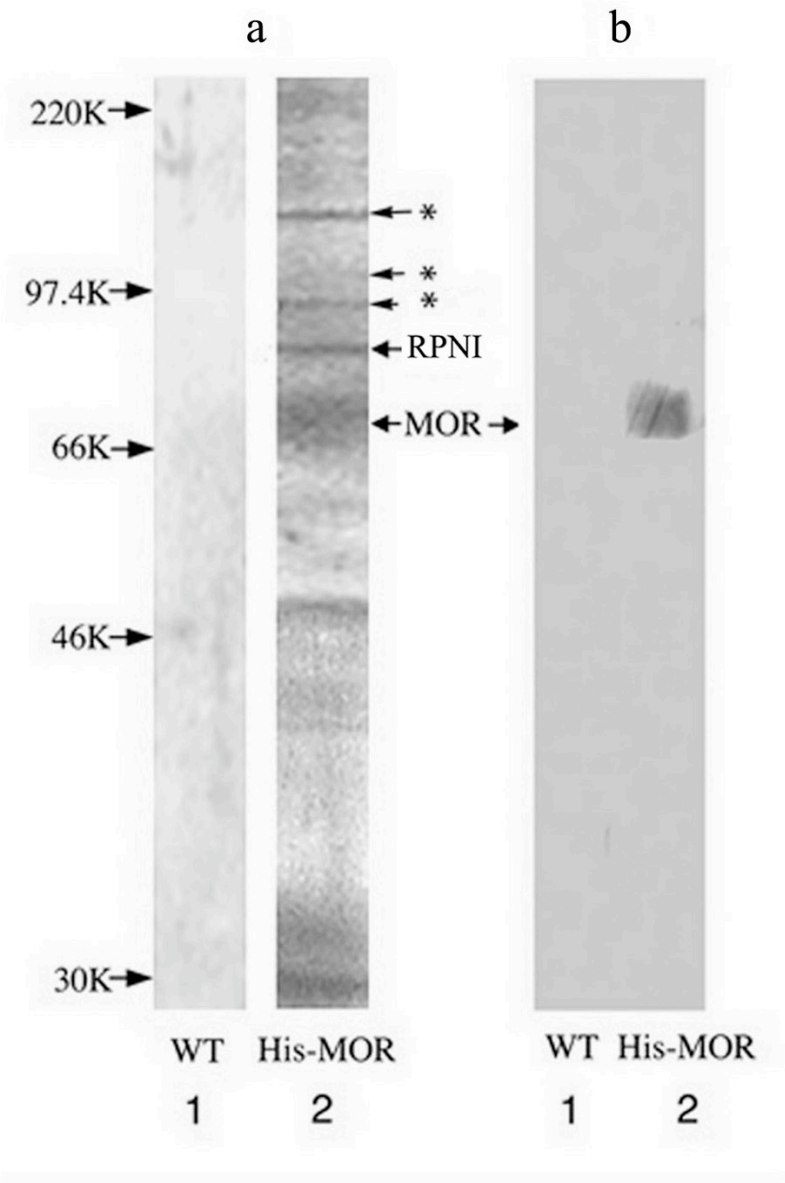

Fig 1.1A. Purification of MOR-associated proteins. MOR-associated proteins from N2A cells stably expressing (His)6-MOR were purified by HisLink Ni2+ affinity resin. Similar purifications starting with wild type N2A cells were carried out. Purified eluate was separated by SDS-PAGE and silver-stained (lanes 1–2). Lane 1 represents eluate from WT N2A cells and lane 2 represents eluate from N2A cells expressing (His)6-MOR. Ribophorin I (RPNI) has an apparent molecular weight around 85 kDa (due to other modification or gel migration). A(b). The presence of MOR was confirmed by Western-blot. The arrows in panel A(a) show all the proteins analyzed by mass spectrometry and the asterisks (*) show other proteins identified.

Tablel.1 Peptides identified using tandem mass spectrometry from mouse RPNI protein.

Peptide	Confidence(1)
AVTSEIAVLQSR	99
LPVALDPGSK	99
NIQVDSPYDISR	99
SEDVLDYGPFK	97
DIPAYSQDTFK	91
DISTLNSGK	23
QPDSGISSIR	6
DTYLENEK	3

Confidence reported from Protein Pilot Results Summary. The percentage of total coverage is 13.6%. High confidence coverage (>90%) is 9%.

MESPVALLLL LLLCLGALAP TPGSASSEAP PLVNEDVKRT VDLSSHLAKV
TAEVVLVHPG GGSTSRASSF VLALEPELES RLAHLGVQIK GEDEEDNNLE
VRETKIKGKS GRFFTVK**LPV** **ALDPGSK**ISV VVETVYTHVL HPYPTQITQS
EKQFVVFEGN HYFYSPYPTK TQTMRVKLAS RNVESYTKLG NPSR**SEDVLD**
YGPFKDIPAY **SQDTFK**VHYE NNSPFLTITS MTRVIEVSHW GIIAVEENVD
LKHTGAVLKG PFSRYDYQRQ PDSGISSIRS FKTILPAAAQ DVYYRDEIGN
VSTSHLLILD DSVEMEIRPR FPLFGGWKTH YIVGYNLPSY EYLYNLGDGY
ALKMRFVDHV FDEQVIDSLT VKIILPEGAK **NIQVDSPYDI** SRAPDELHYT
YLDTFGRPVI VAYKKNLVEQ HIQDIVVHYT TNKVLMLQEP LLVVAAFYIL
FFTVIIYVRL DFSITKDPAA EARMKVACIT EQVLTLVNKR LGLYRHFDET
VNRYKQSR**DI** **STLNSGK**KSL ETEHK**AVTSE** **IAVLQSR**LKT EGSDLCDRVS
EMQKLDAQVK ELVLKSAVEA ERLVAGKLKK DTYLENEKLS SGKRQELVTK
IDHILDAL

Fig 1.2A.LC MS/MS analysis result of the protein band corresponding to RPNI. The sequences in bold and underlined represent the RPNI amino acid sequences identified using tandem mass spectrometry after in-gel digestion of the protein-staining band. The protein sequence refers to gi|31543605.

FLAG epitope was confirmed by direct Western analyses of the total lysates (Figure 1.2B, panel c). Interaction of RPNI with MOR was determined by coimmunoprecipitating the complex with antibodies against the HA epitope, followed by immunoblotting with anti-FLAG antibody. RPNI did not coimmunoprecipitate with the receptor when cells were transfected with either HA-MOR or FLAG-RPNI alone (Figure 1.2B, panel a, lane 1 and 2). However, RPNI was detected in anti-HA immunoprecipitates from cells that were co-transfected with both HA-MOR and FLAG-RPNI, indicating that MOR interacts with FLAG-RPNI in mammalian cells (Fig 1.2B, panel a, lane 3 and 4). Similarly, coimmunoprecipitation of HA-MOR with FLAG-RPNI was observed only in cells co-transfected with both HA-MOR and FLAG-RPNI using anti-FLAG, but not in cells transfected with either one of these two constructs (Figure 1.2B, panel b). Same results were also obtained when digitonin was used to extract the complex in order to preserve the oligosaccharidetransferase (OST) physiological activity (Fig 1.3B). Interestingly, although RPNI showed interaction with MOR in both Triton X-100 treated and digitonin treated immunoprecipitates, other components of OST complex only showed in digitonin treated immunoprecipitates (Fig 1.3B). Such observations could be due to fact that the four components of OST complex link to each other when OST stability was maintained in digitonin (58) during co-IP of RPNI with MOR. RPNI interaction with MOR does not depend on the OST complex glycosylation activity. Only when the OST stability was maintained in digitonin, the individual components of OST complex were co-IP with MOR. Meanwhile, when the stability of OST

complex was disrupted by Triton X-100, only RPNI but not RPNII, OST48, or Dad1 was co-immunoprecipitated with MOR (Fig 1.3).

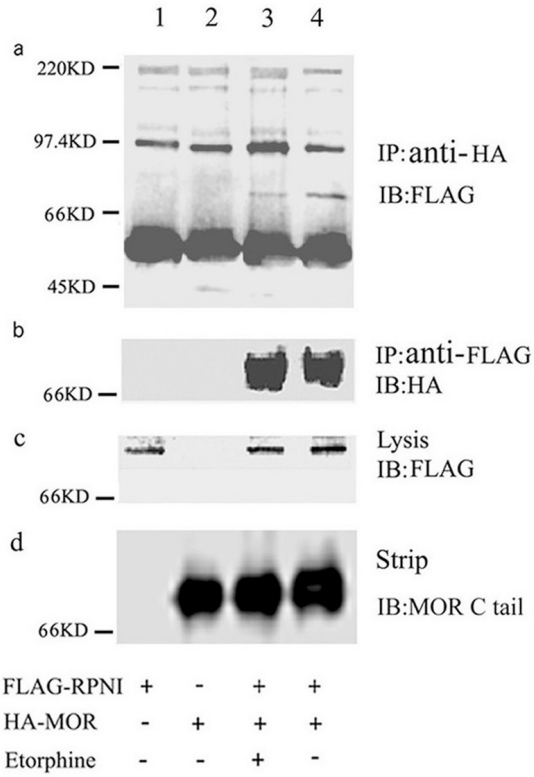

Fig 1.2B. Coimmunoprecipitation experiment of FLAG-RPNI and HA-MOR. Panel a: FLAG-RPNI was detected after HA-MOR was immunoprecipitated (IP) from the cell lysate; panel b: HA-MOR was detected after FLAG-RPNI was immunoprecipitated from the cell lysates; panel c: the expression level of FLAG-RPNI was determined in 1/20 of the total lysate used in IP experiments; panel d: MOR was detected with rabbit polyclonal antibodies directed against the C-tail of MOR after HA-MOR was immunoprecipitated from the cell lysates.

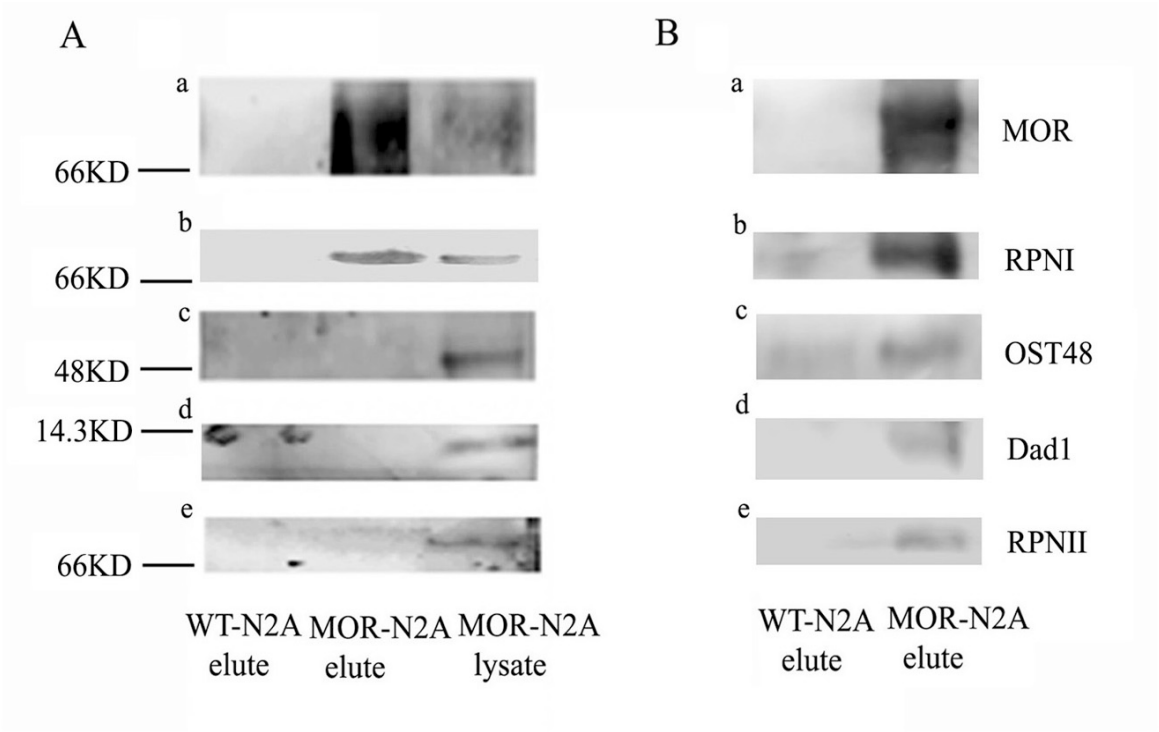

Fig 1.3. (A) WT-N2A cells and HA-MOR-N2A cells were extracted with 1% Triton X-100, which cannot maintain OST complex activity. IP and western analyses were carried out as described in Materials and Methods. Specific antibodies for different components of OST complex were used and the efficacy of each antibody was demonstrated by same amount of lysate; (B) WT-N2A cells and HA-MOR-N2A cells were extracted with 1% digitonin, which can maintain OST complex activity. IP and western analyses were carried out as described in Materials and Methods. In panel (a), MOR expression in WT-N2A cells and HA-MOR-N2A cells was detected by anti-MOR C tail antibodies after immunoprecipitation using anti-HA antibodies; In panel (b), RPNI within the anti-HA immunoprecipitate was detected using anti -RPNI antibodies; In panel (c), OST 48 within the anti-HA immunoprecipitate was detected using anti-OST 48 antibodies; In panel (d), Dad1 within the anti-HA immunoprecipitate was detected using anti-Dad1 antibodies; In panel (e), RPNII within the anti-HA immunoprecipitate was detected using anti-RPNII antibodies.

The RPNI interaction with MOR can be demonstrated to occur within the cellular context, which is not a consequence of detergent extraction by the immunoprecipitation studies with the mixed lysates. When N2A cells separately transfected with MOR or RPNI were mixed together immediately prior to detergent addition for lysate preparations and co-IP, anti-HA did not co-immunoprecipitate FLAG-RPNI from mixed cells transfected with either MOR or RPNI while anti-HA could coimmunopreciptate the FLAG-RPNI from N2A cotransfected with both MOR and RPNI (Fig 1.2C). The direct interaction between RPNI and MOR can be demonstrated further with gel-overlay experiments as described in Materials and Methods. As shown in Figure 1.2D panel a, *in vitro* translation resulted in the production of the full-length FLAG-RPNI. After incubating the Immobilon-P membrane containing the SDS-PAGE separated total lysate from N2A cells with the *in vitro* translated products, positive interaction in the lane containing lysate from MOR-expressed N2A cells, but not in the lane from wild type N2A cells, was observed after excess *in vitro* translated product was removed by repeated washings (Figure 1.2D, panel b). The location of the *in vitro* translated FLAG-RPNI product coincided with the location of HA-MOR, as determined by immunoblotting with anti-HA antibody (Figure 1.2D, panel c). These data indicate that RPNI directly interacts with MOR, not via a protein scaffold or complex.

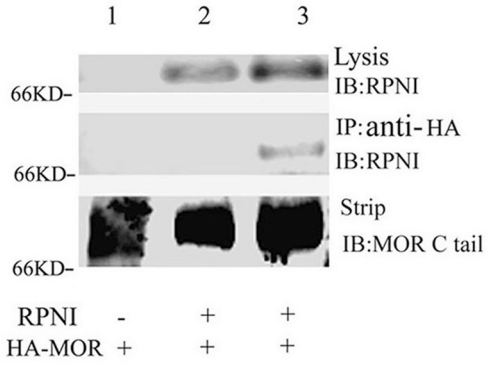

Fig 1.2C. Co-IP of FLAG-RPNI and HA-MOR in mixed cells that individually express FLAG-RPNI and HA-MOR. Lane 1: cells only express HA-MOR as negative control; lane 2: mixed cells that individually express FLAG-RPNI and HA-MOR; lane 3: cells that express both FLAG-RPNI and HA-MOR as positive control.

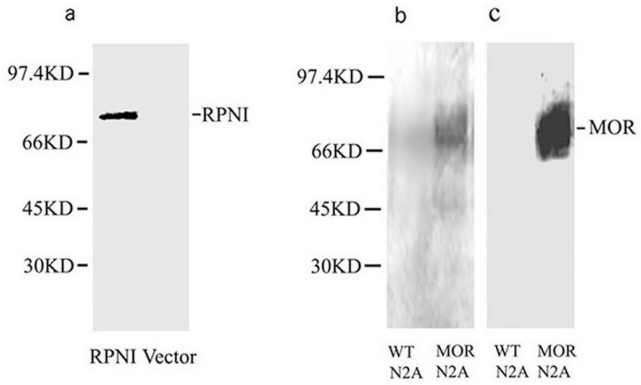

Fig 1.2D. Gel-overlay of RPNI with MOR. Panel a: in vitro translation products of FLAG-RPNI, as indicated by Western analysis using anti-FLAG antibody; panel b: Gel-overlay of FLAG-RPNI on membranes containing SDS-PAGE separated N2A extract from cells expressing or not expressing HA-MOR; panel c: Western analysis of MOR expression.

To demonstrate whether RPNI interacts with MOR endogenously expressed, MOR from mouse hippocampus tissue was immunoprecipitated by the anti-MOR C-tail polyclonal antibodies. Mouse cerebellum was used as the negative control to determine the specificity of the antibodies used. It showed that MOR C-tail antibodies could IP the endogenous RPNI from hippocampus but not from cerebellum extracts (Fig 1.4). In

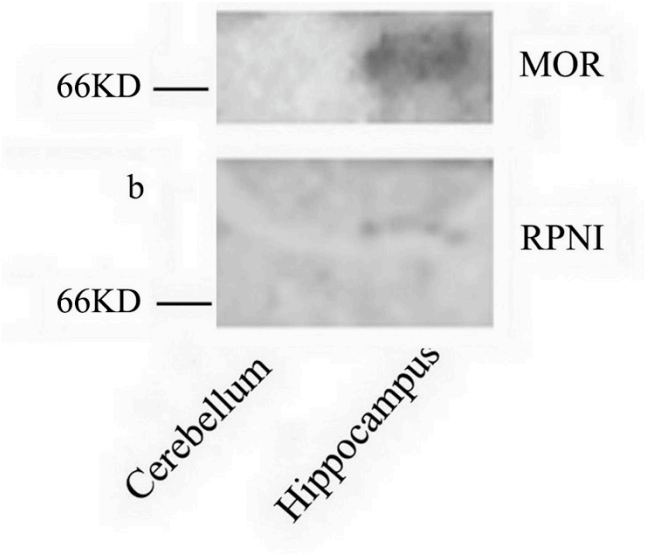

Fig 1.4. To determine whether RPNI interacts with MOR endogenously, different mouse brain sections that has no endogenous MOR expression (cerebellum) or high endogenous MOR expression (hippocampus) were used for IP. IP and western analyses were carried out as described in Materials and Methods. In panel (a), expression level of endogenous MOR was determined by rabbit anti-MOR c-tail antibody used in IP experiments; In panel (b), RPNI was detected by mouse anti-RPNI antibody after endogenous MOR was IP from the brain tissues using specific anti-MOR C-tail antibody.

order to examine whether RPNI could associate with other glycosylated GPCRs, N2A cells were co-transfected with a_{1A}-adrenergic receptor (AR1a) and RPNI transiently. Co-IP studies indicated that RPNI also interacted with AR1a similar to

the RPNI interaction with MOR, i.e., FLAG-RPNI was pulled down by anti-HA only in N2A cells expressing both FLAG-RPNI and HA-AR1a (Fig 1.5A).

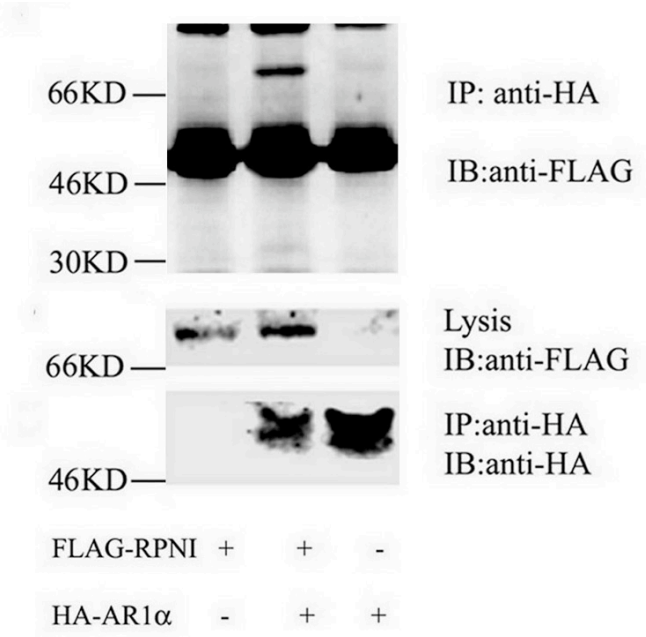

Fig 1.5A. N2A cells were transfected either with empty vector and FLAG-RPNI, with FLAG-RPNI and HA-tagged 1A-adrenergic receptor (HA- 1AAR) or with empty vector and HA- 1AAR

Since RPNI is within the glycosyltransferase complex, the interaction between RPNI and MOR, between RPNI and AR1a can occur within the endoplasmic reticulum (ER), prior to being transported to Golgi during the maturation of these GPCRs. The presence of MOR in ER or Golgi of N2A transiently transfected with MOR can be observed with confocal microscopy

studies using specific organelle markers. The co-localization of MOR and RPNI within the ER was observed in such confocal microscopy studies (Fig 1.6A).

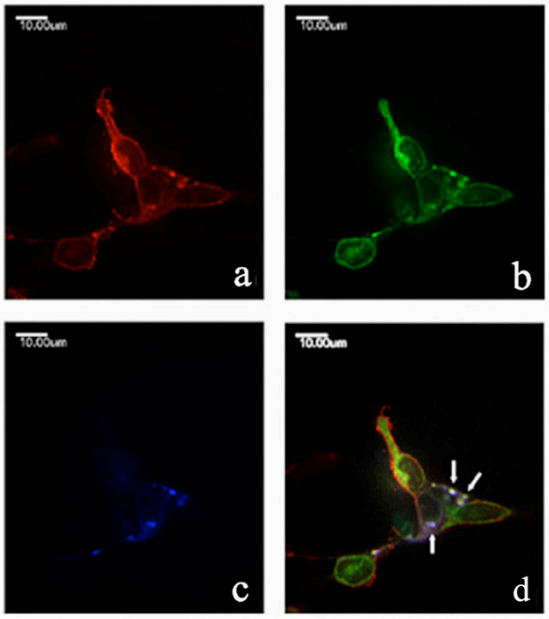

Fig 1.6A. Colocalization of MOR and RPNI in ER. In panel (a), N2A cells expressing HA-MOR were determined by staining with rat anti-HA antibodies and visualized with anti-rat antibodies conjugated with Alexa Fluor 594; In panel (b), N2A cells expressing FLAG-RPNI were determined by staining with rabbit anti-FLAG antibodies and visualized with anti-rabbit antibodies conjugated with Alexa Fluor 488; In panel (c), endogenousER marker-calnexin in N2A cells were determined by staining with mouse anti-calnexinantibodies and visualized with anti-mouse antibodies conjugated with Alexa Fluor 350;in panel (d), the merged image of MOR , RPNI and calnexin. The arrows in the merged image indicate the presence of MOR with RPNI in ER. Scale bar represents 10 μ.

Ability of RPNI to affect cellular location of MOR

To examine the effect of RPNI interaction on MOR cellular trafficking, three RPNI siRNA (#1,2,3) and one scramble siRNA were constructed as described in Materials and Methods. siRNA constructs were transfected into N2A cells and the GFP

fluorescence was used to screen for similar transfection efficiency before lyses. The efficency of RPNI siRNA knocking-down was demonstrated as Fig 1.7A. Only siRNA#3 construct

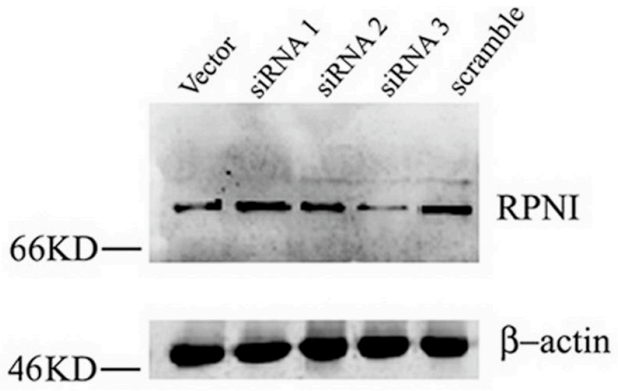

Fig 1.7A. Efficiency of siRNA used on knocking-down endogenous RPNI. siRNA #3 significantly reduced endogenous RPNI expression compared with others. ß-actin was used as control and transfection efficiency was controlled as described in Results.

exhibited significant knock down of the RPNI content in N2A cells. Thus, siRNA#3 and scramble siRNA as control were used in subsequent studies. N2A cells stably expressing HA-MOR were transfected with GFP-pRNAT H1.1/hygro vector (0.1µg), GFP-scramble RPNI siRNA (0.1µg) or GFP-RPNI siRNA#3 (0.1µg). MOR distribution was detected with mouse anti-HA antibody. We observed no difference in MOR distribution among cells transfected with scramble RPNI siRNA and the control vector. Comparing cells with no GFP fluorescence and those with, MOR was detected only on the cell surface in cells transfected with the scramble siRNA (Figure 1.7B). In N2A cells expressing the RPNI siRNA as indicated by the GFP fluorescence, the majority of MOR was detected to be located intracellularly (Figure

1.7C). In the same field, in cells not expressing the RPNI siRNA as indicated by the absence of GFP fluorescence, MOR was observed on the cell surface only. After siRNA transfection, total MOR expression was

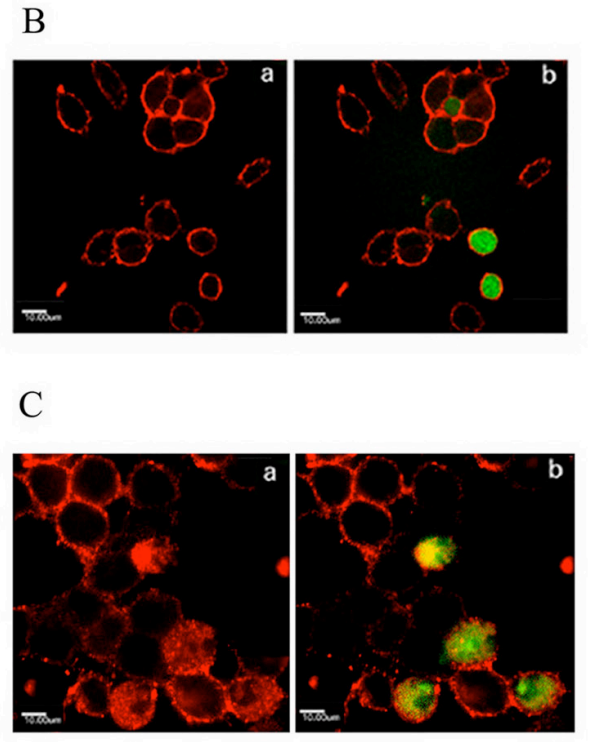

Fig 1.7B&C. (B) Transfection of cells with 0.1 µg of scramble GFP-RPNI siRNA did not affect the expression of MOR on cell surface. (C) Transfection of 0.1 µg GFP-RPNI siRNA decreased the expression of MOR on cell surface. In both (B) and (C), panel a: HA-MOR was stained by the mouse anti-HA monoclonal antibody and detected with the goat anti-mouse antibodies co-njugated with Alexa 594; panel b: merge MOR with GFP-tagged RPNI scramble siRNA or GFP -tagged siRNA. Scale bar equals 10 µ.

not altered as indicated by western analyses of the total lysate (Figure 1.7D). The cell surface MOR level with siRNA transfection was quantified with FACS using N2A cells transfected with GFP-Vector as the basal fluorescence level. The cell surface receptor fluorescence decreased from 100±5.4% to 41.96±2.9% of the basal level

after RPNI siRNA transfection (Figure 1.7D). These data demonstrate that RPNI regulates MOR cell surface expression. To eliminate the possibility that

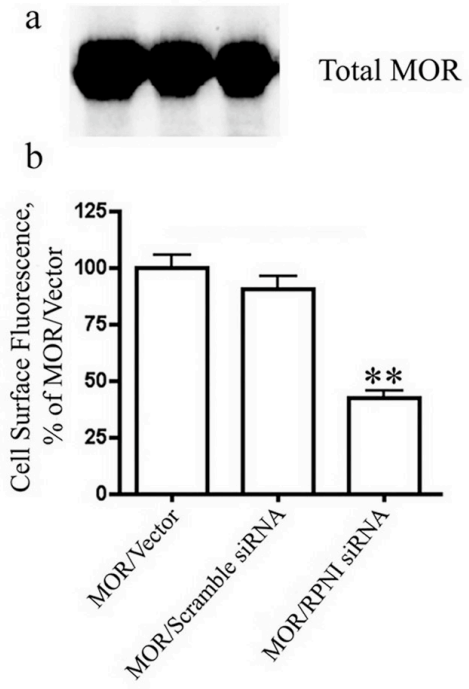

Fig 1.7D. Panel a: expression level of MOR in 1/20 fraction of each sample, which showed total MOR of each sample are almost the same; Panel b: FACS analyses of cell surface MOR expression in N2A cells transfected with RPNI siRNA as described in Materials and Methods. The bars represent the average ± S.E.M. from three separated experiments carried out in triplicate. ** denotes $p < 0.01$ when compared with cells transfected with vector.

knockdown of RPNI could affect the overall MOR glycosylation state leading to the removal of misfolded protein, the glycosylation states of MOR after over-expressing or knocking-down of RPNI were detected by western blot analyses following the treatment with Endoglycosidase H (EndoH) and PNGase F (EndoF). As summarized in Fig 1.8A panel a, majority of MOR migrated in SDS PAGE with a molecular weight ~65-70 KDa. There was a minor protein band with M.W. ~45-46 KDa

detected by the HA antibodies, probably the immature form of MOR. Pretreatment of the lysate with EndoH for deglycosylation enzyme digestion reduced

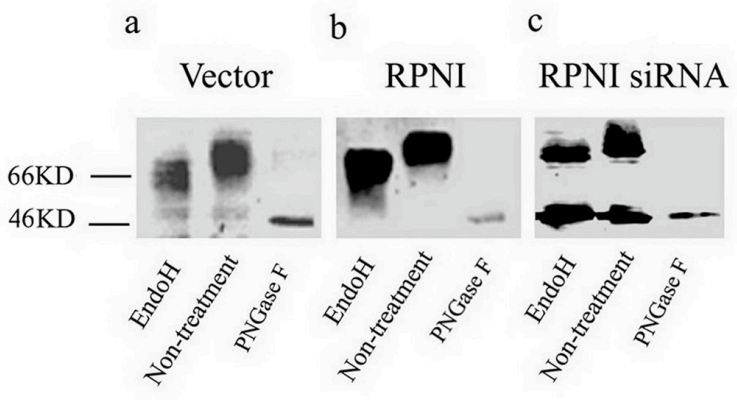

Fig 1.8A. Western-blot to detect MOR, MOR after EndoH digestion, and MOR after PNGase F digestion. panel (a): MOR in extract from N2A-MOR transfected with vector, after EndoH digestion, and after PNGase F digestion; panel (b): extract from N2A-MOR over-expressing RPNI, after EndoH digestion, and after PNGase F digestion ; panel (c): MOR in extract from N2A-MOR transfected with RPNI siRNA, MOR after EndoH digestion, and MOR after PNGase F digestion.

the M.W. of MOR slightly, while pretreatment with EndoF reduced the M.W. of MOR to ~ 46 KDa, similar to that of the nascent polypeptide. Over-expression of RPNI eliminated the non-matured MOR protein band, but did not alter the receptor sensitivity toward EndoH and EndoF (Figure 1.8A, panel b). siRNA knockdown of RPNI resulted in an increase in the amount of immature MOR form, but did not alter the receptor sensitivity to these two enzymes (Figure 1.8A, panel c). Therefore, the observed cellular location of MOR under the conditions of over-expression of RPNI or knock-down of RPNI with siRNA does not reflect an alteration in the glycosylation states of the receptor.

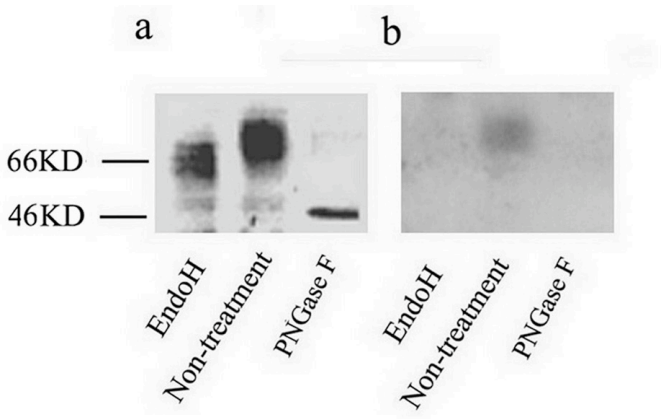

Fig 1.8B. Gel-overlay of RPNI with MOR, EndoH digested MOR, and PNGase F digested MOR. panel (a): Western-blot to detect N2A extract from cells expressing MOR, EndoH digested MOR, and PNGase F digested MOR. Panel (b): gel-overlay of in vitro translated FLAG-RPNI on membrane containing SDS-PAGE separated N2A extract from cells expressing MOR, EndoH digested MOR, and PNGase F digested MOR were carried out as described in Methods and Materials.

Interestingly, interaction of RPNI with MOR appears to involve the glycosylation states of the receptor. As shown in Figure 1.8B, gel overlay studies with the *in vitro* translated RPNI product indicated that only MOR not treated with the enzymes could bind with RPNI. Pretreatment of MOR with either EndoH or EndoF eliminated the RPNI interaction with the receptor (Figure 1.8B, panel b). Since western analyses indicated similar level of receptor among various enzyme treatments (Figure 1.8B, panel a), the absence of interaction in such gel overlay studies suggested the high mannose or some hybrid types of N-linked carbohydrates on MOR were essential for RPNI interaction. Combined with the data of RPNI IP from mixed cell lysates (Fig 1.2C), it indicates that carbohydrate (CHO) moiety is indispensable for RPNI binding. To further demonstrate whether RPNI interacts directly with the CHO moiety or not, the MOR partially purified with wheat germ agglutinin was digested with PNGase F and gel overlay studies were carried out with the *in vitro* translation

product of RPNI. No interaction was observed between RPNI and MOR in the PNGase F treated sample (Fig 1.8B, panel b).

The inability of RPNI to interact with the PNGase F treated MOR could be due to the changes in the receptor's conformation after enzyme digestion thus affecting the recognition between these proteins, the role of CHO in RPNI binding was investigated with other GPCRs. Since our data showed RPNI could bind to glycosylated adrenergic receptor (α_{1A} AR) (Fig 1.5A), whether RPNI could have distinct interaction among GPCRs that exhibit high sequence homology but different glycosylation states was investigated, such as the non-glycosylated α2B-AR and the highly glycosylated α2C-AR. As shown in Fig 1.5B and Fig 1.5C, RPNI was not co-IP with α2B-AR while RPNI did co-IP with α2C-AR.

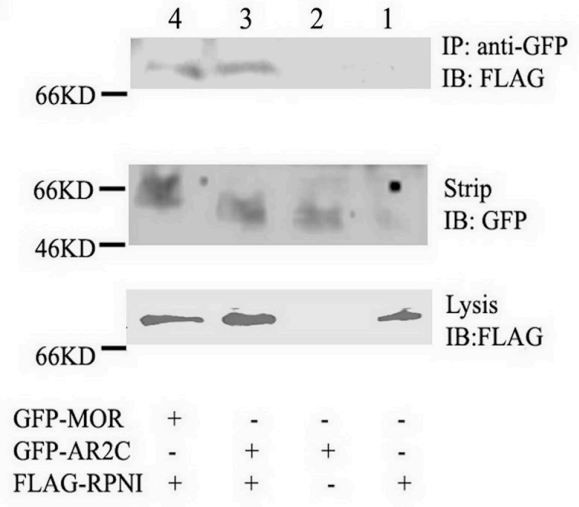

Fig 1.5B. N2A cells were transfected either with empty vector and FLAG-RPNI (lane 1), with empty vector and GFP- 2CAR (lane 2), with FLAG-RPNI and GFP-tagged 2C-AR (lane 3), or with FLAG-RPNI and GFP-tagged R (lane 4) as positive control

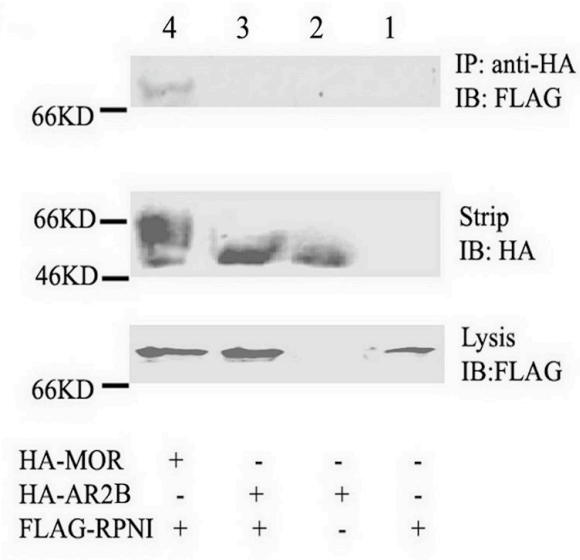

Fig 1.5C. N2A cells were transfected either with empty vector and FLAG-RPNI(lane 1), with empty vector and HA- 2BAR(lane 2), with FLAG-RPNI and HA-tagged 2B-AR(lane 3), or with FLAG-RPNI and HA-tagged R (lane 4) as positive control.

Despite the highly conserved motifs of them (59), our data suggested that there might not be specific binding motif for RPNI. N-glycosylation plays an important role in RPNI interaction with GPCR.

RPNI enhances cell surface expression of the C2 mutant, but not the 5 N-glycosylation mutant

Previous studies indicated that the export of MOR could be facilitated by a chemical chaperone such as naloxone (60). In particular, naloxone could rescue an export-deficient MOR mutant lacking a motif at the proximal carboxyl tail ^{344}KFCTR^{348} (C2). Colocalization of C2 and MOR in ER has been reported (61). The C2 mutant

receptor had similar glycosylation state as the wild type receptor (Fig 1.9A), which gel-overlay studies indicated it could interact with RPNI directly (Fig 1.8C, panel a).

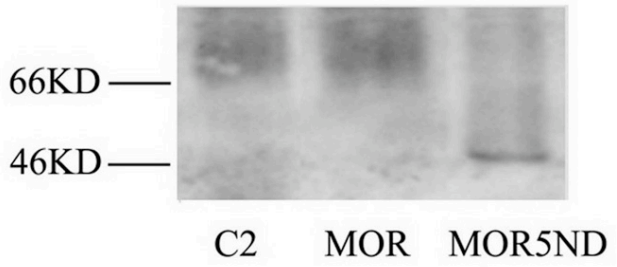

Fig 1.9A. Western-blot to detect receptor glycosylation state from N2A extract of cells expressing MOR C2 mutant, MOR, MOR5ND mutant.

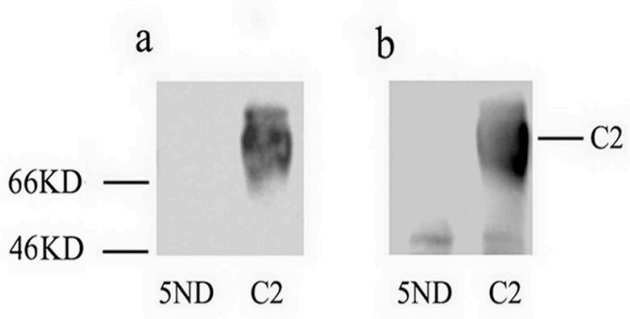

Fig 1.8C. Gel-overlay of in vitro translated FLAG-RPNI with MOR C2 mutant or MOR5ND mutant. Panel a: Gel-overlay of FLAG-RPNI on membranes containing SDS-PAGE separated N2A extract from cells expressing MOR C2 mutant or MOR5ND mutant; panel b: Western analysis used to detect different glycosylated forms of MOR C2 and MOR5ND mutants using anti-MOR C tail polyclonal antibody.

Whether RPNI could increase the export of the C2 mutant was examined with confocal microscopy using anti-HA conjugated with Alexa^{488} to detect the receptor location and goat anti-mouse antibody conjugated with Alexa^{594} to detect the FLAG-RPNI. As shown in Fig 1.10A, cell surface expression of C2 mutant was observed only in N2A cells expressing both C2 mutant and RPNI. Meanwhile, in N2A cells without RPNI expression, i.e., cells exhibiting only the Alexa^{488} fluorescence, majority of the C2 mutant was detected intracellularly (Fig 1.10A, panel b). RPNI and naloxone appear to have similar mechanisms in regulating C2 mutant expression. Using FACS analyses to determine the cell surface C2 level, we could demonstrate that the cell surface expression of C2 was dependent on the amount of RPNI plasmid used to transfect the cells. The addition of 1 μM naloxone in cells expressing RPNI increased the amount of C2 on cell surface, but only at the lower RPNI plasmid concentration (Figure 1.10B). The level of C2 expressed on cell surface in the presence of naloxone and RPNI did not significantly exceed the level observed when naloxone alone was used to rescue the C2 export. The inability of naloxone to increase the cell surface expression of C2 in N2A cells over-expressed with RPNI could be the exhaustion of the intracellular located receptor export pools at the high level of RPNI. However, this did not appear to be the case since intracellular located C2 could be observed in N2A cells over-expressing RPNI (Figure 1.10A). These data suggest that RPNI may have chaperone activities similar to that observed with the chemical chaperone naloxone.

Since RPNI was known to have oligosaccharyltransferase activity (62) and RPNI could not interact with MOR pretreated with EndoH or EndoF (Figure 1.8B), we

investigated whether the putative glycosylation residues, Asn at the N-terminal domain

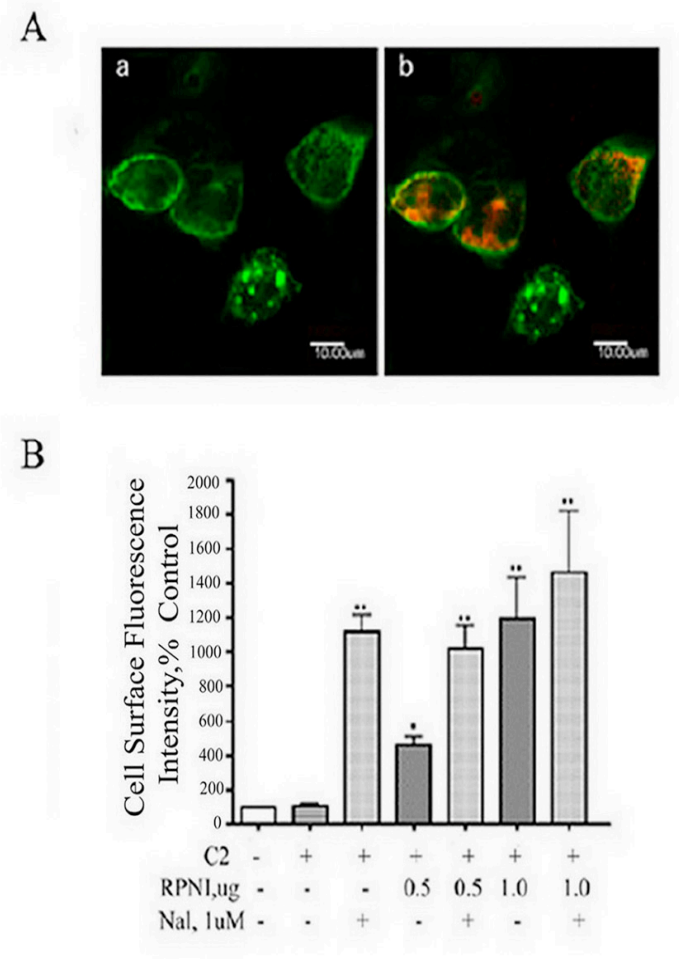

Fig 1.10 A&B. (A) RPNI up-regulate the cell surface expression of export deficient MOR C2 mutant. Panels a: WT N2A cells were cotransfected with HA-MOR C2 mutant and FLAG-RPNI. C2 mutant expression was detected by rabbit anti-HA antibody conjugated with Alexa 488; panels b: merge of MOR C2 mutant and FLAG-RPNI that was determined by staining with mouse anti-FLAG monoclonal antibody and detected with goat anti-mouse antibodies conjugated with Alexa 594; Scale bar equals 10 µ. (B) FACS analyses of C2 cell surface expression in the presence of naloxone and over-expression of RPNI. N2A cells were transiently transfected with vector or 0.5 µg RPNI or 1 µg RPNI and MOR C2 mutant. The bars represent averages ± SEM of immunofluorescence in cells treated and not treated with 1 µM naloxone after transfection in n=3 experiments.

of MOR, had roles in RPNI export function. The putative glycosylation sites in MOR (Asn^{9}, Asn^{31}, Asn^{38}, Asn^{46} and Asn^{53}) were all mutated to Asp (MOR5ND). MOR5ND transiently transfected into N2A cells was observed to be retained at the ER (Fig 1.9B).

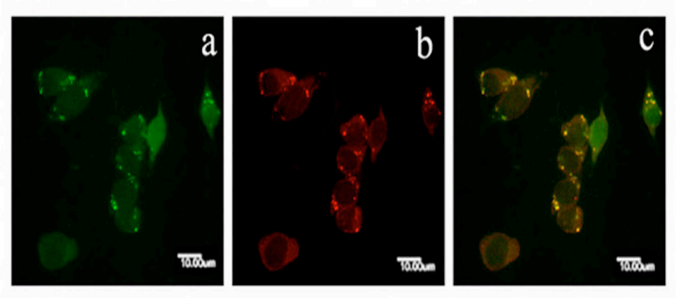

Fig 1.9B. Colocalization of MOR5ND and ER marker-calnexin. In panel (a), N2A cells expressing (His)6-MOR5ND were determined by staining with rabbit anti-(His)6 antibodies and visualized with anti-rabbit antibodies conjugated with Alexa Fluor 488; In panel (b), endogenous ER marker-calnexin protein in N2A cells were determined by staining with mouse anti-calnexin antibodies and visualized with anti-mouse antibodies conjugated with Alexa Fluor 594;in panel (c), the merged image of panel (a)and panel (b). The arrows in the merged image indicate the presence of MOR with ER. Scale bar represents 10 μ.

Similar to the mobility of the PNGase F pretreated MOR, MOR5ND in SDS-PAGE exhibited an apparent MW of ~46KDa (Figure 1.9A). Also, gel-overlay studies indicated that MOR5ND, similar to MOR pretreated with EndoH or PNGase F, was unable to interact with RPNI (Figure 1.8C, panel a). When the cellular location of the receptor was monitored by confocal microscopy, MOR5ND was observed as intracellular location despite over-expression of RPNI (Figure 1.10C). Majority of the

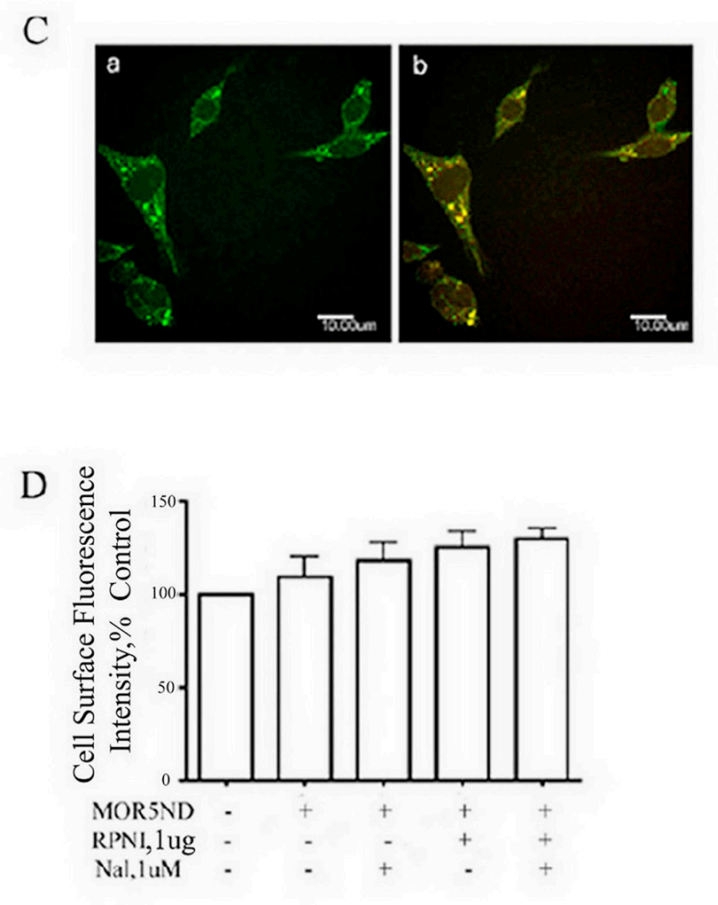

Fig1.10C&D. (C) RPNI failed to regulate the export of 5 N-glycosylation-site mutants of MOR (MOR5ND). Panels a: WT N2A cells were cotransfected with (His)6-MOR-5ND mutant and FLAG-RPNI. MOR5ND mutant expression was detected by rabbit anti-(His)6 antibody conjugated with Alexa 488; panels b: merge of MOR5ND mutant and FLAG-RPNI that was determined by staining with mouse anti-FLAG monoclonal antibody and detected with goat anti-mouse antibodies conjugated with Alexa 594; Scale bar equals 10 μ. (D) Inability of RPNI or naloxone to rescue cell surface expression of MOR5ND as determined by FACS analyses. The bars represent the averages ± SEM of 3 separate experiments carried out in triplicate.

receptor immunofluorescence was detected intracellular in regardless of RPNI level (Figure 1.10C, panel b). Similarly, FACS analyses of the MOR5ND receptor mutant demonstrated minimal cell surface expression. Over-expression of RPNI resulted in slight, but not significant change in cell surface MOR5ND mutant receptor immunofluorescence. Interestingly, addition of naloxone did not result in an increase in cell surface expression of MOR5ND receptor mutant either, regardless of the presence or absence of RPNI over-expression (Fig 1.10D).

To determine whether chaperone function of RPNI is dependent on N-glycosylation, single mutation mutants in each of the 5 putative glycosylation Asn sites of MOR were generated. As shown in Fig 1.11B, all 5 single glycosylation site mutants exhibited a slightly faster mobility in SDS-PAGE, indicative of a smaller molecular weight protein species than wild type MOR. In some regards, their molecular weights are similar to that of MOR pretreated with EndoH (Fig 1.8A). Interestingly, in contrast to the wild type MOR, all the single glycosylation site mutants could not pull down the FLAG-RPNI (Fig 1.11A). Hence, RPNI should have minimal consequence on these mutants' intracellular trafficking. When the cell surface expression of these mutants was determined by FACS analyses, it was shown that RPNI could not regulate the plasma membrane insertion of these mutants (Fig 1.12B). Although variable degrees of cell surface expression of the mutant receptors were observed (Fig 1.12A), co-expression of RPNI with any one of the five mutants did not increase these mutant receptors export to the cell surface. Such data suggest RPNI's interaction with MOR and subsequent chaperone function requires full N-glycosylation of the receptor.

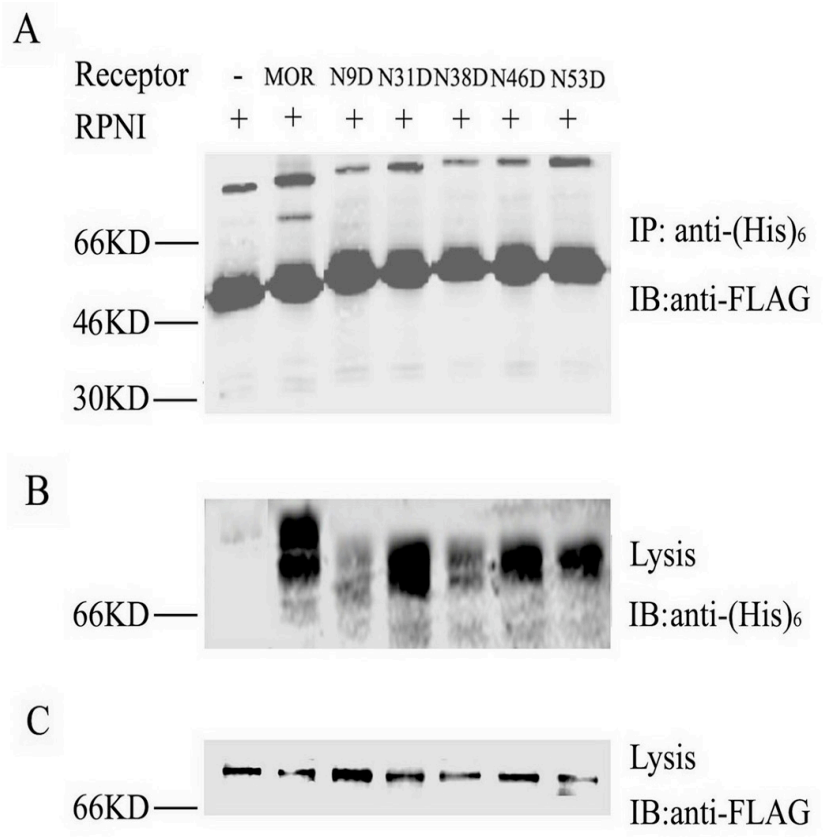

Fig 1.11. N2A cells were transfected FLAG-RPNI with (His)6-tagged vector, (His)6-MOR, and (His)6-tagged MOR single glycosylation-site mutant (i.e. N9D, N31D, N38D, N46D, N53D). IP and western analyses were carried out as described in Materials and Methods. In panel (A), RPNI was detected after (His)6-tagged vector, (His)6-MOR, and (His)6-tagged MOR single glycosylation-site mutant was immunoprecipitated from the cell lysate using anti-(His)6 antibody; In panel (B), glycosylation level of (His)6-tagged vector, (His)6-MOR, and (His)6-tagged MOR single glycosylation-site mutant was detected by rabbit anti-(His)6 antibody in 1/20 of total lysate used in IP experiments; In panel (C), expression level of FLAG-RPNI was determined in 1/20 of total lysate used in IP experiments.

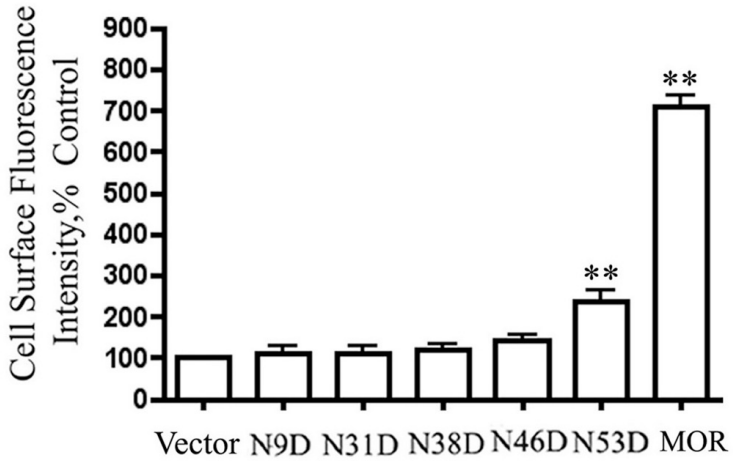

Fig 1.12A. N2A cells were transiently transfected either with MOR mutant or MOR for 48 hours before cell surface receptor levels were determined by FACS analyses, as described in Materials and Methods. The bars represent the averages ± SEM of 3 separate experiments carried out in triplicate

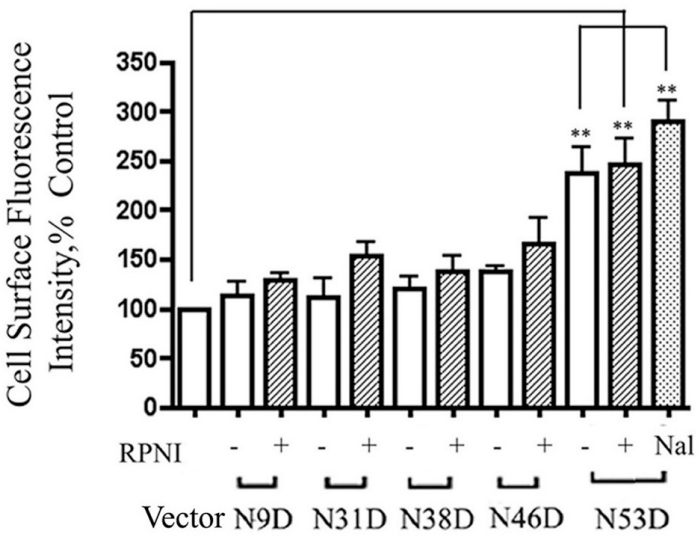

Fig 1.12B. N2A cells were transiently transfected either with MOR mutant and vector, or MOR mutant and 1 μg RPNI for 48 hours before cell surface receptor levels were determined by FACS analyses, as described in Materials and Methods. The bars represent the averages ± S.E.M. in 3 separated experiments carried out in triplicate in the absence and presence of RPNI overexpression or treatment with 1 naloxone respectively, ** p denotes < 0.01 when compared with cells transfected with vector.

RPNI rescues C2 without increasing the mutant receptor interaction with calnexin The transit of proteins from ER is determined by its interaction with calnexin. Pharmacological chaperones were reported to rescue some GPCR mutants by altering their interaction with calnexin (63). It is probable that RPNI-enhanced cell surface expression of MOR is a reflection of the receptor interaction with calnexin. Hence, the export deficient mutant C2 was used to examine whether RPNI could increase C2 glycosylation level and subsequent calnexin binding. MOR and the C2 mutant were immunoprecipitated from N2A cells transfected either with HA-MOR and vector (Fig 1.13A, lane 1), with HA-C2 and RPNI (Fig 1.13A, lane 2), with HA-C2 and vector treated with naloxone (Fig 1.13A, lane 3), with HA-C2 and vector treated with the proteosome inhibitor MG132 (Fig 1.13A, lane 4), or with HA-C2 and

vector treated with saline (Fig 1.13A, lane 5). The relative C2 receptor level was determined using HA-MOR as the reference. The increase in the total cellular level of C2 in N2A cells over-expressed RPNI was similar to those observed in cells treated with naloxone or proteosome inhibitor MG132 (Fig 1.13B). However, FACS analysis showed that overexpression of RPNI, like addition of naloxone(60), increased the total C2 cell surface level while MG132 did not (Fig 1.13C). Also, in contrast to wild type MOR, in which strong interaction with calnexin was detected in the immunoprecipitate (Fig 1.13A lane 1 and Fig 1.13D), C2 did not exhibit strong interaction with calnexin (Fig 1.13A lane 2-5 and Fig 1.13D). Over-expression of RPNI or pretreatment with naloxone did not increase the receptor-calnexin interaction. These data suggest that the RPNI chaperone function, similar to that of naloxone, is not due to an increase in calnexin binding to MOR.

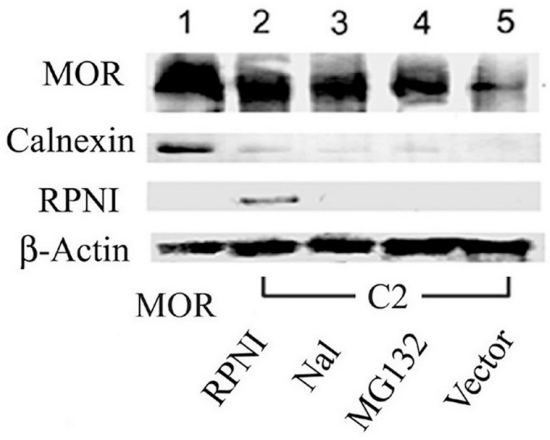

Fig 1.13A. N2A cells were transfected either with HA-MOR and vector (panel A, lane 1), with HA-C2 mutant and FLAG-RPNI (panel A, lane 2), with HA-C2 mutant and vector treated with naloxone (panel A, lane 3), with HA-C2 mutant and vector treated with 10 μM MG132 16 hours prior to harvesting (panel A, lane 4), or with HA-C2 mutant and vector (panel A, lane 5). Immunopreciptation and western analyses were carried out as described in Materials and Methods.

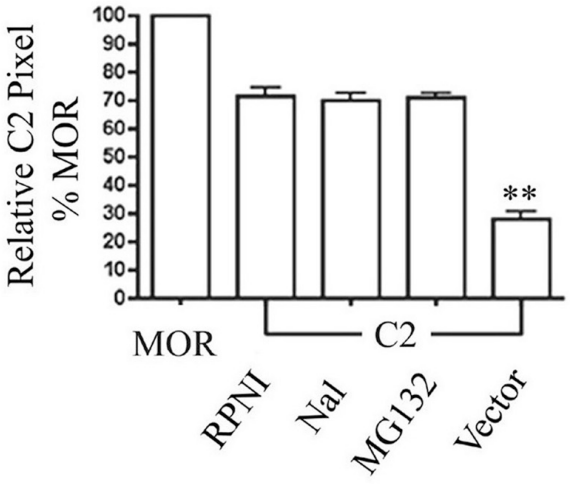

Fig 1.13B. Relative intensities of C2 mutant levels using HA-MOR as a reference, and the amount of ß-actin immunoactivities in each lane was used for loading control. The bars represent the average ± SEM of 3 separate experiments.

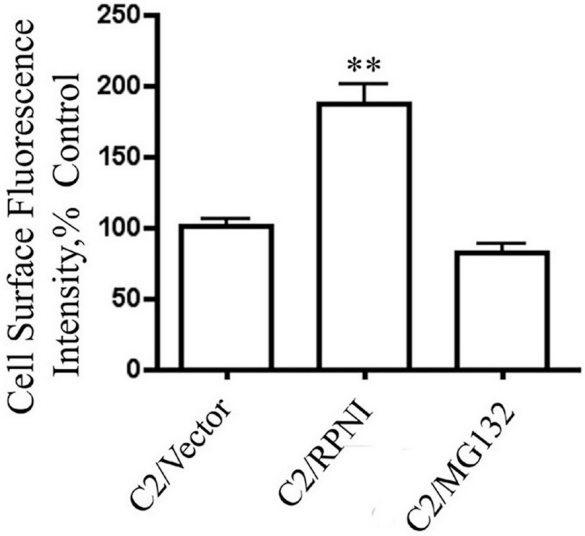

Fig 1.13C. FACS analyses of cell surface MOR C2 mutant after overexpression of RPNI, or the addition of MG132.

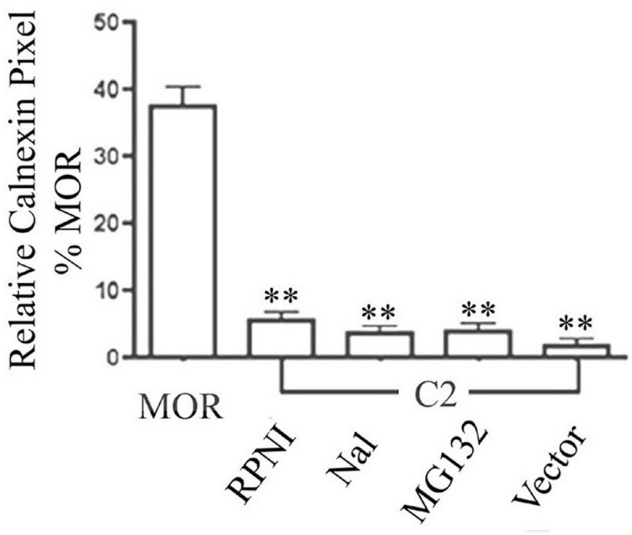

Fig 1.13D. relative intensities of calnexin co-IP with HA-MOR using HA-MOR immunoreactivity as a reference, and ß-actin immunoactivities in each lane were used for loading control. The bars represent the average ± SEM of 3 separate experiments.

RPNI interacts with DOR and KOR and enhances their export

Since RPNI was shown to interact with other highly glycosylated GPCR such as AR1ąand a2C- but not a2B-AṚ(Figure 1.5), whether RPNI could interact with δ-opioid receptor (DOR) or κ-opioid receptor (KOR) and had similar effect in these receptors' export was investigated. Coimmunoprecipitation studies were performed in lysate from N2A cells transiently transfected with HA-DOR or HA-KOR, together with either FLAG-RPNI or vector control. Similar to our observations with MOR, RPNI was observed to co-IP with DOR and KOR (Fig 1.14A and 1.14C). RPNI was not co-immunoprecipitated with anti-HA when N2A cells were not transfected with the HA-DOR or HA-KOR. FACS analyses indicated that RPNI also could affect DOR or KOR export. Overexpression of RPNI significantly increased the DOR level

on the cell surface by 33.2±7.8% (Fig 1.14B), but did not significantly increase KOR cell surface expression (Fig 1.14D). In comparison, when N2A cells were transfected with RPNI siRNA, both DOR and KOR cell surface expression were significantly reduced by 38.1±3.9% and 22±4.4%, respectively.

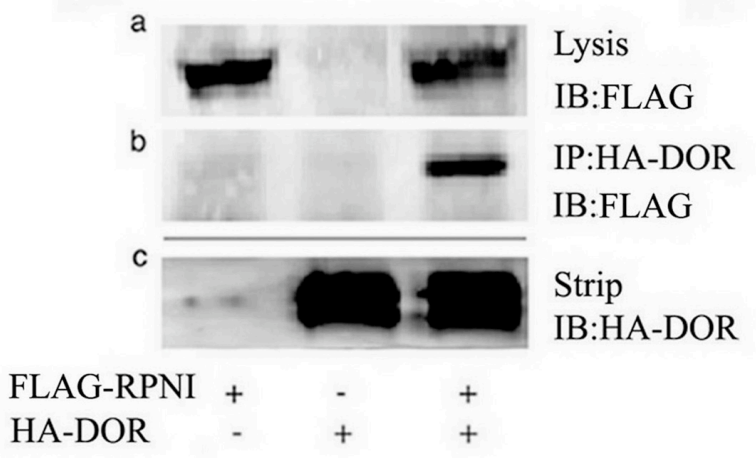

Fig 1.14A. Co-IP of RPNI with DOR. N2A cells were transiently transfected either with vector and HA-DOR, vector and FLAG-RPNI, or FLAG-RPNI and HA-DOR, as described in Materials and Methods. Panel a: RPNI expression was detected with mouse anti-FLAG antibody in 1/20 total cell lysates; panel b: RPNI was detected with rabbit anti-FLAG after HA-DOR was immunoprecipitated from the cell lysates using mouse anti-HA antibodies; panel c: the amount of HA-DOR immunoprecipitated and loaded on each lane was demonstrated after stripping the blots used to detect RPNI.

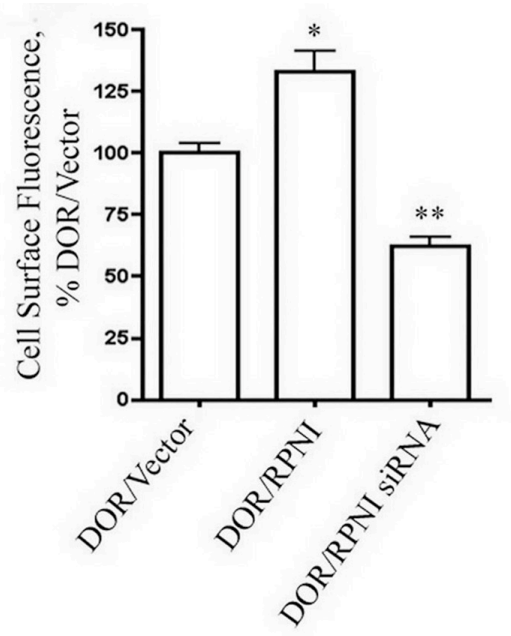

Fig 1.14B. Increase of DOR export by RPNI. N2A cells were transiently transfected either with HA-DOR and vector, HA-DOR and RPNI, or HA -DOR and RPNI siRNA for 48 hours before cell surface receptor levels were determined by FACS analyses, as described in Materials and Methods. The bars represent the averages±S.E.M. of n=3 experiments carried out in triplicate. * p denotes < 0.05, ** p denotes < 0.01 when compared with cells transfected with vector.

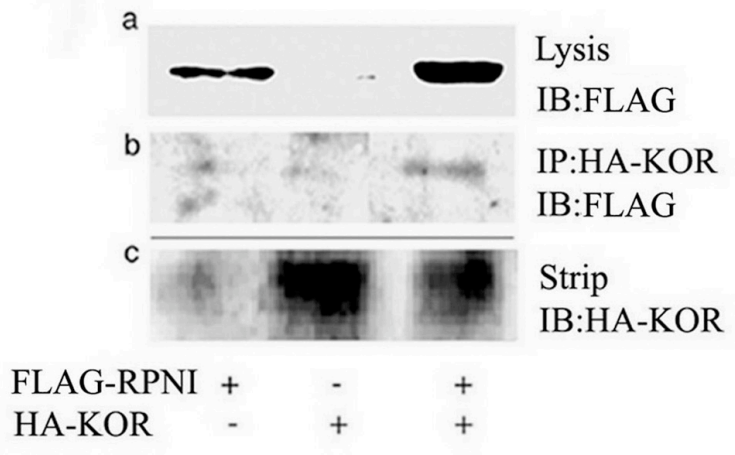

Fig 1.14C. Co-IP of RPNI with KOR. N2A cells were transfected either with vector and HA-KOR, vector and FLAG-RPNI, or FLAG-RPNI and HA-KOR, as described in Materials and Methods. Panel a: RPNI expression was detected with mouse anti-FLAG antibody in 1/20 total cell lysates; panel b: RPNI was detected with rabbit anti-FLAG after HA-KOR was immunopreciptated from the cell lysates using mouse anti-HA antibodies; panel c: the amount of HA-KOR immunoprecipitated and loaded on each lane was demonstrated after stripping the blots used to detect RPNI.

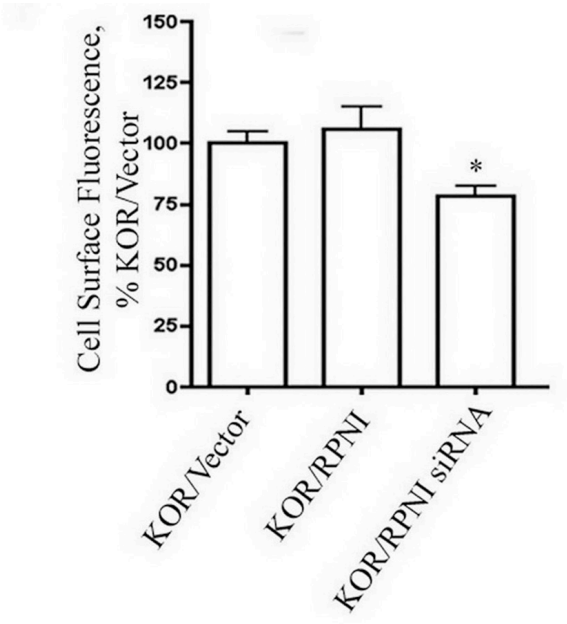

Fig 1.14D. Decrease in KOR export after RPNI knock-down. N2A cells were transiently transfected either with HA-KOR and vector, HA-KOR and FLAG- RPNI, or HA-KOR and RPNI siRNA for 48 hours before cell surface receptor levels were determined by FACS analyses, as described in Materials and Methods. The bars represent the averages±S.E.M. of n=3 experiments carried out in triplicate. * p denotes < 0.05 when compared with cells transfected with vector.

Chapter 2:

Identification of GRIN1 Binding to MOR

In order to identify components of MOR signaling complexes, $(His)_6$-MOR stably expressed in N2A cells were partially purified with a Ni^{2+} resin column as described in previously published paper (64). Eluted samples containing MOR complexes were denatured by SDS-PAGE sample buffer at 65°C for 30 minutes. Silver-staining of the gels revealed multiple protein bands including $(His)_6$-MOR, which migrated as a diffusive band with molecular weight between 65-70 KDa. The consistency in protein isolation can be demonstrated in the silver-staining results from three different experiments(64). These silver-stained bands were demonstrated to be proteins associated with $(His)_6$-MOR by their absence in Ni^{2+} resin eluates of N2A wild type cells. The identity of MOR was further confirmed by parallel Western-blot analysis, using anti-MOR carboxyl tail polyclonal antibody (64,65). The protein band around 110 KDa was identified as GRIN1 by MALDI-TOF spectrometry analysis, indicating that GRIN1 was in the purified MOR complex. Equivalent protein candidates reported were gi|5901688, gi|5901688. They all refer to the sequence of GRIN1 (Fig 1.1A).

The specific interaction between MOR and GRIN1 can be demonstrated with the co-immunoprecipitation experiments. In order to eliminate protein interaction after disruption of cellular boundaries during extraction, cells expressing either FLAG-MOR or HA-GRIN1 were mixed together immediately prior to detergent addition. Contrary to cells cotransfected with both FLAG-MOR and HA-GRIN1 (Fig 2.1A, lane 4), mixed cells transfected with either MOR or GRIN1 alone did not co-immunoprecipitate together (Fig 2.1A, lane 3). Furthermore, GRIN1 interaction with

MOR appears to be affected by agonist treatment. When the N2A cells

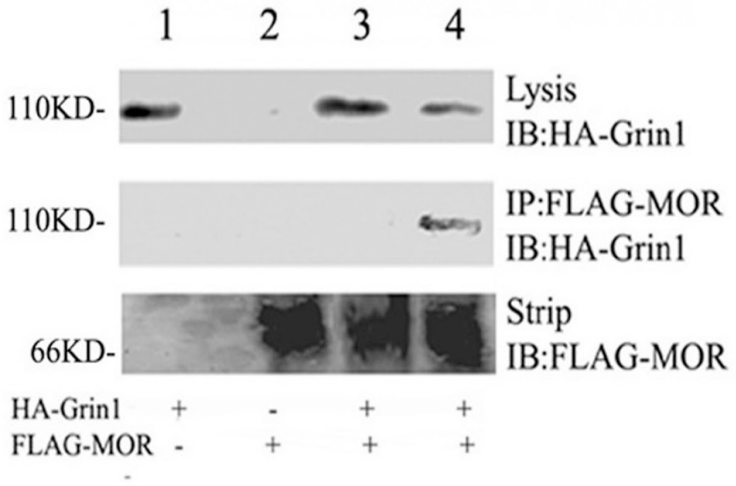

Fig 2.1A. Coimmunoprecipitation of FLAG-MOR and HA-GRIN1 in cells only express HA-GRIN1 (lane 1); in cells only express FLAG-MOR (lane 2); in mixed cells that individually express FLAG-MOR and HA-GRIN1 (lane 3); and in cells that express both FLAG-MOR and HA-GRIN1 (lane 4).

transiently transfected with HA-GRIN1 and FLAG-MOR were treated with 100 nM etorphine for 10 min, a reduction in the amount of GRIN1 co-immunoprecipitated by MOR was observed (Fig 2.1B). Quantitation of the band indicated around 60±10.8% reduction in GRIN1-MOR co-immunoprecipitated (Fig 2.1B). Western analyses of HA-GRIN1 in the total lysate and amount of FLAG-MOR immunoprecipitated indicated the observed reduction was not due to the differences in these two protein levels in the control and etorphine treated cells.

Since the observed GRIN1-MOR interaction was demonstrated with the heterologous expression system N2A cells, in order to demonstrate whether GRIN1 interacts with MOR endogenously, mouse hippocampi were used subsequently. MOR from mouse hippocampus tissue was immunoprecipitated with the anti-MOR C-tail polyclonal antibodies (65). Mouse cerebellum was used as the negative control to

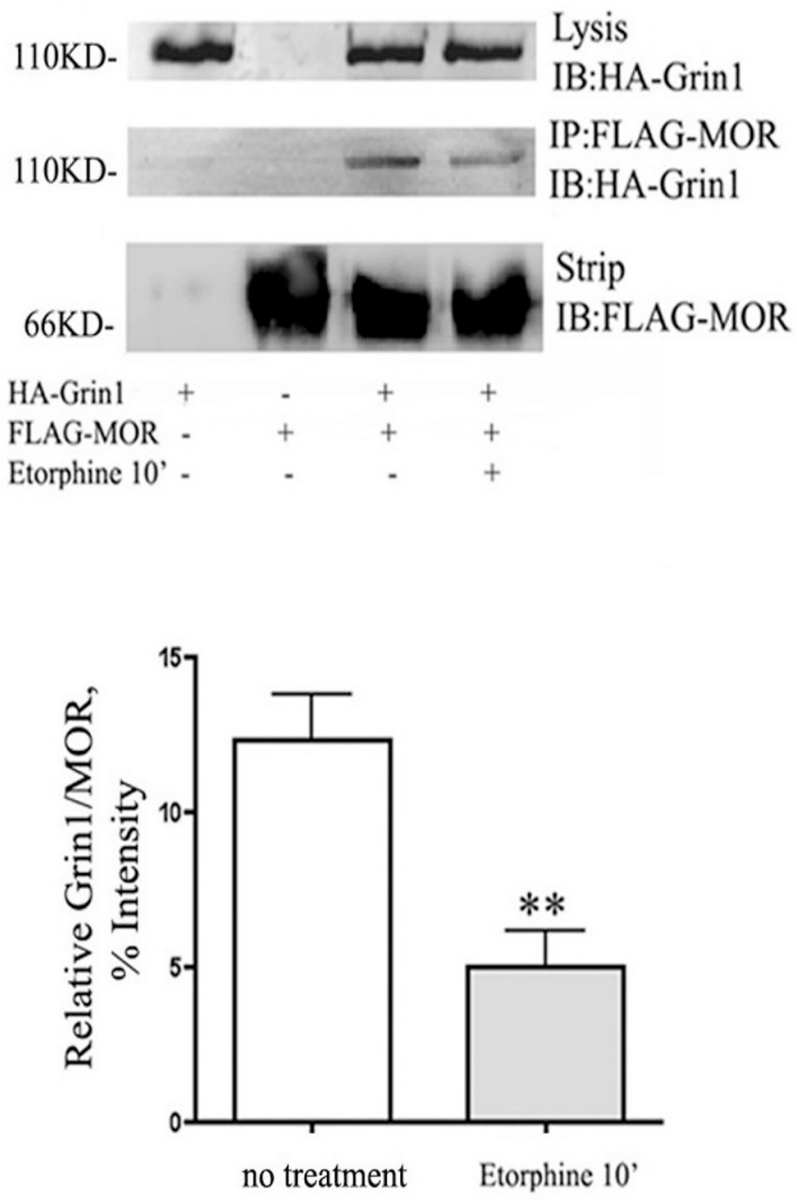

Fig 2.1B. Effect of 100 nM etorphine on the co-immunoprecipitation of GRIN1 with MOR in cells overexpressed with both HA-GRIN1 and FLAG-MOR.

determine the specificity of the antibodies used. As shown in Fig 2.1D, MOR C-tail antibodies could immunoprecipitate the endogenous GRIN1 from hippocampus. Proteins with molecular weight similar to GRIN1 were not observed with the MOR C-tail antibodies immunoprecipitates of the cerebellum extracts with or without PTX pretreatment, which indicated GRIN1 bound to MOR endogenously regardless of G protein (Fig 2.1C).

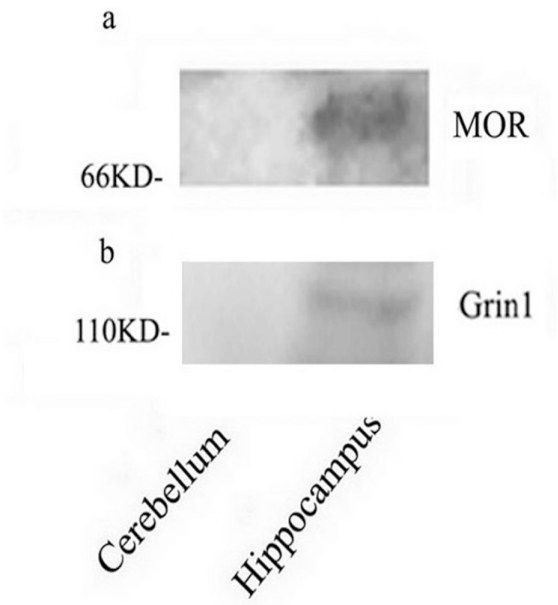

Fig 2.1C. Co-immunoprecipitation of GRIN1 with MOR in mouse brain region with no endogenous MOR expression (cerebellum) or with high endogenous MOR expression (hippocampus). Endogenous MOR was determined by rabbit anti-MOR C-tail antibody (panel a) and GRIN1 was detected by anti-GRIN1 (T116) antibody (panel b).

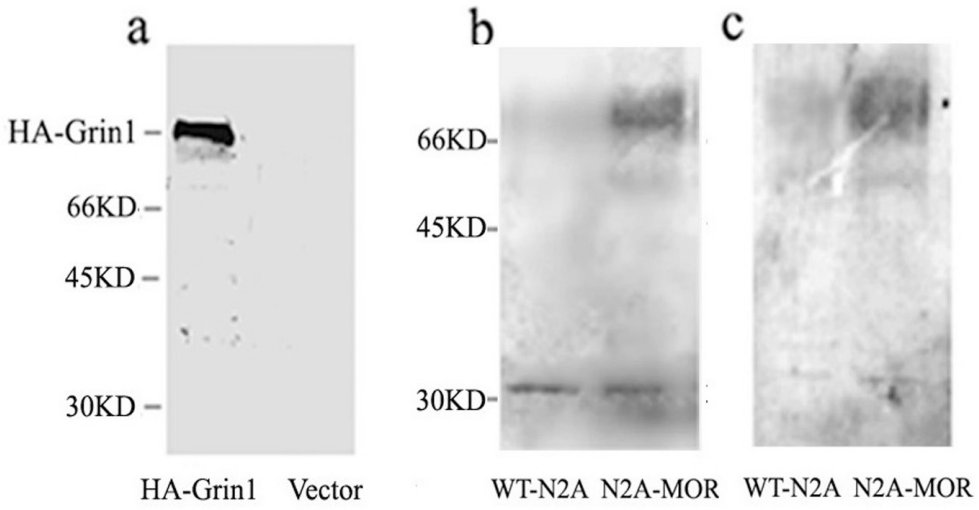

Fig 2.1D. Gel-overlay of HA-GRIN1with N2A-MOR. Panel a: in vitro translation products of HA-GRIN1, as detected by anti-HA antibody; panel b: Gel-overlay of HA-GRIN1 on membranes containing SDS-PAGE separated N2A extract from cells expressing or not expressing MOR; panel c: same blot was stripped and MOR expression was detected using anti-MOR C tail antibody.

Since GRIN1 has been shown to interact with Gα (50), the co-immunoprecipitation of GRIN1 with the receptor antibodies or receptor epitope antibodies could be the result of receptor-G protein interaction. To further determine whether GRIN1 directly interacts with MOR or not, gel-overlay experiments were performed. *In vitro* translation products of GRIN1 was shown as in Fig 2.1D, panel a. The total lysate of N2A cells expressing FLAG-MOR was first separated with SDS-PAGE and transferred to Immobibon-P membrane. Then, the membrane was incubated with the *in vitro* translation products of GRIN1 construct, which molecular weight was around 85 KDa, probably due to the absence of post-translational modification. After excess *in vitro* translated product was removed by repeated washings, GRIN1 positive band was observed in lane containing lysate from MOR-expressed N2A cells, but not in lane from wild type N2A cells (Fig 2.1D, panel b). The location of the *in vitro* translated HA-GRIN1 product coincided with the location

of FLAG-MOR, as determined by parallel experiment of western-blot using anti-FLAG antibody (Fig 2.1D, panel c). These data indicated that GRIN1 directly interacted with MOR. Another GRIN1 positive band was also observed in both wide type N2A cells and MOR-expressed N2A cells, which is around 30 KDa and confirmed to be endogenous Giα subunit by western analysis using anti-Giα antibody (data not shown).

GRIN1 directly interacted with the MOR third intracellular loop

Next, we examined the MOR sequence involved in the binding to GRIN1 by using GST-fusion protein pull-down approaches. Because of the intracellular location of GRIN1, only the putative intracellular domains of MOR were used in the pull-down studies. GST or GST-MOR 2nd, GST-MOR 3rd intracellular loop and GST-MOR C-tail fusion proteins (see Table 2.1 for specified amino acid sequences) were expressed in *E. coli* and purified. To avoid the influence of G protein interaction, the *in vitro* translation GRIN1 product was used instead of total cell lysates, in the GST-fusion protein pull-down experiments. As shown in Fig 2.2A, the GST-MOR 3rd intracellular loop bound GRIN1 *in vitro* translation product to a much greater extent than GST-MOR 2nd intracellular loop and GST-MOR C-tail fusion protein, which showed similar binding as GST alone. These results indicate that GRIN1 interacts directly with the GST-MOR 3rd intracellular loop but not with the GST-MOR 2nd intracellular loop or the GST-MOR C-tail. To explore which domain in the 3rd intracellular loop is critical for binding GRIN1, co-immunoprecipitation experiment was performed with the 3rd loop deletion mutants.

Table 2.1 Amino acid sequence of GST- fusion protein

GST-fusion protein	***Amino acid sequence***
GST-MOR 2nd IL	GST-//- DRYIAVCHPVKALDFRTPR
GST-MOR 3rd IL	GST-//- LMILRLKSVRMLSGSKEKDRNLRRITR
GST-MOR C tail	GST-//- DENFKRCFREFCIPTSSTIEQQNSSR VRQNTREHPSTANTVDRTNHQLENLEAETAPLP

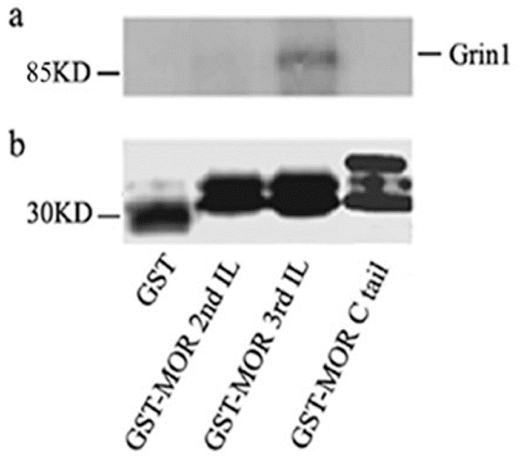

Fig 2.2A MOR 3rd intracellular loop is involved in direct interaction with GRIN1- (A) GST-MOR 3rd intracellular loop bound GRIN1. Panel a: in vitro translation product of GRIN1 binding to GST, GST-MOR 2nd intracellular loop, GST-MOR 3rd intracellular loop or GST-MOR C-tail fusion protein; Panel b: Expression level of respective fusion proteins as determined with commassiee blue staining.

Five amino acids in the 3rd intracellular loop were systematically deleted to generate the 3rd loop deletion mutants as described previously (66). The sequences that were deleted in the mutants were summarized in Fig 2.2B. Interestingly, GRIN1 could still bind to the ^{267}GSKEK^{271} (i3-3) within the 3rd intracellular loop completely abolished the GRIN1 and

	TM5	(Third intracellular loop)	TM6
WT	MLL	RLKSVRMLSGSKEKDRNLRRITR	MVL
i31	MLL	----------RMLSGSKEKDRNLRRITR	MVL
i32	MLL	RLKSV-------SGSKEKDRNLRRITR	MVL
i33	MLL	RLKSVRMLS----------DRNLRRITR	MVL
i34	MLL	RLKSVRMLSGSKEK---------RRITR	MVL
i35	MLL	RLKSVRMLSGSKEKDRNL----------	MVL

Fig2.2B Amino acid sequences of MOR 3rd intracellular loop, and the corresponding sequences of MORi3-1, MORi3-2, MORi3-3, MORi3-4, and MORi3-5 mutants.

MOR interaction. Among those mutants, domain i3-5 was determined to be pivotal for MOR/ G protein interaction (66). Although GRIN1 has been reported to interact with $G\alpha_{i/o}$ directly (50), these data also suggest that GRIN1 directly binds to MOR regardless of whether the receptor can interact with the G protein. Since GST-Il3 pulled down GRIN1 in vitro translation product (Fig 2.2A), it indicated that GST tagged MOR binding motif still possessed the characteristics for directly binding to GRIN1 in vitro translation product. To further confirm the deleted sequence ^{267}GSKEK^{271} is pivotal for directly binding to GRIN1, gel-overlay experiment using the premixing of in vitro translation product of GRIN1 and GST-MORi33 or GST-MORi35 was performed as described in Experimental Procedures. As shown in

Fig2.2E, there was no difference between gel-overlay with in vitro translation product of GRIN1 and with the premixing of in vitro translation product of GRIN1 and GST-MORi33, which implicated GST-MORi33 could not occupy the binding site of GRIN1 for MOR. In contrast, GST-MORi35 blocked GRIN1 direct interaction with MOR, which demonstrated that GST-MORi35 interacted with GRIN1 in the premixing and led to attenuation of the direct interaction between in vitro translation product of GRIN1 and MOR.

C

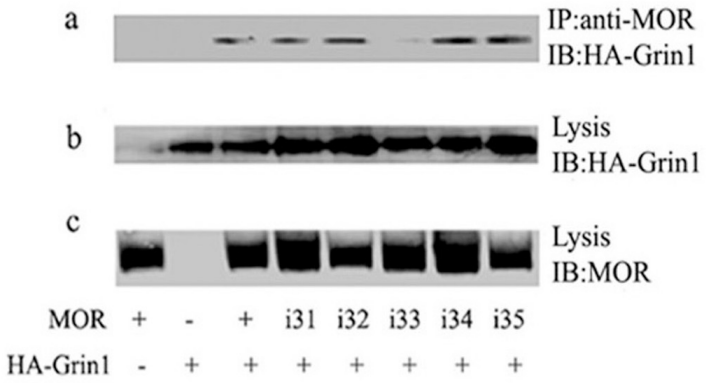

D

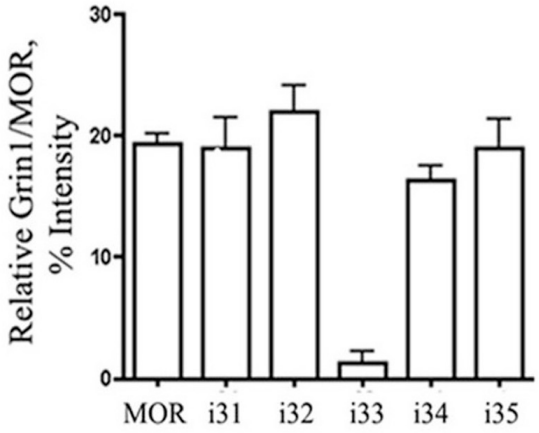

Fig 2C&D (C) Co-immunoprecipitation of GRIN1 with different MOR 3rd intracellular loop mutant. Panel a: GRIN1 was detected with anti-HA in the co-immunoprecipitates; panel b: the expression level of HA-GRIN1 in 1/20 of the total lysates used in IP experiments; panel c: the amount of MOR in the immunoprecipitates detected with anti-MOR C-tail antibodies after the blots were stripped (D) Quan -tification and statistic analysis of the relative percentage of immunoprecipitated GRIN1 vs MOR or each MOR 3rd intracellular loop mutants.

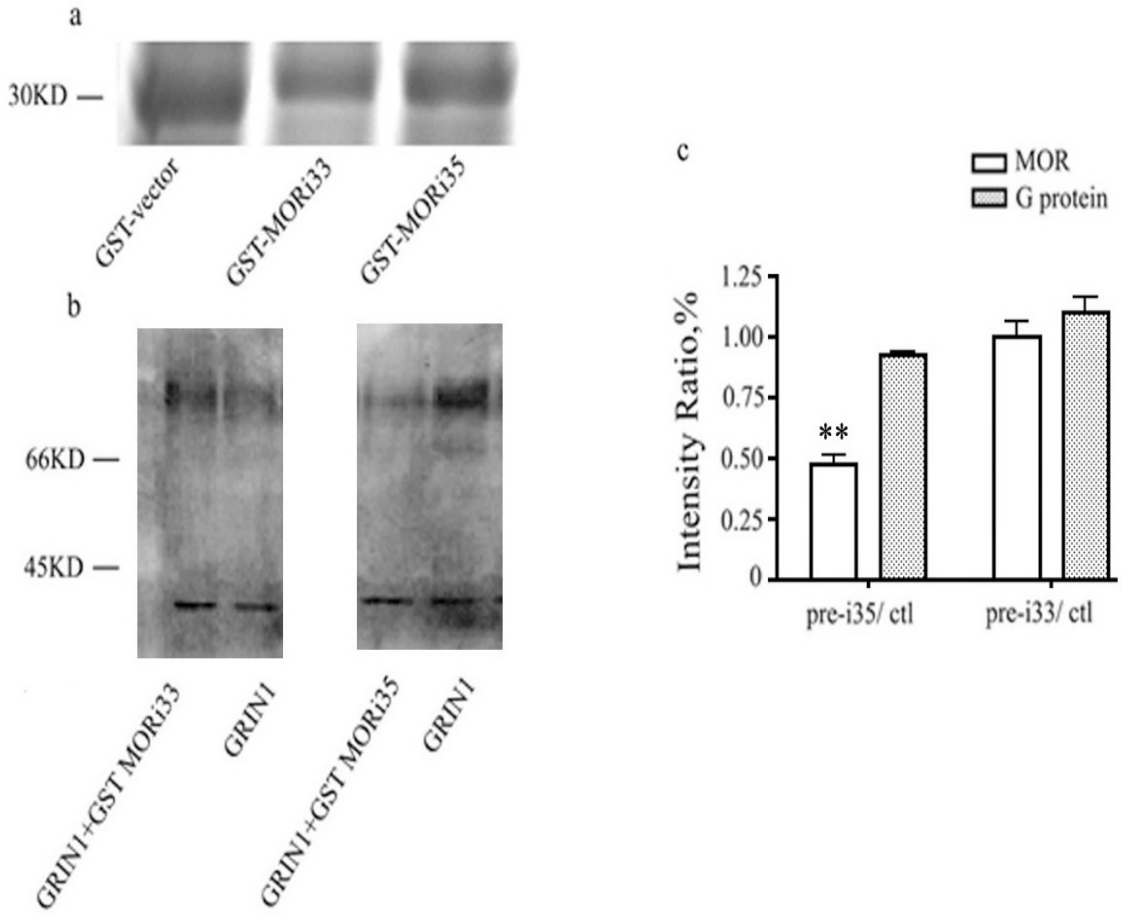

Fig 2.2E Gel-overlay of HA-GRIN1 or pre-combination of HA-GRIN1/GST-i33 or HA-GRIN1/GST-i35 with N2A-MOR. Panel a: Expression level of GST-i33 or GST-i35 fusion proteins as determined by commassiee blue staining; panel b: Gel -overlay of HA-GRIN1 or pre-combination of HA-GRIN1/GST-i33 or HA-GRIN1/GST-i35 on membranes containing SDS -PAGE separated N2A extract from cells expressing MOR; panel c: Quantification and statistic analysis of the relative percentage of MOR vs G protein. Quantification results expressed as percentage of GRIN1-overlayed control values, represented as mean ± S.E.M. *, $P < 0.05$.

GRIN1 serves as a tether for MOR and Gα_i

It has been reported that GRIN1 can bind to activated G$\alpha_{i,}$, Gα_o, and Gα_z(50). To illustrate which subtype of Gα is associated with GRIN1 when MOR is activated, adenovirus was used to over-express PTX-resistant subtypes of Gα in N2A cells

($G\alpha_{i2}$, $G\alpha_{i3}$, and $G\alpha_{o}$) and PTX was employed to suppress the receptor-mediated activation of the endogenous Gα proteins, then each Gα was pulled down under the conditions with or without etorphine as described in Materials and Methods. $G\alpha_{i2}$ was found to bind GRIN1 when MOR was activated by etorphine (Fig 2.3). There was 54.5±8.9% increase in the amount of HA-GRIN1 immunoprecipitated by the $G\alpha_{i2}$ antibodies in the presence of etorphine. The amount of HA-GRIN1 immunoprecipitated by the $G\alpha_{i3}$ or $G\alpha_{o}$ antibodies remained the same in the absence or presence of etorphine.

The association of GRIN1 with the MOR signaling complex could still be due to the protein interaction with $G\alpha$ subunits within the complex. In order to eliminate such possibility, a GRIN1(1-717) mutant that lacked G protein binding motif (51) was constructed. As expected, the full length GRIN1 could be co-immunoprecipitated with $G\alpha_{i2}$ (Fig 2.4A, lane 4) while the truncated mutant GRIN1(1-717) could not be co-immunoprecipitated with $G\alpha_{i2}$ (Fig 2.4A, lane 3). On the other hand, the truncated GRIN1(1-717) mutant could be co-immunoprecipitated by MOR only when both were co-transfected together (Fig 2.4B). Additionally, when MOR was uncoupled from $G\alpha_{i2}$ after pertussis toxin (PTX) pretreatment, the interaction between MOR and GRIN1 decreased significantly (Fig 2.4C&D). In contrast, PTX pretreatment did not perturb the $G\alpha_{i2}$–GRIN1 interaction. The amount of GRIN1 co-immunoprecipitated with the antibodies against $G\alpha_{i2}$ enhanced after PTX pretreatment (Fig 2.4E&F).

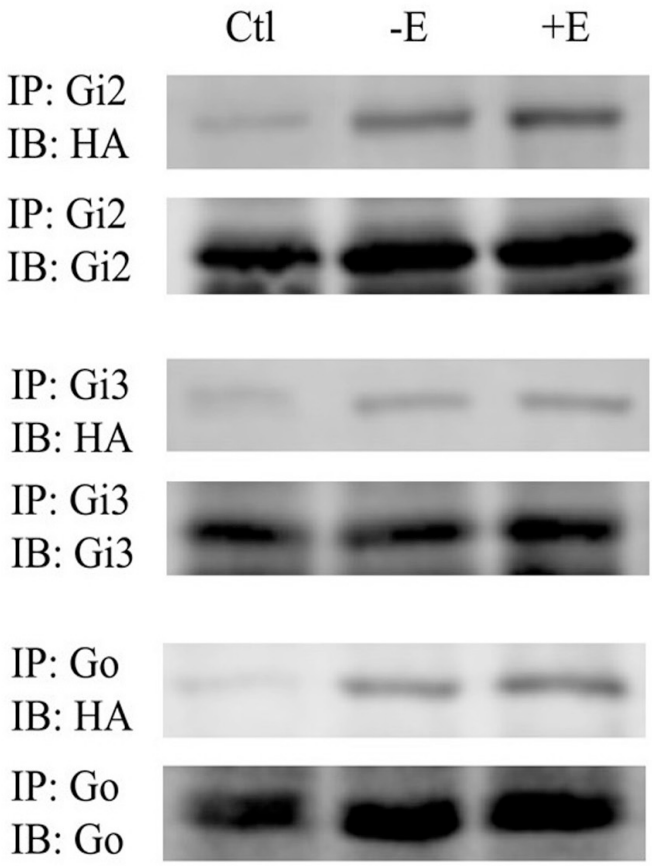

Fig 2.3A N2A cells stably-expressing MOR were infected with PTX-insensitive adeno-Gi 2-Leu, adeno-Gi 3-Leu, or adeno-Go -Leu viruses, transfected with HA-GRIN1 and treated with PTX to inactivate endogenous Gi/o proteins. After cells were treated with or without 100 nM Etorphine for 10 min, Gi 2 (upper two panels), Gi 3 (middle two panels) or Go (lower two panels) proteins were immnunoprecipitated (IP) by their corresponding antibodies and then the immunoprecipitate was blotted (IB) with anti-HA for HA-GRIN1 and with Gi 2, Gi 3, Go antibodies. The blots are representative of similar blots from three independent experiments. Ctl, control, where the cells were not infected with the adeno-viruses but were transfected with HA-GRIN1; –E, untreated control ; +E, treated with 100 nM etorphine for 10 min.

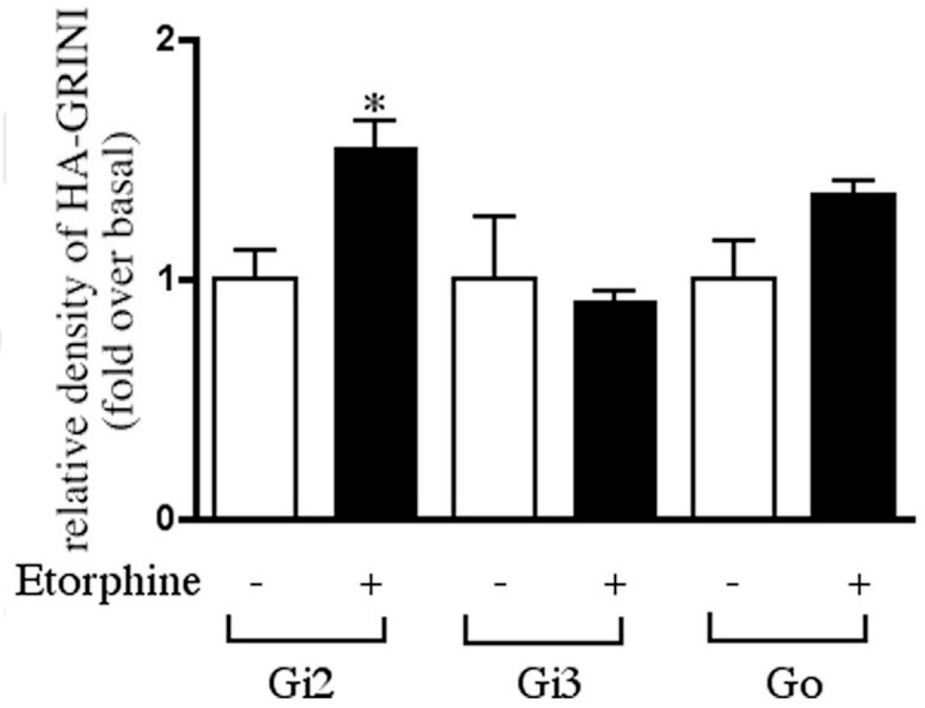

Fig 2.3B Quantification analysis of data in (A). The basal represents cells untreated with agonist. Data are means ± S.E.M. *, $P < 0.05$ versus the basal.

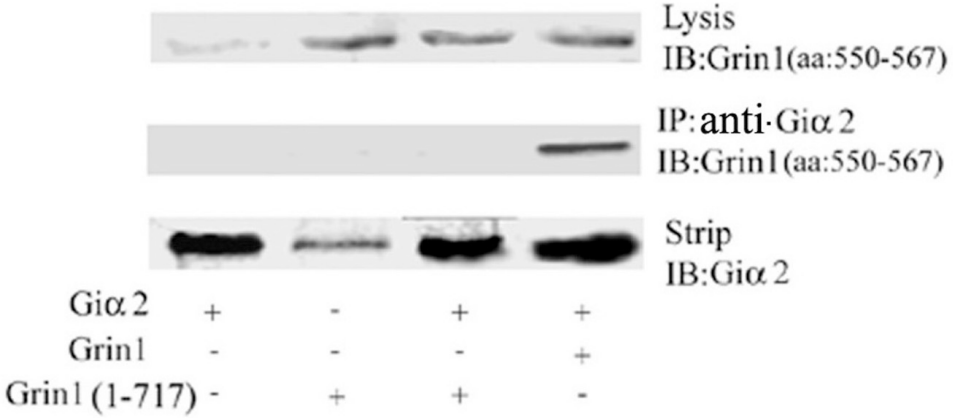

Fig 2.4A Co-IP of GRIN1 1-717 mutant with Gi 2.panel a: the expression level of HA-GRIN1 in 1/20 of the total lysates used in IP experiments;Panel b: GRIN1 was detected with anti-HA in the co-immunoprecipitates; panel c: the amount of Gi 2 in the immunoprecipitates detected with anti -Gi 2 antibodies after the blots were stripped.

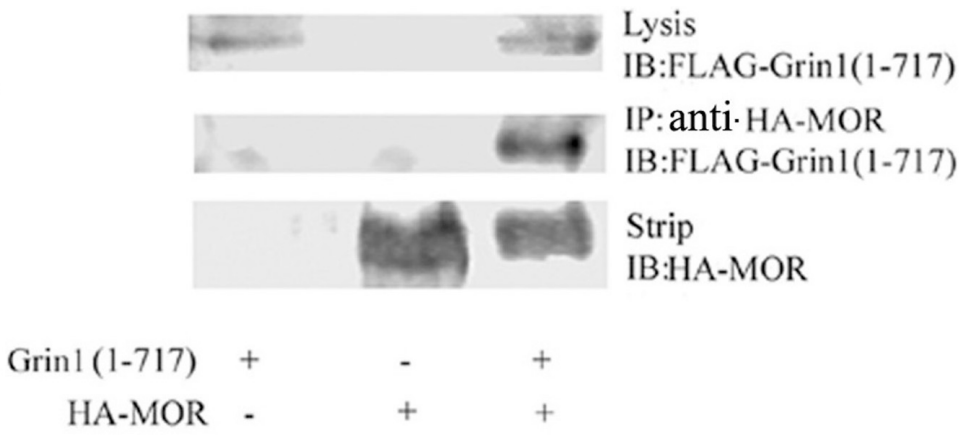

Fig 2.4B Co-IP of GRIN1 1-717 mutant with MOR. panel a: the expression level of FlAG-GRIN1 in 1/20 of the total lysates used in IP experiments;Panel b: GRIN1 was detected with anti-FLAG in the co-immunoprecipitates; panel c: the amount of MOR in the immunoprecipitates detected with anti-MOR C-tail antibodies after the blots were stripped

These data suggested that GRIN1 might associate with both MOR and $G\alpha_{i2}$ as a tether and that the association between MOR and GRIN1 could be affected by the receptor interaction with the $G\alpha$.

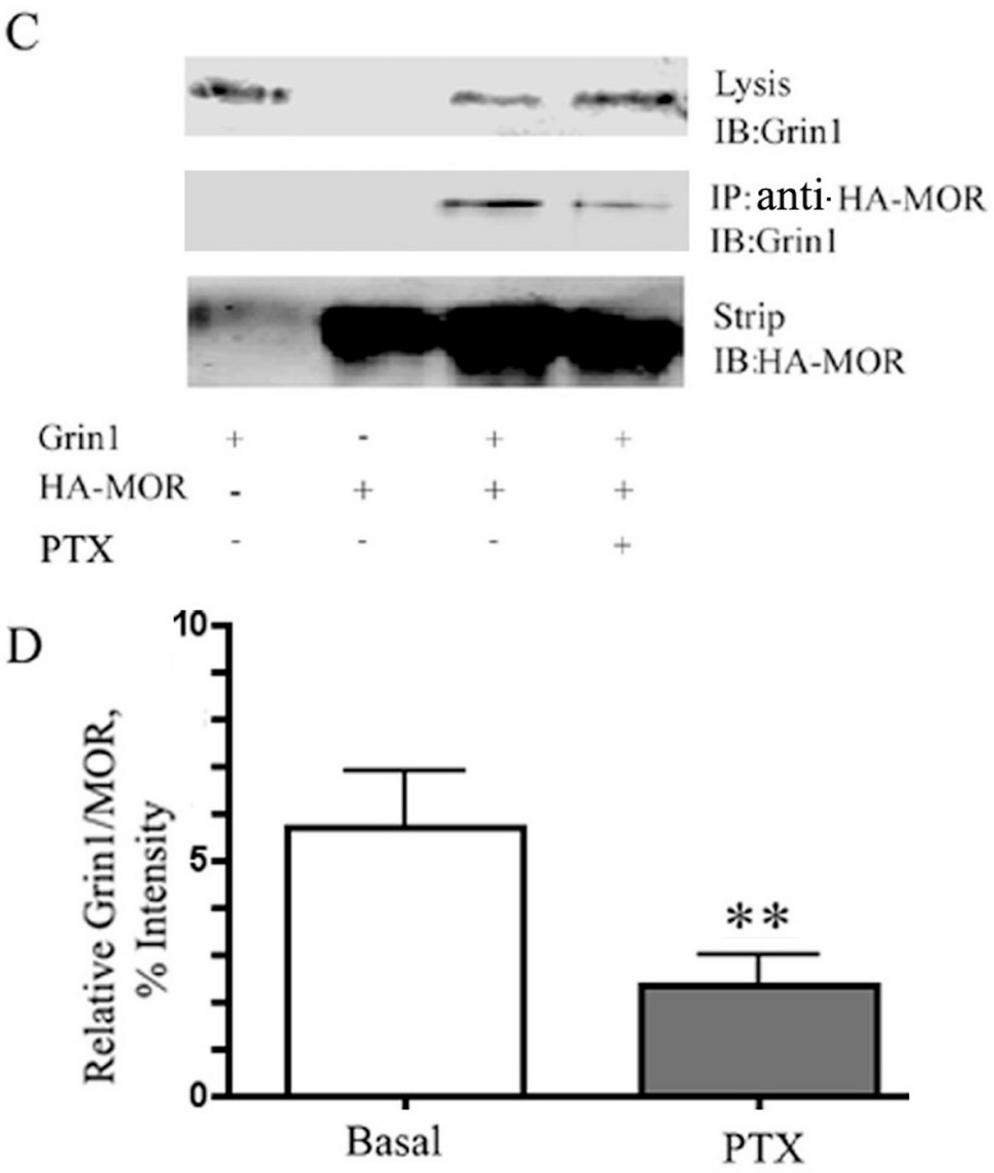

Fig 2.4C&D (C) Co-IP of GRIN1 with MOR with or without PTX pretreatment. (D) Quantification analysis of immunoprecipitated GRIN1 with MOR with or without PTX pretreatment.

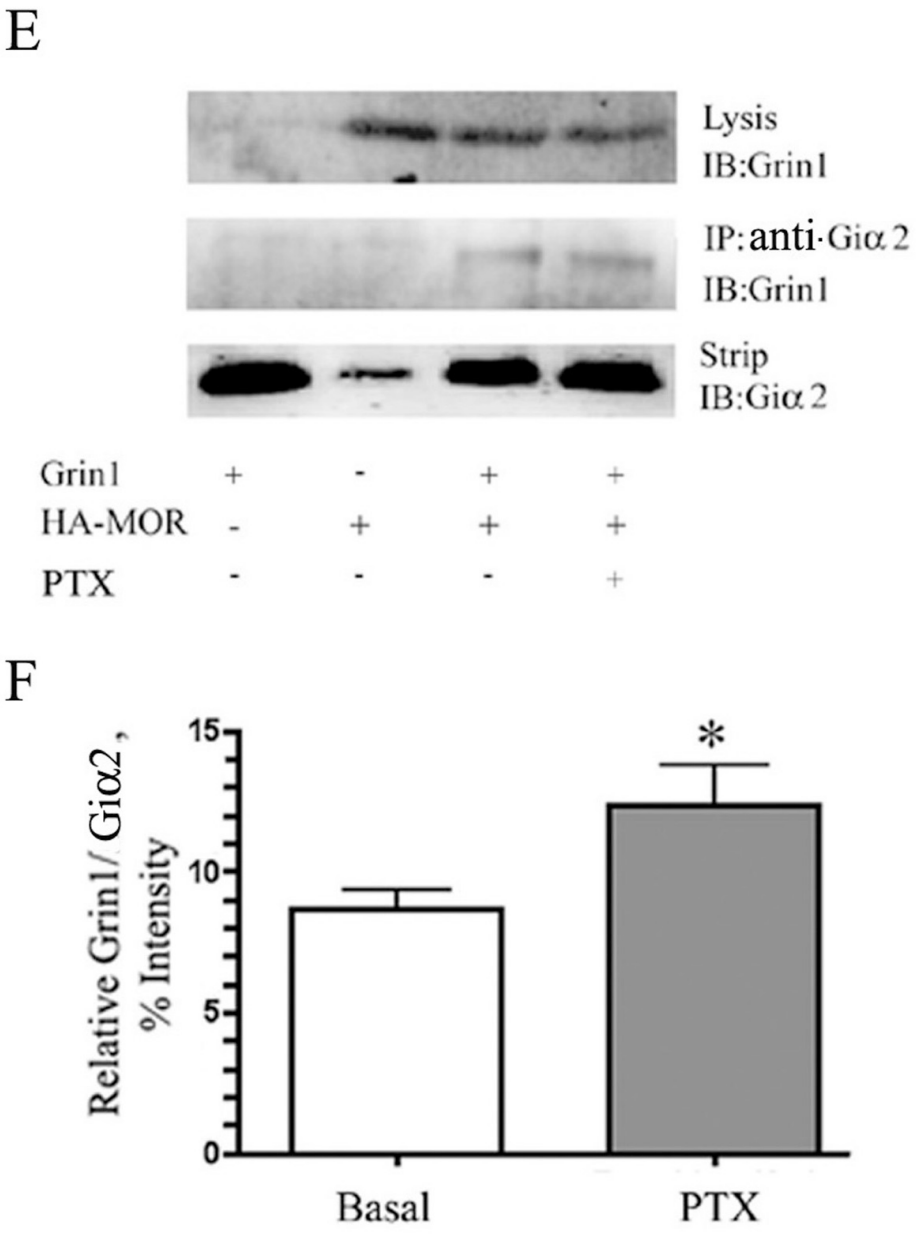

Fig 2.4E&F (E) Co-IP of GRIN1 with Gi 2 with or without PTX pretreatment. (F) Quantification analysis of immunoprecipitated GRIN1 with Gi 2 with or without PTX pretreatment.

Over-expression of GRIN1 maintained the activated MOR in lipid raft

Previous studies indicate that MOR location in lipid raft is critical for the receptor activities (57,67). Further, etorphine but not morphine could induce the redistribution of MOR from lipid rafts, which resulted in pathway selective signaling of these opioid agonists (42). Most intriguingly is that $G\alpha_{i2}$ was shown to involve in the anchoring of MOR within these microdomains (42). Since our current studies suggested GRIN1 could tether the receptor and $G\alpha_{i2}$ together, whether GRIN1 could affect MOR translocation upon agonist activation was examined. N2A cells were transfected with GFP-vector or GFP-GRIN1, with or without etorphine treatment. Each sample was tested to be around 80% transfection efficiency by determining GFP fluorescence under microscopy before cells were lyzed. To isolate lipid raft fractions, N2A cells were extracted and subjected to sucrose density gradient centrifugation as described in Materials and Methods. The gradient was fractionated and the fractions were analyzed for MOR, GRIN1, $G\alpha_{i2}$ and non-raft marker-transferrin. The results are presented in Figure 2.5A. Fractions 4 & 5 were reported to be raft fractions while other fractions referred as non-raft fractions (57). Western blot analysis demonstrated that non-raft marker-transferrin was present in fractions except fraction 4 and 5 while $G\alpha_{i2}$ was found in fraction 4 and 5, presumably the lipid raft fractions. In agreement with a previous report (42), activation of MOR with etorphine resulted in a translocation of the receptor to non-raft domain, which was not observed with morphine pretreatment (Fig 2.5A, panel c&e).

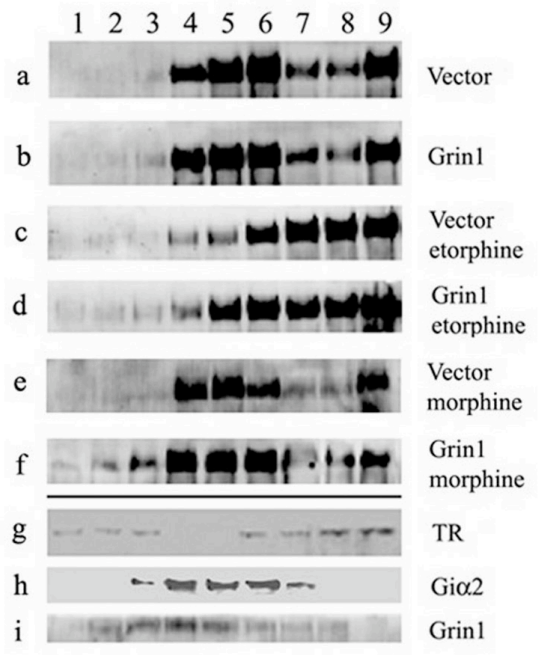

Fig 2.5A N2A cells stably expressing MOR were tansfected with GFP-vector or GFP-GRIN1, with or without agonist treatment for 10 minutes after 48-hour transfection. Lipid raft and non-raft fractions were separated as described under Experimental Procedures. In panel a to f, MOR level in all the gradient fractions were determined with anti-HA. In panels g, h and i, the levels of Transferrin receptor (TR), Gi 2 and GRIN1 were detected with their respective antibodies. The locations of MOR in GFP-vector transfected N2A cells with no drug treated (panel a), 100 nM etorphine treated (panel c) or 100 nM morphine treated (panel e) were determined. Likewise, the MOR distributions with the sucrose gradient fractions from N2A cells over-expressed with GRIN1 and no drug treaed (panel b), 100 nM etorphine treated (panel d) and 100 nM morphine treated (panel f) were determined.

Surprisingly, over-expression of GRIN1 did not significantly alter the microdomain distribution of MOR (Fig 2.5A, panel b). However, when GRIN1 was over-expressed, the amount of MOR redistributed to the non-raft fraction after etorphine treatment was reduced (Fig 2.5B & C). Since the etorphine-induced translocation of MOR did not involve the parallel translocation of $G\alpha_{i2}$ (42), the increase in the amount of MOR within the lipid raft after GRIN1 over-expression suggested that GRIN1 tethered the receptor with $G\alpha_{i2}$ and enhanced MOR distribution in the lipid rafts.

To demonstrate further the GRIN1-MOR interaction can affect MOR lipid raft location, lipid raft fractionation of MOR i33 mutant was also performed with or without etorphine treatment. The co-immunoprecipitation experiments suggested that the 3rd intracellular loop sequence, ^{267}GSKEK^{271} is involved in the GRIN1-MOR interaction (Fig 2.2). The deletion of this sequence from MOR (i33 mutant) resulted in the non-raft distribution of the receptor mutant as compared with the wide type MOR (Fig 2.5D, panel a & b). Over-expression of GRIN1 couldn't rescue i33 mutant back to lipid raft because there was minimal interaction between i33 mutant and GRIN1 (Fig 2.5D, panel c). Moreover, under the condition of PTX pretreatment that can further uncouple $G\alpha_{i2}$ from i33 mutant, a dramatic decrease of the receptor in lipid rafts was observed (Fig 2.5D, panel d). Similarly, the deletion of the sequence ^{276}RRITR^{280} from the 3rd intracellular loop of MOR (i35 mutant) resulted in the uncoupling of the receptor from $G\alpha_{i2}$ that also responsible for MORs' anchoring in lipid raft (66), i35 mutant can be minimally detected in the lipid raft fractions of the gradient (Fig 2.5D, panel e). Over-expression of GRIN1 could rescue partial of MOR i35 mutant back into lipid raft, but no significant difference was observed (Fig 2.5D, panel e & f). Probably, the ability of i35 mutant to interact with

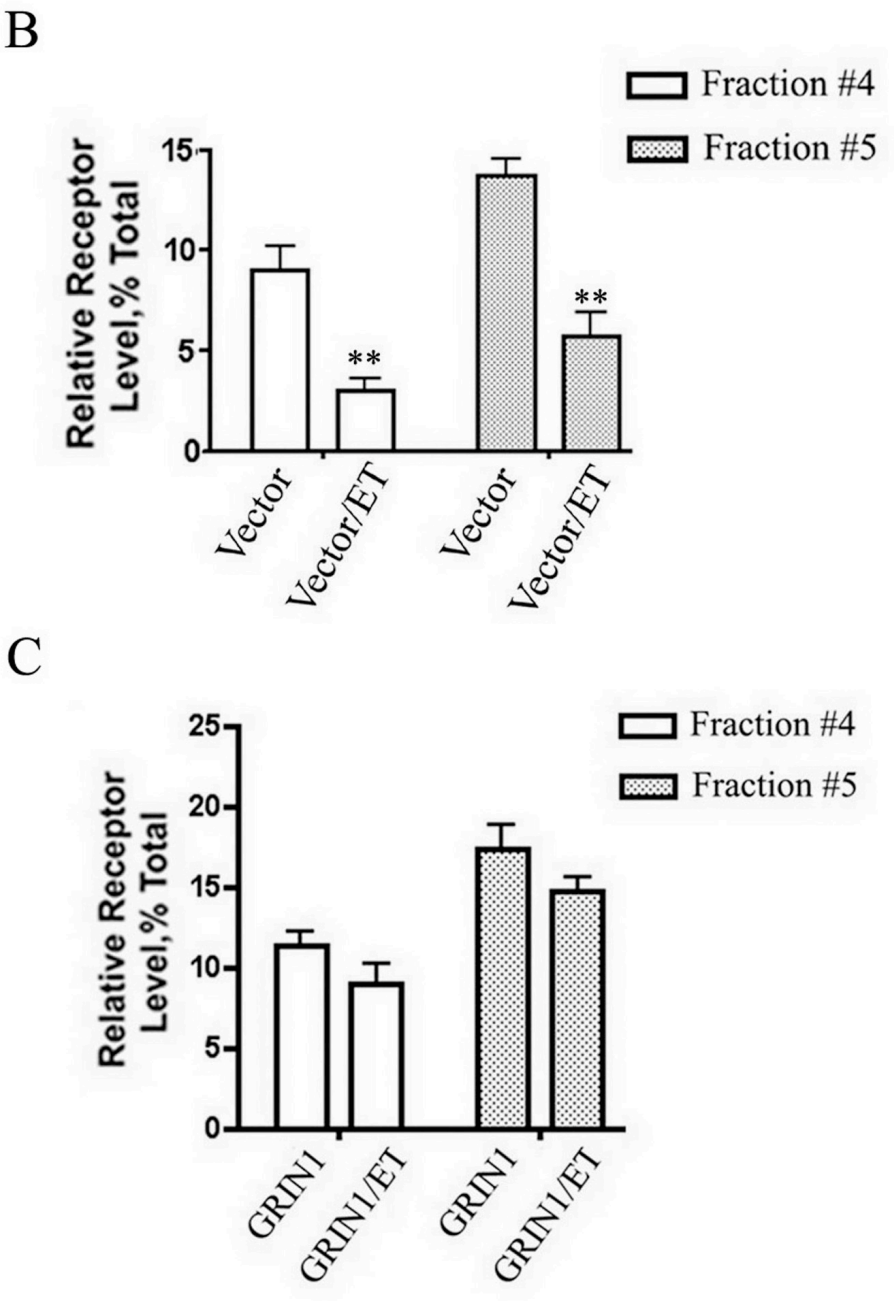

Fig 2.5B&C (B) Statistic analysis of MOR distribution by determining the percentage of MOR in lipid raft fractions vs total MOR level when transfected with vector, with or without etorphine treatment. (C) Statistic analysis of MOR distribution in lipid raft fractions vs total MOR when transfected with GRIN1, with or without etorphine treatment.

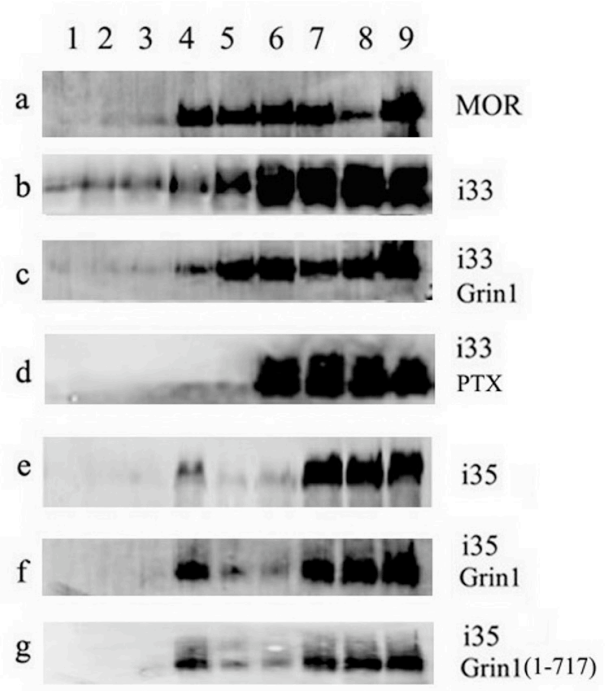

Fig 2.5D N2A cells stably expressing MOR, or MORi35 mutant, or MORi33 mutant with or without GRIN1 over-expression after 48-hour transfection. Distribution of MOR, MORi35 mutant, or MORi33 mutant on the sucrose gradients were determined as in (A).

GRIN1 enables some of receptors to be retained in the lipid rafts. Further knocking-down of G protein-GRIN1 interaction by GRIN1 (1-717) mutant didn't change the receptor distribution pattern. These data suggest that MOR-GRIN1 interaction same as MOR-G protein interaction can keep MOR located in lipid raft, which is mostly because GRIN1 serves as a tether between MOR and G protein. The results obtained by endogenous rat brain fractionation also demonstrated that lentivirus-mediated GRIN1 siRNA (Fig 2.8A) could further remove MOR out of lipid raft in addition to precluding G protein function by PTX pretreatment (Fig 2.5E), which indicated that GRIN1 could affect MOR distribution in lipid raft physiologically.

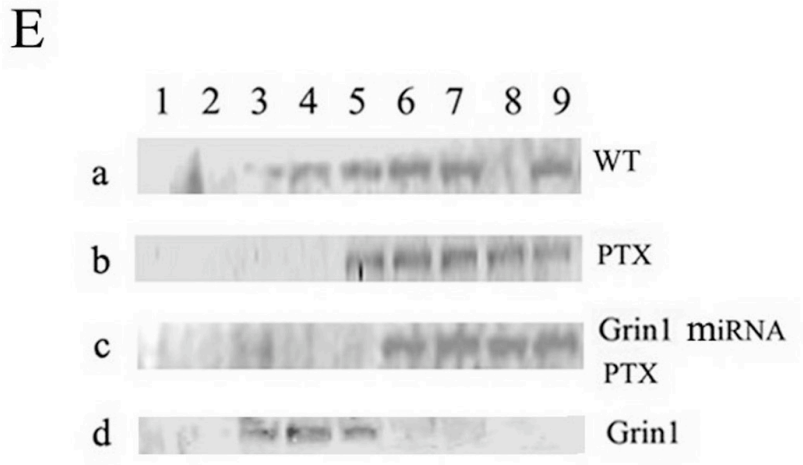

Fig 2.5E Lipid raft and non-raft fractions were separated using rat brain slices with endogenous MOR expression as described under Experimental Procedures. In panel a to c, MOR level in all the gradient fractions were determined with anti-MOR purified antibody (provided by Dr.Chen). In panel d, the level of GRIN1 was detected with anti-GRIN1 antibody (T116).

GRIN1 potentiates the MOR-mediated regulation of Src kinase activity

Since GRIN1 can stabilize the receptor complex within the lipid rafts, it is reasonable to hypothesize that GRIN1-MOR interaction can potentiate the signaling of the receptor. GRIN1 is known to induce neurite outgrowth. Thus, it is probable that GRIN1 can modulate the MOR-mediated regulation of the signaling pathway such as Src kinase known to affect neurite extension (67,68). Confocal Microscopy experiment showed that PP2, a specific inhibitor for Src kinase, could reduce neurite outgrowth that promoted by GRIN1 over-expression (Fig 2.6C). N2A cells stably expressing MOR (MOR-N2A) were transfected with GFP-vector, GFP-GRIN1 or GFP-GRIN1 siRNA, with or without etorphine treatment. Each sample was tested to be around 80% transfection efficiency by screening GFP fluorescence under

microscopy before cells were lyzed. Cell lysates were subjected to lipid raft fractionation as described in Materials and Methods. Only the fractions (#4&5) containing lipid raft were used in determining the Src kinase activity. Using the antibodies specific for the phospho-Tyr^{416} to detect the activated kinase and the antibodies specific for total Src to determine percentage of Src being activated, ten-minute etorphine treatment was shown to activate Src only in the N2A-MOR cells transfected with GRIN1. Meanwhile, etorphine was shown to decrease Src activities when the N2A-MOR cells were transfected with GRIN1 siRNA (Fig 2.6A). At the same time, disruption of lipid raft by pretreatment of MβCD blocked the etorphine-induced Src kinase activation in the N2A-MOR cells over-expressed GRIN1, suggesting that MOR location within the lipid raft was critical for Src activation (Fig 2.6B).

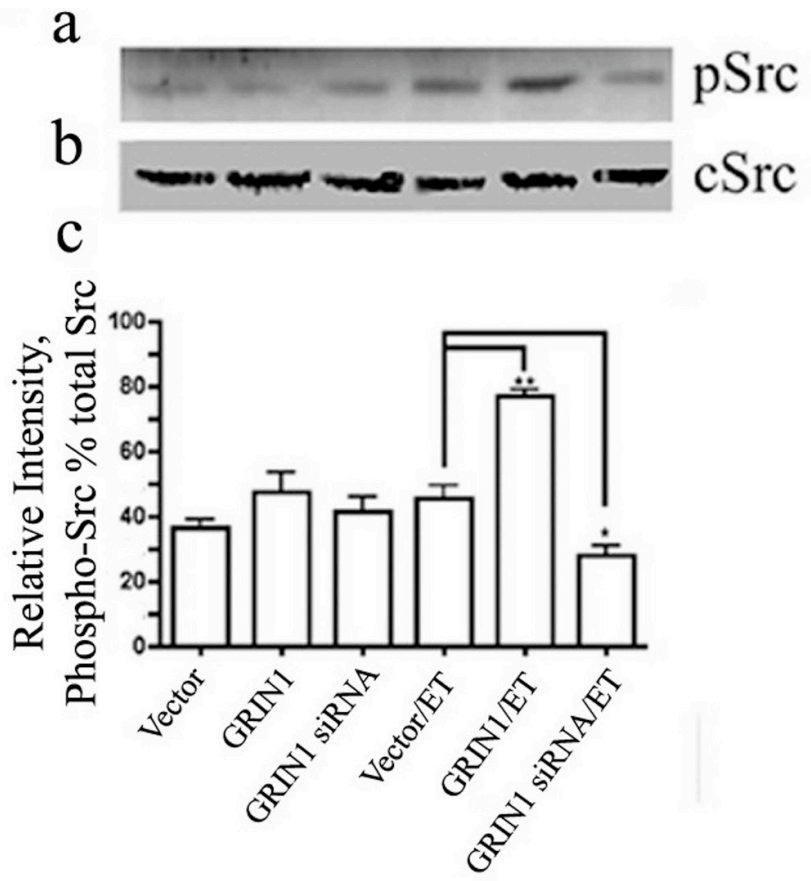

Fig 2.6A Src kinase activity in lipid raft fractions increased when N2A-MOR cells were over-expressed with GRIN1 and treated with etorphine.Panel a represents the level of activated Src kinase as determined by the amount pY416 phosphorylated Src kinase in lipid raft; Panel b represents total Src kinase level in lipid raft; Panel c: statistic analysis of Src kinase activity by determining the percentage of intensity pixels of phosphorylated Src kinase vs total Src kinase.

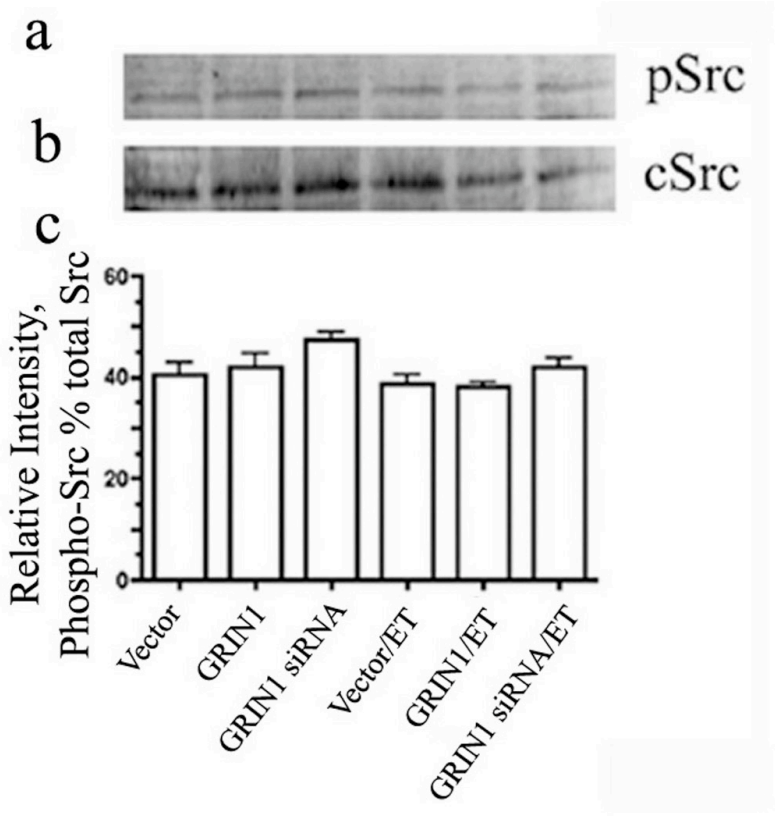

Fig 2.6B Overexpression of GRIN1 cannot increase Src kinase activity in lipid raft when cells were treated with MβCD.Panel a represents the level of activated Src kinase as determined by the amount pY416 phosphorylated Src kinase in lipid raft; Panel b represents total Src kinase level in lipid raft; Panel c: statistic analysis of Src kinase activity by determining the percentage of intensity pixels of phosphorylated Src kinase vs total Src kinase.

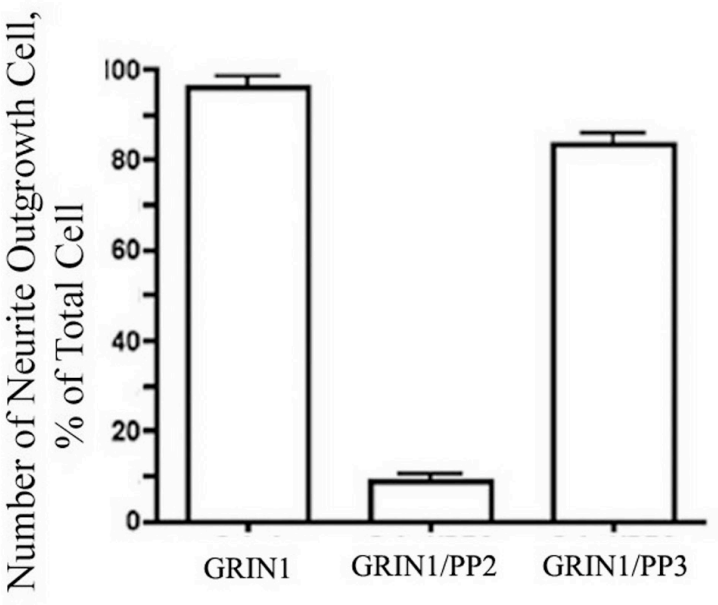

Fig 2.6C Statistic analysis of cell number possessing neurite outgrowth in GRIN1-overexpressed N2A-MOR cells 48 hours after etorphine treatment when pre-treated with saline, 10 M PP2 or PP3 for 30 min at 37°C. The bars represents the summary from the cells observed in >20 different fields of confocal images, **p denotes <0.01.

Etorphine-induced neurtite outgrowth is mediated by GRIN1

Since GRIN1 is reported to induce neurite outgrowth (50,51), whether the tethering of the receptor and $G\alpha_{i2}$ by GRIN1 could affect the neurite outgrowth activity of this protein molecule was investigated. N2A-MOR cells were transfected with GFP-vector, GFP-GRIN1 or GFP-GRIN1 siRNA (GRIN1 siRNA #3, GRIN1 siRNA efficiency was demonstrated as Fig 2.7A). The cells were then exposed to 100 nM etorphine for 10 minutes. Afterwards, the medium was removed, and neurites were induced by replacing the medium with serum free DMEM. Live cell images of the same cells were recorded up to 48 hrs as described in Materials and Methods. There was significant difference in the ratio of neurite outgrowth between cells transfected with GRIN1 and cells without

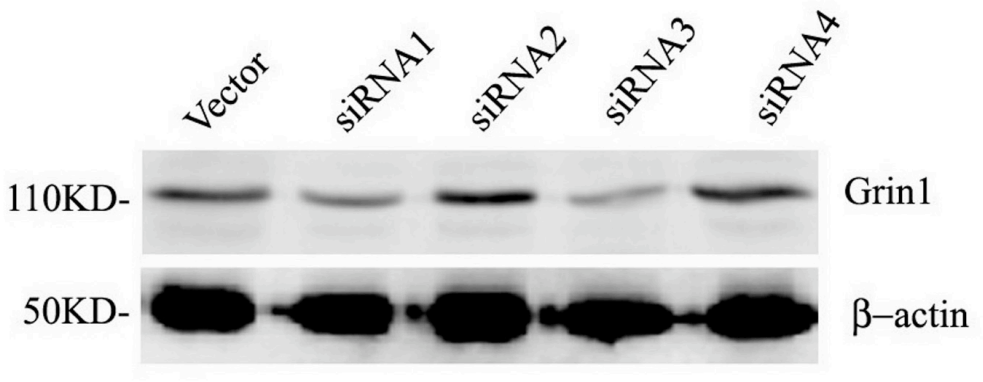

Fig 2.7A Efficency of each designed GRIN1 siRNA to alter the endogenous GRIN1 level in N2A cells

GRIN1 over-expression. Approximately 70% of cells overexpressing with GRIN1 possessed long neuritis or growing dendrites after 48-hour induction of differentiation (Fig 2.7B&D). In contrast, almost none of GFP-GRIN1 siRNA transfected cells and only around 8% of GFP-vector transfected cells possessed long neuritis or growing dendrites at 48 hours after induction of differentiation (Fig 2.7D). These data indicated that over-expression of GRIN1 and etorphine treatment together could induce neurite outgrowth significantly, contrary to etorphine treatment alone. On the other hand, 100 nM morphine could induce neurite outgrowth regardless of GRIN1 over-expression. There was little difference in the morphine effect on neurite outgrowth between cells transfected with vector and those over-expressed GRIN1 (Fig 2.7E). Above data implicate the selectivity of MOR agonist in inducing neurite outgrowth when GRIN1 is over-expressed. When the cells were pretreated with PTX or naloxone, the ability of etorphine to induce neurite outgrowth was blocked regardless of whether GRIN1 was over-expressed or not (Fig 2.9), suggesting GRIN1-promoted neurite outgrowth was dependent on the association of

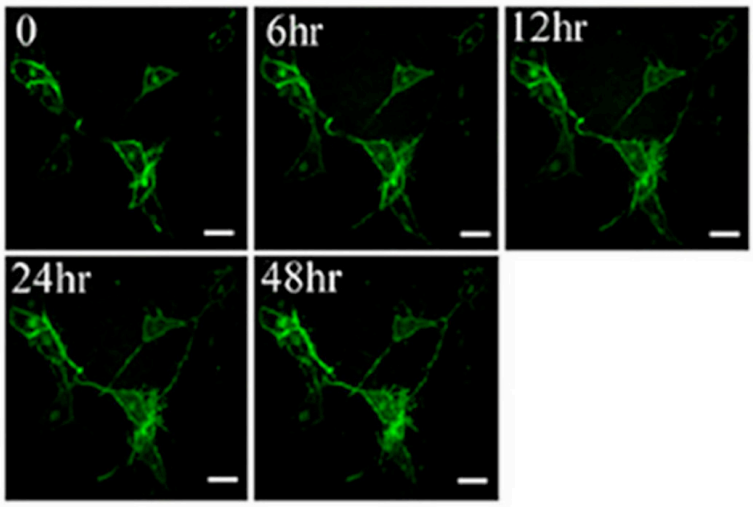

Fig 2.7B Live cell images of etorphine-induced neurite outgrowth in N2A stably expressing MOR and transiently transfected with GFP-GRIN1;Panel a: N2A cells after removal of 10-minute 100 nM etorphine treatment, time "0"; Panel b: 6 hour; Panel c: 12 hour; Panel d: 24 hour; and Panel e: 48 hour after etorphine treatment. Scale bar equals 10 μm.

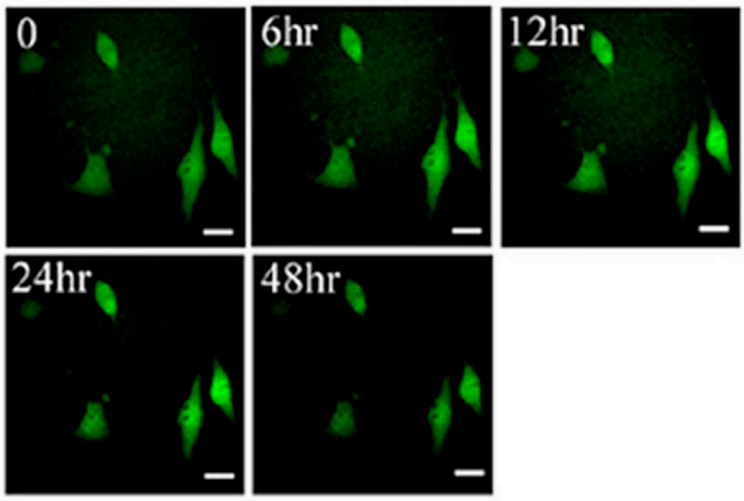

Fig 2.7C Live cell imagse of etorphine-induced neurite outgrowth in N2A-MOR cells transfected GFP-GRIN1 siRNA. Panel a: N2A cells after removal of 10-minute 100 nM etorphine treatment, time "0"; Panel b: 6 hour; Panel c: 12 hour; Panel d: 24 hour; and Panel e: 48 hour after etorphine treatment. Scale bar equals 10 μm.

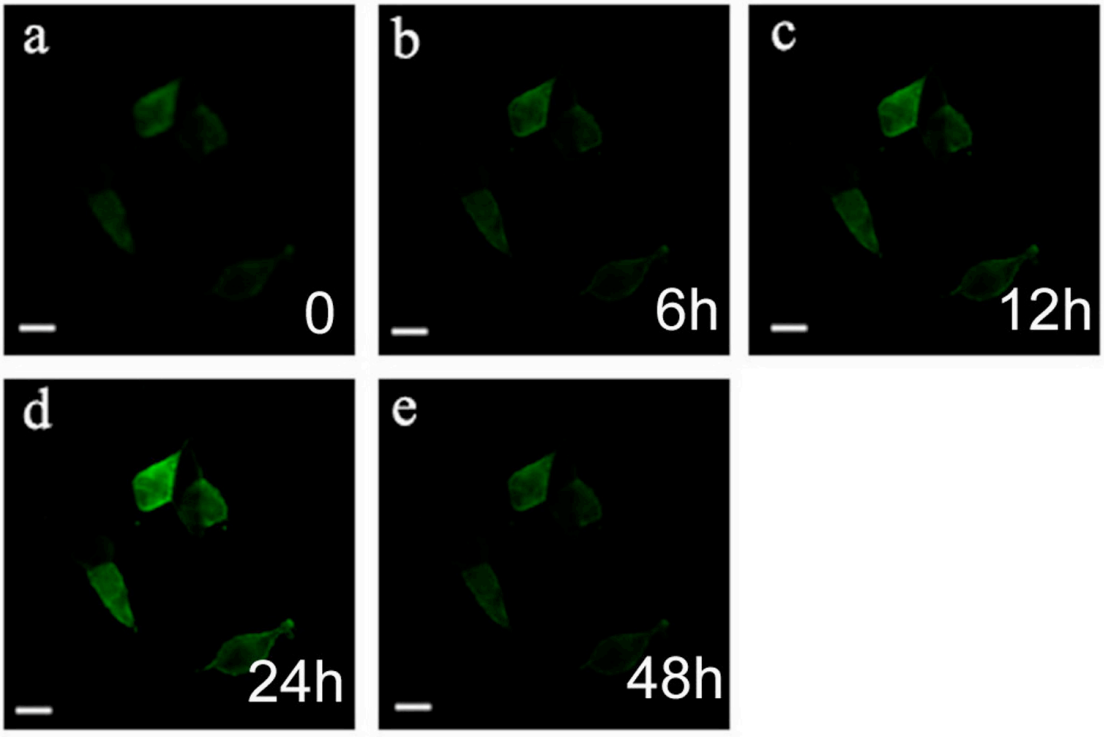

Fig 2.9A Live image of GFP-Grin1 did not promoted neurite outgrowth through PTX pretreated MOR; Panel a: N2A cells after transfection were pretreated with PTX or naloxone for 12 hours and then treated with 100 nM etorphine for 10 minutes as start time point "0"; Panel b: 6 hour after etor -phine treatment; Panel c: 12 hour after etorphine treatment; Panel d: 24 hour after etorphine treatment; Panel e: 48 hour after etorphine treatment. Scale bar equals 10ul.

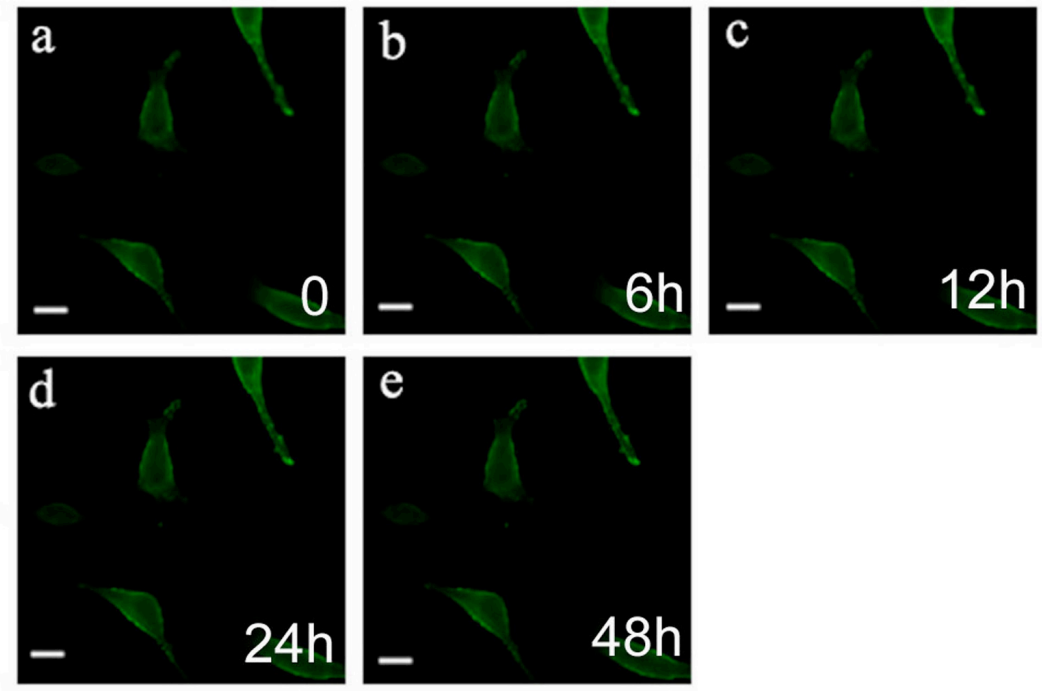

Fig 2.9B Live image of GFP-Grin1 did not promoted neurite outgrowth through naloxone pretreat -ed MOR. Panel a: N2A cells after transfection were pretreated with PTX or naloxone for 12 hours and then treated with 100 nM etorphine for 10 minutes as start time point "0"; Panel b: 6 hour after etorphine treatment; Panel c: 12 hour after etorphine treatment; Panel d: 24 hour after etorphine treat -ment; Panel e: 48 hour after etorphine treatment. Scale bar equals 10ul.

activated MOR and G protein. Similarly, knocking down endogenous GRIN1 in N2A-MOR cells with GRIN1 siRNA blunted the etorphine-induced long neuritis or growing dendrites 48 hours after serum removal (Fig 2.7C&D). The siRNA studies support the important role of GRIN1 in MOR-induced neurite outgrowth.

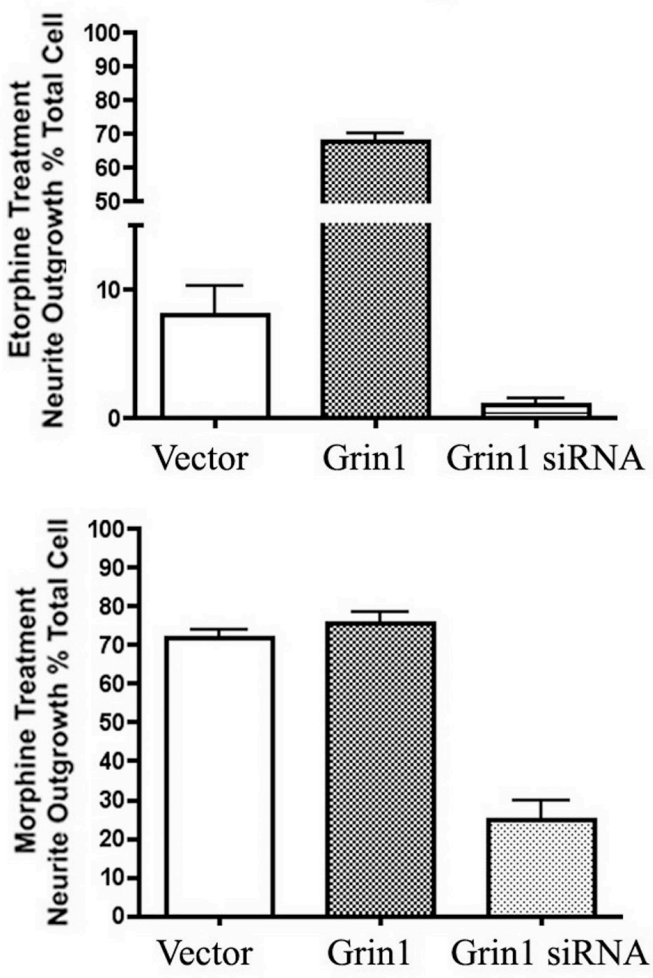

Fig 2.7D&E (D) Statistic analysis of cell number possessing neurite outgrowth when N2A cells were transfected with GFP-vector, GFP-GRIN1 and GFP-GRIN1 siRNA calculated from >20 different fields of confocal images after etorphine treatment, **p denotes <0.01. (E) Statistic analysis of cell number possessing neurite outgrowth when N2A cells were transfected with GFP-vector, GFP-GRIN1 and GFP-GRIN1 siRNA calculated from >20 different fields of confocal images after 100nM morphine treatment, **p denotes <0.01.

To further confirm the interaction between MOR and GRIN1 is crucial for MOR-activation induced neurite outgrowth, MORi33 mutant and MORi35 mutant were used for nurite outgrowth studies. In accordance with previous report, MORi35 mutant showed decreased interaction with endogenous $G\alpha_{i2}$ (Fig 2.10A). Meanwhile, MORi33 mutant showed minimal interaction with endogenous GRIN1 (Fig

2.2&2.10A). N2A cells differentiated in the absence of serum, and approximately 80% of cells possessed long neuritis or growing dendrites after 48-hour induction of differentiation when overexpressed with GRIN1. In contrast, although the deletion of ^{276}RRITR^{280} resulted in the complete blockade of agonist-mediated inhibition of adenylyl cyclase activity (42,66), around 7% of MORi35 mutant transfected cells exhibited long neurite and growing dendrite 48 hrs after serum removal and etorphine treatment (Fig 2.10B). On the other hand, even with no measurable difference in the agonist ability to regulate adenylyl cyclase activity in cells expressing the ^{267}GSKEK^{271} deletion mutant (66), 20% of MORi33 mutant transfected cells possessed long neuritis or growing dendrites at 48 hours after serum removal (Fig 2.10B). These data suggest the importance of the interaction between MOR and GRIN1 in the opioid agonist-induced neurite outgrowth.

To further explore whether the receptor location within the lipid raft is critical for GRIN1-mediated neurite outgrowth, live image experiment was performed with cells treated with MβCD to extract cholesterol so as to disrupt the lipid raft. The effect of MβCD on neurite outgrowth was compared with the cells treated with MβCD together with addition of cholesterol in order to restore lipid raft structure. As shown in Fig 2.11A & B, addition of cholesterol or MβCD plus cholesterol did not affect the etorphine-induced neurite outgrowth in the GRIN1 transfected N2A-MOR cells. However addition

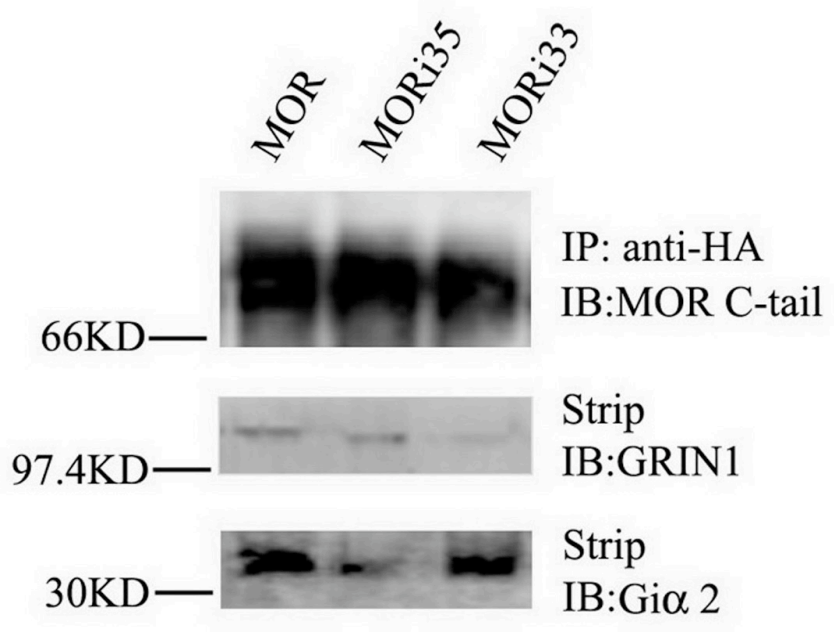

Fig 2.10A Co-IP of MOR, MORi35 mutant, or MORi33 mutant with endogenous GRIN1 or Gi 2. Panel a: MOR was detected withMOR C-tail antibody in the co-immunoprecipitates; panel b: the amount of GRIN1 in the immunoprecipitates detected with anti-GRIN1 antibodies after the blots were stripped; panel c: the amount of Gi 2 in the immunoprecipitates detected with anti-Gi 2 anti -bodies after the blots were stripped.

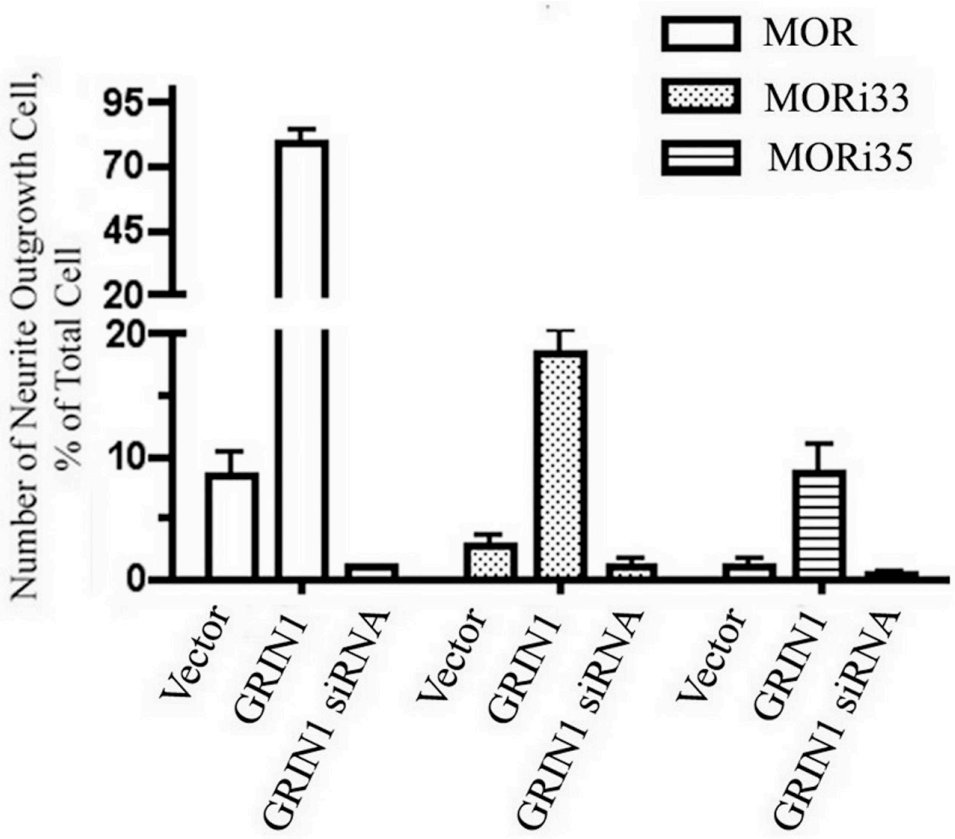

Fig 2.10B Ratio of N2A cells possessing neurite outgrowth under etorphine treatment when individually expressing MOR, MORi33 mutant, or MORi35 mutant in combination with GRIN1 or GRIN1 siRNA .

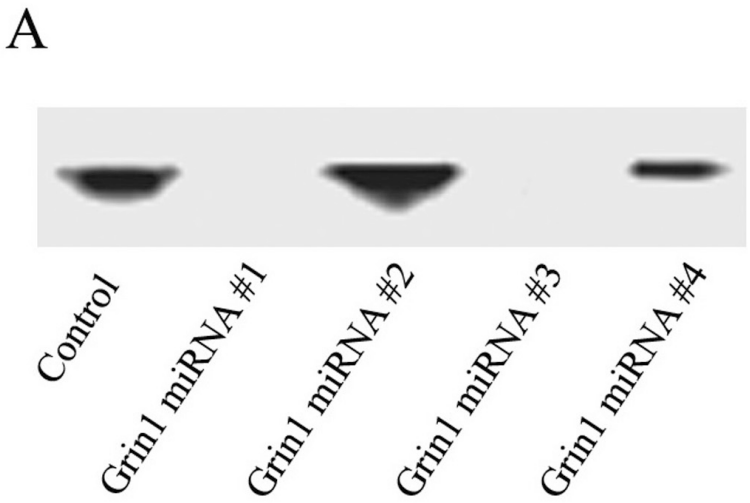

Fig 2.8A lentivirus-mediated GRIN1 miRNA efficiency. lentivirus-mediated GRIN1 miRNA #1,2,3, 4 were constructed as described in Experimental Procedures. GRIN1 miRNA constructs were transfected into HEK293FT cells and virus were collected to infect rat brain slices for 48 hours. Slices were homogenized and centrifuged at 13,000rpm for 30min and subjected for Western-blot analysis by detecting GRIN1 expression using anti-GRIN1 antibody (T116).

B

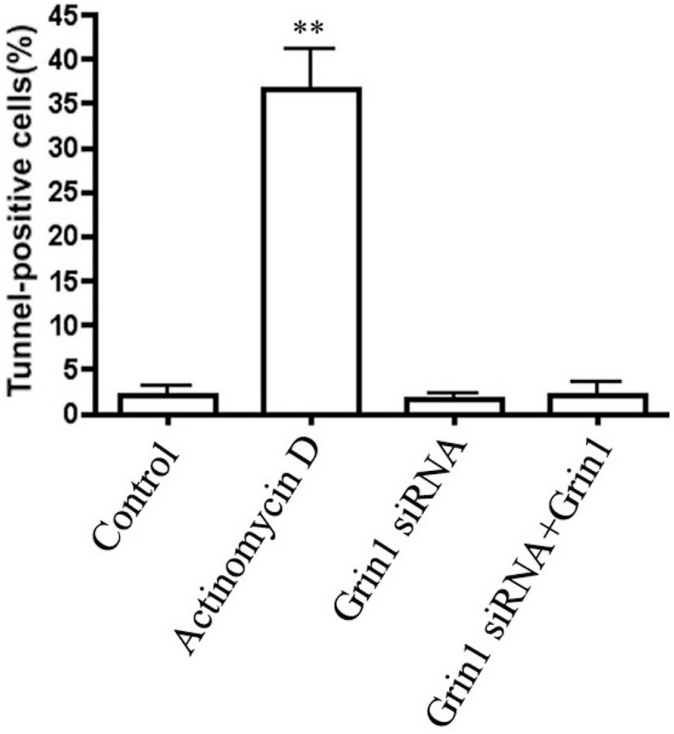

Fig 2.8B GRIN1siRNA cannot cause cell apoptosis, as detected by the Tunnel assay. Analysis and score of Tunel-positive cells - a graphical representation of the scores of the Tunel-positive cells. N2A-MOR cells was either left untreated (control) or treated with Actinomycin D in 0.1% DMSO for 15 minutes to induce apoptosis (positive control) or transfected with GFP-tagged GRIN1 siRNA or transfected with GFP-tagged GRIN1siRNA and rescued with GRIN1 over-expression as described in Experimental procedures.

of MβCD by itself significantly blocked the etorphine-induced GRIN1-promoted neurite outgrowth (Fig 2.11A&B). Thus, MOR location within the lipid raft is critical for etorphine to induce neurite outgrowth, and the GRIN1 tethering of MOR and $G\alpha_{i2}$ enhances the lipid raft location of the receptor leading to the promotion of neurite outgrowth in the presence of etorphine.

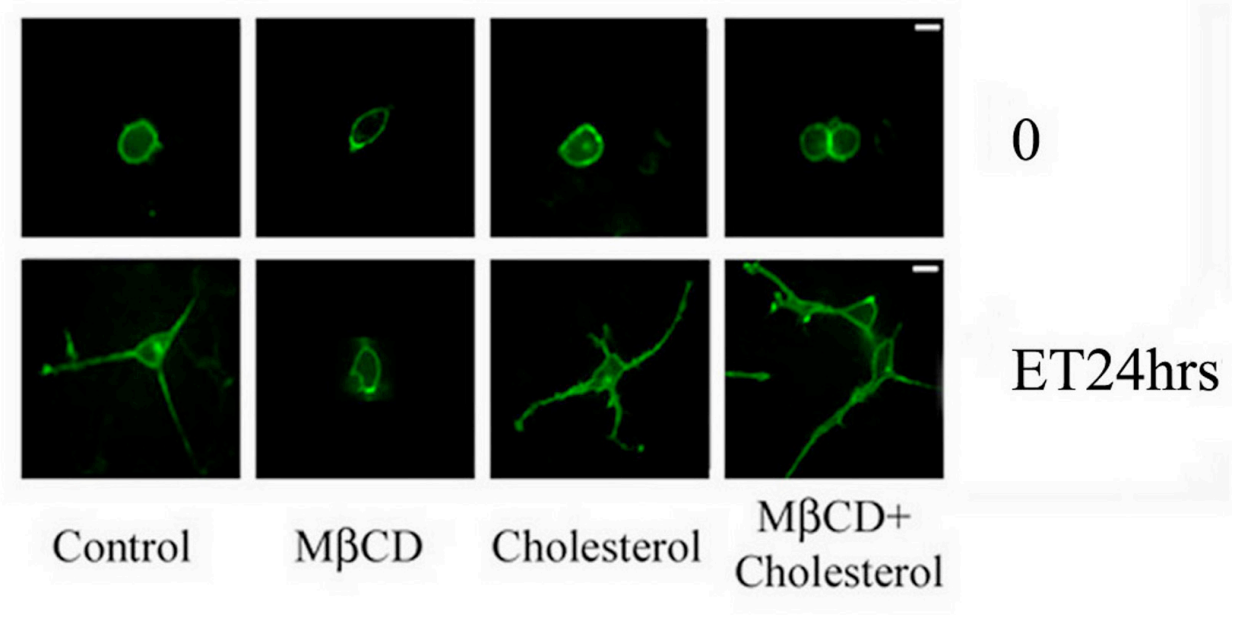

Fig 2.11A Live cell images of neurite outgrowth in GRIN1 transfected cells when treated with saline as control, M CD, cholesterol or M CD plus cholesterol 24 hours after 100 nM etorphine treatment for 10 minutes.

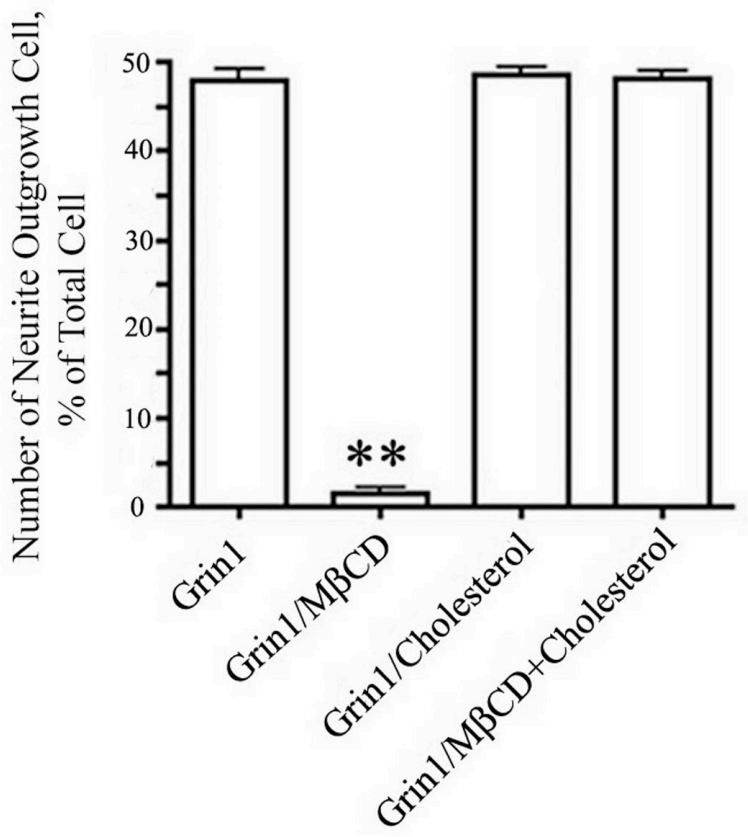

Fig 2.11B Statistic analysis of cell number possessing neurite outgrowth in GRIN1 transfected cells calculated from >20 different vision fields of confocal images when treated with saline, M CD, chol -esterol or M CD plus cholesterol 24 hours after etorphine treatment, **p denotes <0.01.

Part V: Conclusions

Chapter 1:

RPNI was originally identified as an integral component of rough microsomal membranes and appeared to be related to the bound ribosomes (69). Currently, RPNI is accepted to be a member of the oligosaccharyltransferase (OST) family. The mammalian OST is an oligomeric complex composed of three membrane proteins located within the ER: ribophorin I (RPNI), ribophorin II (RPNII) and OST48 (62). Later, DAD1, a anti-apoptotic protein, also was found to be a subunit of the mammalian OST (70). The biosynthesis of membrane proteins at the ER involves the integration of the polypeptide at the Sec61 translocon, together with a number of maturation events that can occur both during and after synthesis, such as N-glycosylation and signal sequence cleavage (71). The transmembrane domain of RPNI has been suggested to function as a dolichol binding site (62). It is also reported that RPNI may function to retain potential substrates in close proximity to the catalytic subunit of the OST (sttp3), thereby stochastically improving the efficiency of the N-glycosylation reaction *in vivo* (71). Other evidence has shown that RPNI may be multifunctional and facilitate additional processes, for example, ER quality control (71).

Using an affinity column purification paradigm, we have identified RPNI as a MOR-interacting protein. The interaction between RPNI and MOR was confirmed by coimmunoprecipitation studies in transiently transfected N2A cells and direct gel overlay studies using the *in vitro* translation products of a RPNI cDNA construct. By means of both confocal immunofluorescence microscopy and FACS analysis, our

data demonstrated that the expression level of MOR could be regulated by RPNI level. RPNI appears to mediate MOR exocytotic activity, which is clearly related to its OST activity. For example, RPNI can stimulate the transport of the MOR C2 mutant from the ER to the cell surface, but not the export of the glycosylation-deficient MOR mutant-MOR5ND. This phenomenon suggests that RPNI not only is involved in biosynthesis of nascent polypeptides as previously reported, but also plays a pivotal role in their maturation and plasma membrane expression.

How RPNI can regulate MOR plasma membrane expression requires further investigation. However, our studies reveal several possible scenarios in which RPNI may affect MOR export.

First, our data showed that RPNI rescuing MOR C2 mutant was not due to ERAD (endoplasmic reticulum associated degradation) because ERAD substrate MOR could not rescue C2 (72) and MG132 only enhanced intracellular accumulation of C2 mutant but not on cell surface, in contrary to RPNI overexpression (Fig 1.13C). Furthermore, over-expression of RPNI has differential effects on the export of various opioid receptors and MOR mutants (Fig 1.10&1.14).

Second, our data suggested that RPNI could serve as chaperone for MOR. RPNI has been suggested to be involved in ER quality control. (71,73). Antibodies produced against the cytoplasmic domain of RPNI interfere with protein translocation across the rough ER by preventing ribosome targeting to the Sec61 complex (74). OST was demonstrated to be adjacent to the protein translocation channel (75), allowing the cotranslational modification of the nascent polypeptide as it enters the lumen of the rough ER (76). Most newly synthesized membrane and secretory

proteins are delivered to the Sec61 translocon that mediates their integration into the lipid bilayer (77). The Sec61 translocon forms an aqueous pore that is gated by the lumenal Hsp70—BiP (78,79). Accumulating evidence has revealed that the ER molecular chaperone BiP is a master regulator of ER function. BiP is responsible for maintaining the permeability barrier of the ER during protein translocation, directing protein folding and assembly, and targeting misfolded proteins for retrograde translocation so they can be degraded by the proteasomes (78,80). Hsp70 (BiP), together with RPNI, already has been found to interact with the ACE receptor (81). Interestingly, we identified one of the proteins co-purified with $(His)_6$-MOR to be Bip. Thus, similar to the chemical chaperone of MOR—naloxone (60), RPNI/Hsp70 could function as chaperone to rescue MOR C2 mutant transport to cell surface.

As the prelude of chaperone-assisted folding and oligomerization, formation of disulfide bonds already has started when the growing nascent peptide chains enter the luminal compartment (82,83). Proteins that fail to fold or oligomerize properly are prevented from export and are degraded (84-86). During folding, polypeptides with N-linked oligosaccarides interact transiently and specifically with two ER-unique chaperones, calnexin and calreticulin. Calnexin transiently interacts with different glycoproteins during folding and maturation (87). The disulfide bonds in the opioid receptor may link to calnexin and affect the plasma membrane expression of the opioid receptor. Interestingly, C2 mutant is different from some other calnexin-retained GPCR mutants -V2 vasopressin receptor and V1b/V3 receptor mutants (63,88), which may account for different mutants having different effect on the interaction of calnexin. From Figure 1.13, calnexin was detected when MOR was

immunoprecipitated, contrary to C2 coexpressed with RPNI. Coexpression of C2 and RPNI didn't affect the total amount of cellular glycosylated receptor, compared to C2 with naloxone and C2 with proteosome inhibitor MG132. Under all these conditions, interaction between C2 and calnexin was not detected (Fig 1.13D). However, the co-expression of RPNI with C2 helps to stabilize C2 and prevents its degradation, as compared to C2 co-transfected with vector control (Fig 1.13A&B). The data suggested that overexpression of RPNI could enhance cell surface expression of C2, which might reflect RPNI-associated ER quality control processes to facilitate C2 mutant's export out of ER other than the calnexin pathway.

The chaperone activity of RPNI appears to be connected to its OST activities. Contrary to the MOR C2 mutant, another MOR plasma membrane expression deficient mutant in which all 5 Asn residues at the N-terminus were mutated to Asp (MOR5ND), was unable to be expressed in plasma membrane despite RPNI over-expression. Furthermore, addition of naloxone did not result in cell surface expression of MOR5ND. On the other hand, one of the single Asn mutants, N53D, was shown to express on the cell surface (Fig 1.12) and interact with calnexin (Fig 1.15). Over-expression of RPNI or naloxone treatment did not increase the expression of the N53D mutant (Fig 1.12). These results suggest that N-glycosylation is critical for naloxone or RPNI to function as a chaperone. A new model for OST recently was proposed in which RPNI might act as a chaperone or as an escort to promote the N-glycosylation of selected substrates by the catalytic STT3 subunits (89). The importance of N-glycosylation in opioid receptor plasma membrane expression was demonstrated further with other opioid receptors–DOR and KOR, and the

endoglycosidases studies. Although RPNI is known to form a complex with these two receptors, RPNI, as a chaperone, exhibits differential effects in their plasma membrane expressions. KOR has less N-glycosylation sites and over-expression of RPNI has minimal effect on KOR plasma membrane expression. However, by knocking-down RPNI level with siRNA, KOR plasma membrane expression decreased, illustrating that RPNI was important in KOR final destination. All these data suggest that RPNI's function depends not only on the glycosylation state of the receptor but also on the number of glycosylation sites.

Collectively, a major finding of this study is the interaction of MOR with RPNI in neuroblastoma cells and the potential function of this association in regulating opioid receptor plasma membrane expression. Our data indicate that RPNI has functions other than being an oligosaccharyltransferase. The interaction of RPNI with MOR suggests that RPNI serves as a chaperone or controller of MOR transport from the ER to the cell surface. It remains to be determined whether RPNI and its interaction with MOR can regulate or be regulated by receptor signaling.

Chapter 2:

In long-term pain relief, the biggest clinical issue is that repeated opiate exposure can lead to the development of tolerance, sensitization and physical dependence, which involves the change of neuron synaptic plasticity, neurogenesis, the brain reward circuit (90,91). These phenomena can be considered adaptive processes similar to other experience-dependent changes in the brain, such as learning and neural development (90-94). Formation and extension of axons and dendrites, so-called neurite outgrowth, is a crucial event in neuronal differentiation and maturation during

development of nervous system (95,96). Substantial evidence also showed that alteration of opioid receptor activity disturbed the neurobehavioral development of newborns(97), indicating the involvement of the opiate system in neuronal differentiation. Endogenous activity of opioid receptor could affect neurite outgrowth(98), which is demonstrated to be critical in other addiction progresses (99,100). Meanwhile, it was also reported that etorphine and another mu-selective ligand -DAMGO ([D-Ala2, N-MePhe4, Gly-ol]-enkephalin) suppressed neurite outgrowth on cultured neurons (101,102) but morphine at ultra low concentrations enhanced neurite outgrowth of spinal and cortical neurons via a naloxone-independent mechanism(103). All these data suggested that activation of opioid receptor by different ligands could selectively affect neurite outgrowth.

Through mass spectrometry analysis and GST pull-down experiment, GRIN1 was found to be directly associated with MOR at its 3rd intracellular loop (Fig 2.1&2.2). Coimmunoprecipitation data demonstrated that MOR, $G_i\alpha 2$ and GRIN1 associated with each other and formed a distinctive signaling complex (Fig 2.4). This particular protein-protein association suggested that GRIN1 had other function when MOR was activated besides acting as a down-stream signal of $G_i\alpha$. Within the membrane-targeting region of GRIN1 (772–827), potential palmitoylation sites were found at Cys818 and Cys819 that could facilitate GRIN1 translocation into lipid rafts(51), as observed in our current studies (Fig 2.5). MOR signaling complex has been reported to be associated with $G\alpha_{i2}$ in lipid rafts (104-106). Many signaling proteins are selectively distributed inside or outside lipid rafts (29), which are rich in cholesterol and sphingolipids at the plasma membrane. One of the most important characteristics

of lipid rafts is that they can retain or expel proteins to variable extents. Proteins possessing raft affinity include glycosylphosphatidylinositol (GPI)-anchored proteins, doubly acylated proteins, such as Src kinase family or the α-subunits of heterotrimeric G proteins, cholesterol-linked and palmitoylated proteins such as Hedgehog, and transmembrane proteins, particularly palmitoylated ones (107-111). Being a member of GPCR superfamily, MOR was also demonstrated to be located in lipid raft (57). However, when activated by etorphine, MOR translocated out of lipid raft due to the fact that agonist-receptor complex switched its interaction with $G_i\alpha 2$ to ß-arrestin (42). The translocation of the receptor from lipid rafts could be one of the determinants in the observed agonist-dependent pathway-selective signaling. By tethering the receptor with $G\alpha_{i2}$, GRIN1 stabilized MOR complex within the lipid rafts thereby altered the receptor signaling of those agonists that could translocate MOR out of lipid raft (i.e. etorphine). This is demonstrated by our current studies in which Src kinase activation and subsequent neurite outgrowth induced by etorphine were dramatically affected by GRIN1 expression. As expectedly, the activities of agonist such as morphine, which does not induce MOR translocation from lipid rafts, were not affected by the GRIN1 expression.

It was reported that the stability of lipid raft was very important in PC12 neurite outgrowth (112), which was consistent with our data that the stability of lipid raft also was crucial for MOR-activation-induced neurite outgrowth (Fig 2.11). Disrupting the structure of lipid raft by MβCD could suppress neurite outgrowth and recovery of lipid raft by adding cholesterol continued neurite outgrowth (Fig 2.11). Thus, it is reasonable to suggest that MOR-activation-induced neurite outgrowth take place in

lipid raft. Overexpression of GRIN1 minimizes the removal of MOR out of lipid raft in the presence of etorphine and subsequently amplifying the signals involved in neurite outgrowth. Once MOR was activated in lipid raft, c-Src kinase activity increased (Fig 2.6), which could lead to a series change of down-stream signal to induce neurite outgrowth (33,113-117). The ability of PP2, a general Src kinase inhibitor and not PP3 to inhibit MOR-mediated neurite outgrowth supported the Src involvement in such process (data not shown). Scanning GRIN1 binding motif, we found the possible proline-rich region (PRR) at its C-terminal, which suggested that GRIN1 might bind to Src kinase and other proteins through Src-homology 2 (SH2) region and Src-homology 3 (SH3) region(118-121). Detailed mapping of GRIN1 for motifs involved in modulating neurite outgrowth needs to be demonstrated in the future.

Combination of such information and our data can depict a picture that GRIN1 can assist the interaction of MOR and $G_{i/o}$ in lipid rafts and further recruit down-stream signal molecules to amplify the neurite outgrowth signal transduction. The change of GRIN1 expression level results in variable degree of functional MOR signaling complex in lipid rafts, which also account for other distinct signaling transductions (i.e. adenylyl cyclase (data not shown)). Thus, the selective influence of GRIN1 on signaling activity of different opiate drugs such as etorphine may trigger different posttranslational modifications and trafficking, and finally the change of body tissue partitioning and metabolism that involved in the establishment of brain reward circuit and drug dependence.

Part VI: References

1. Bockaert, J., Roussignol, G., Becamel, C., Gavarini, S., Joubert, L., Dumuis, A., Fagni, L., and Marin, P. (2004) Biochem Soc Trans 32(Pt 5), 851-855
2. Tong, H., Rockman, H. A., Koch, W. J., Steenbergen, C., and Murphy, E. (2004) Circ Res 94(8), 1133-1141
3. Rosenfeld, J. L., Knoll, B. J., and Moore, R. H. (2002) Receptors Channels 8(2), 87-97
4. Ueda, H., Harada, H., Nozaki, M., Katada, T., Ui, M., Satoh, M., and Takagi, H. (1988) Proc Natl Acad Sci, Sep;85(18):7013-7017.
5. Neubig, R. R., and Siderovski, D. P. (2002) Nat Rev Drug Discov 1(3), 187-197
6. Zhong, H., and Neubig, R. R. (2001) J Pharmacol Exp Ther 297(3), 837-845
7. Claing, A., Perry, S. J., Achiriloaie, M., Walker, J. K., Albanesi, J. P., Lefkowitz, R. J., and Premont, R. T. (2000) Proc Natl Acad Sci U S A 97(3), 1119-1124
8. Whistler, J. L., Enquist, J., Marley, A., Fong, J., Gladher, F., Tsuruda, P., Murray, S. R., and Von Zastrow, M. (2002) Science 297(5581), 615-620
9. Yerbury, J. J., Stewart, E. M., Wyatt, A. R., and Wilson, M. R. (2005) EMBO Rep 6(12), 1131-1136
10. Zhang, J., Ferguson, S. S., Barak, L. S., Bodduluri, S. R., Laporte, S. A., Law, P. Y., and Caron, M. G. (1998) Proc Natl Acad Sci U S A 95(12), 7157-7162
11. Whistler, J. L., Chuang, H. H., Chu, P., Jan, L. Y., and von Zastrow, M. (1999) Neuron
12. Evans, C. J., Keith, D. E., Jr., Morrison, H., Magendzo, K., and Edwards, R. H. (1992) Science 258(5090), 1952-1955
13. Kieffer, B. L., Befort, K., Gaveriaux-Ruff, C., and Hirth, C. G. (1992) Proc Natl Acad Sci U S A 89(24), 12048-12052
14. Chen, Y., Mestek, A., Liu, J., Hurley, J. A., and Yu, L. (1993 Jul) Mol Pharmacol., 44(41):48-12.
15. Mullaney, I., Magee, A. I., Unson, C. G., and Milligan, G. (1988 Dec 1) Biochem J., 256(252):649-256.
16. Miller, R. J., and Dawson, G. (1980) Adv Biochem Psychopharmacol 21, 11-20
17. Heydorn, A., Sondergaard, B. P., Ersboll, B., Holst, B., Nielsen, F. C., Haft, C. R., Whistler, J., and Schwartz, T. W. (2004 Dec 24) J Biol Chem., 279(252):54291-54303. Epub 52004 Sep 54227.
18. Milligan, G., Murdoch, H., Kellett, E., White, J. H., and Feng, G. J. (2004) Biochem Soc Trans 32(Pt 5), 878-880
19. Onoprishvili, I., Andria, M. L., Kramer, H. K., Ancevska-Taneva, N., Hiller, J. M., and Simon, E. J. (2003) Mol Pharmacol 64(5), 1092-1100
20. Guang, W., Wang, H., Su, T., Weinstein, I. B., and Wang, J. B. (2004) Mol Pharmacol 66(5), 1285-1292
21. Koch, T., Brandenburg, L. O., Schulz, S., Liang, Y., Klein, J., and Hollt, V. (2003) J Biol Chem 278(11), 9979-9985

22. Chen, C., Li, J. G., Chen, Y., Huang, P., Wang, Y., and Liu-Chen, L. Y. (2006) J Biol Chem 281(12), 7983-7993
23. Silberstein, S., and Gilmore, R. (1996) Faseb J 10(8), 849-858
24. Kreibich, G., Sabatini, D. D., and Adesnik, M. (1983) Methods Enzymol 96, 530-542
25. Abeijon, C., and Hirschberg, C. B. (1992) Trends Biochem Sci 17(1), 32-36
26. Kornfeld, R., and Kornfeld, S. (1985) Annu Rev Biochem 54, 631-664
27. Helenius, A., and Aebi, M. (2001) Science 291(5512), 2364-2369
28. Petaja-Repo, U. E., Hogue, M., Laperriere, A., Walker, P., and Bouvier, M. (2000) J Biol Chem 275(18), 13727-13736
29. Cohen, A. W., Hnasko, R., Schubert, W., and Lisanti, M. P. (2004) Physiol Rev 84(4), 1341-1379
30. Chun, M., Liyanage, U. K., Lisanti, M. P., and Lodish, H. F. (1994) Proc Natl Acad Sci U S A 91(24), 11728-11732
31. Lisanti, M. P., Scherer, P. E., Tang, Z., and Sargiacomo, M. (1994) Trends Cell Biol 4(7), 231-235
32. Lisanti, M. P., Scherer, P. E., Vidugiriene, J., Tang, Z., Hermanowski-Vosatka, A., Tu, Y. H., Cook, R. F., and Sargiacomo, M. (1994) J Cell Biol 126(1), 111-126
33. Head, B. P., Patel, H. H., Roth, D. M., Murray, F., Swaney, J. S., Niesman, I. R., Farquhar, M. G., and Insel, P. A. (2006) J Biol Chem 281(36), 26391-26399
34. Pike, L. J., Han, X., and Gross, R. W. (2005) J Biol Chem 280(29), 26796-26804
35. Balbis, A., Parmar, A., Wang, Y., Baquiran, G., and Posner, B. I. (2007) Endocrinology 148(6), 2944-2954
36. Rozengurt, E. (2007) J Cell Physiol 213(3), 589-602
37. Monastyrskaya, K., Hostettler, A., Buergi, S., and Draeger, A. (2005) J Biol Chem 280(8), 7135-7146
38. Navratil, A. M., Bliss, S. P., Berghorn, K. A., Haughian, J. M., Farmerie, T. A., Graham, J. K., Clay, C. M., and Roberson, M. S. (2003) J Biol Chem 278(34), 31593-31602
39. Carter, B. D., and Medzihradsky, F. (1992) J Neurochem 58(5), 1611-1619
40. McKenzie, F. R., and Milligan, G. (1990) Biochem J 267(2), 391-398
41. Xu, W., Yoon, S. I., Huang, P., Wang, Y., Chen, C., Chong, P. L., and Liu-Chen, L. Y. (2006) J Pharmacol Exp Ther 317(3), 1295-1306
42. Zheng, H., Chu, J., Qiu, Y., Loh, H. H., and Law, P. Y. (2008) Proc Natl Acad Sci U S A 105(27), 9421-9426
43. Ohkubo, S., and Nakahata, N. (2007) Yakugaku Zasshi 127(1), 27-40
44. Reversi, A., Rimoldi, V., Brambillasca, S., and Chini, B. (2006) Am J Physiol Regul Integr Comp Physiol 291(4), R861-869
45. Philip, F., and Scarlata, S. (2004) Biochemistry 43(37), 11691-11700
46. Resh, M. D. (2006) Sci STKE 2006(359), re14
47. Barnett-Norris, J., Lynch, D., and Reggio, P. H. (2005) Life Sci 77(14), 1625-1639
48. Head, B. P., and Insel, P. A. (2007) Trends Cell Biol 17(2), 51-57

49. Evans, B. J., Wang, Z., Mobley, L., Khosravi, D., Fujii, N., Navenot, J. M., and Peiper, S. C. (2008) Biochem Biophys Res Commun 377(4), 1067-1071
50. Chen, L. T., Gilman, A. G., and Kozasa, T. (1999) J Biol Chem 274(38), 26931-26938
51. Nakata, H., and Kozasa, T. (2005) Mol Pharmacol 67(3), 695-702
52. Kapphahn, R. J., Ethen, C. M., Peters, E. A., Higgins, L., and Ferrington, D. A. (2003) Biochemistry 42(51), 15310-15325
53. Shilov, I. V., Seymour, S. L., Patel, A. A., Loboda, A., Tang, W. H., Keating, S. P., Hunter, C. L., Nuwaysir, L. M., and Schaeffer, D. A. (2007) Mol Cell Proteomics
54. Smith, K. E., Gibson, E. S., and Dell'Acqua, M. L. (2006) J Neurosci 26(9), 2391-2402
55. Zhang, L., Tetrault, J., Wang, W., Loh, H. H., and Law, P. Y. (2006) Mol Pharmacol 69(6), 1810-1819
56. Roerig, S. C., Loh, H. H., and Law, P. Y. (1992) Mol Pharmacol 41(5), 822-831
57. Zhao, H., Loh, H. H., and Law, P. Y. (2006) Mol Pharmacol 69(4), 1421-1432
58. Fu, J., Ren, M., and Kreibich, G. (1997) J Biol Chem 272(47), 29687-29692
59. Dong, C., and Wu, G. (2006) J Biol Chem 281(50), 38543-38554
60. Chaipatikul, V., Erickson-Herbrandson, L. J., Loh, H. H., and Law, P. Y. (2003) Mol Pharmacol 64(1), 32-41
61. Chaipatikul, V., Erickson-Herbrandson, L. J., Loh, H. H., and Law, P. Y. (2003) Molecular Pharmacology. 64(1), 32-41
62. Kelleher, D. J., Kreibich, G., and Gilmore, R. (1992) Cell 69(1), 55-65
63. Robert, J., Auzan, C., Ventura, M. A., and Clauser, E. (2005) J Biol Chem 280(51), 42198-42206
64. Ge, X., Loh, H. H., and Law, P. Y. (2009) Mol Pharmacol
65. Arvidsson, U., Riedl, M., Chakrabarti, S., Lee, J. H., Nakano, A. H., Dado, R. J., Loh, H. H., Law, P. Y., Wessendorf, M. W., and Elde, R. (1995) J Neurosci 15(5 Pt 1), 3328-3341
66. Chaipatikul, V., Loh, H. H., and Law, P. Y. (2003) J Pharmacol Exp Ther 305(3), 909-918
67. Zhang, L., Zhao, H., Qiu, Y., Loh, H. H., and Law, P. Y. (2009) J Biol Chem 284(4), 1990-2000
68. Mukherjee, A., Arnaud, L., and Cooper, J. A. (2003) J Biol Chem 278(42), 40806-40814
69. Kreibich, G., Freienstein, C. M., Pereyra, B. N., Ulrich, B. L., and Sabatini, D. D. (1978) J Cell Biol 77(2), 488-506
70. Kelleher, D. J., and Gilmore, R. (1997) Proc Natl Acad Sci U S A 94(10), 4994-4999
71. Wilson, C. M., Kraft, C., Duggan, C., Ismail, N., Crawshaw, S. G., and High, S. (2005) J Biol Chem 280(6), 4195-4206
72. Law, P. Y., Erickson-Herbrandson, L. J., Zha, Q. Q., Solberg, J., Chu, J., Sarre, A., and Loh, H. H. (2005) J Biol Chem 280(12), 11152-11164
73. de Virgilio, M., Weninger, H., and Ivessa, N. E. (1998) J Biol Chem 273(16), 9734-9743

74. Yu, Y. H., Sabatini, D. D., and Kreibich, G. (1990) J Cell Biol 111(4), 1335-1342
75. Shibatani, T., David, L. L., McCormack, A. L., Frueh, K., and Skach, W. R. (2005) Biochemistry 44(16), 5982-5992
76. Chen, W., Helenius, J., Braakman, I., and Helenius, A. (1995) Proc Natl Acad Sci U S A 92(14), 6229-6233
77. Lecomte, F. J., Ismail, N., and High, S. (2003) Biochem Soc Trans 31(Pt 6), 1248-1252
78. Alder, N. N., Shen, Y., Brodsky, J. L., Hendershot, L. M., and Johnson, A. E. (2005) J Cell Biol 168(3), 389-399
79. Alder, N. N., and Johnson, A. E. (2004) J Biol Chem 279(22), 22787-22790
80. Hendershot, L. M. (2004) Mt Sinai J Med 71(5), 289-297
81. Santhamma, K. R., and Sen, I. (2000) J Biol Chem 275(30), 23253-23258
82. Bergman, L. W., and Kuehl, W. M. (1979) J Supramol Struct 11(1), 9-24
83. Bergman, L. W., and Kuehl, W. M. (1979) J Biol Chem 254(13), 5690-5694
84. Parodi, A. J. (2000) Annu Rev Biochem 69, 69-93
85. Hurtley, S. M., and Helenius, A. (1989) Annu Rev Cell Biol 5, 277-307
86. Doms, R. W. (1990) Methods Enzymol 191, 841-854
87. Hebert, D. N., Foellmer, B., and Helenius, A. (1996) Embo J 15(12), 2961-2968
88. Morello, J. P., Salahpour, A., Petaja-Repo, U. E., Laperriere, A., Lonergan, M., Arthus, M. F., Nabi, I. R., Bichet, D. G., and Bouvier, M. (2001) Biochemistry 40(23), 6766-6775
89. Wilson, C. M., and High, S. (2007) J Cell Sci 120(Pt 4), 648-657
90. Moron, J. A., Abul-Husn, N. S., Rozenfeld, R., Dolios, G., Wang, R., and Devi, L. A. (2007) Mol Cell Proteomics 6(1), 29-42
91. Besson, J. M. (1999) Lancet 353(9164), 1610-1615
92. Kahn, L., Alonso, G., Normand, E., and Manzoni, O. J. (2005) Eur J Neurosci 21(2), 493-500
93. Trujillo, K. A. (2002) Neurotox Res 4(4), 373-391
94. Williams, J. T., Christie, M. J., and Manzoni, O. (2001) Physiol Rev 81(1), 299-343
95. Van Ooyen, A., Van Pelt, J., and Corner, M. A. (1995) J Theor Biol 172(1), 63-82
96. Zhang, W., and Benson, D. L. (2002) J Neurosci Res 69(4), 427-436
97. Connaughton, J. F., Jr., Finnegan, L. P., Schut, J., and Emich, J. P. (1975) Addict Dis 2(1-2), 21-35
98. Yeh, G. C., Hsieh, T. H., and Chang, S. F. (1998) Neurosci Lett 252(1), 25-28
99. Nassogne, M. C., Gressens, P., Evrard, P., and Courtoy, P. J. (1998) Brain Res Dev Brain Res 110(1), 61-67
100. Kabbani, N., Woll, M. P., Levenson, R., Lindstrom, J. M., and Changeux, J. P. (2007) Proc Natl Acad Sci U S A 104(51), 20570-20575
101. Yin, D. L., Ren, X. H., Zheng, Z. L., Pu, L., Jiang, L. Z., Ma, L., and Pei, G. (1997) Neurosci Res 29(2), 121-127
102. Miller, J. H., and Azmitia, E. C. (1999) Brain Res Dev Brain Res 114(1), 69-77

103. Brailoiu, E., Hoard, J., Brailoiu, G. C., Chi, M., Godbolde, R., and Dun, N. J. (2004) Neurosci Lett 365(1), 10-13
104. Gilman, A. G. (1987) Annu Rev Biochem 56, 615-649
105. Ross, E. M. (1995) Curr Biol 5(2), 107-109
106. Macdonald, J. L., and Pike, L. J. (2005) J Lipid Res 46(5), 1061-1067
107. Zhang, L., Zhao, H., Qiu, Y., Loh, H. H., and Law, P. Y. (2008) J Biol Chem
108. Di Vizio, D., Adam, R. M., Kim, J., Kim, R., Sotgia, F., Williams, T., Demichelis, F., Solomon, K. R., Loda, M., Rubin, M. A., Lisanti, M. P., and Freeman, M. R. (2008) Cell Cycle 7(14), 2257-2267
109. Oneyama, C., Hikita, T., Enya, K., Dobenecker, M. W., Saito, K., Nada, S., Tarakhovsky, A., and Okada, M. (2008) Mol Cell 30(4), 426-436
110. Sugawara, Y., Nishii, H., Takahashi, T., Yamauchi, J., Mizuno, N., Tago, K., and Itoh, H. (2007) Cell Signal 19(6), 1301-1308
111. Harder, T., Scheiffele, P., Verkade, P., and Simons, K. (1998) J Cell Biol 141(4), 929-942
112. Zhang, W., Duan, W., Cheung, N. S., Huang, Z., Shao, K., and Li, Q. T. (2007) J Neurochem 103(3), 1157-1167
113. He, J. C., Gomes, I., Nguyen, T., Jayaram, G., Ram, P. T., Devi, L. A., and Iyengar, R. (2005) J Biol Chem 280(39), 33426-33434
114. Oh, D. Y., Park, S. Y., Cho, J. H., Lee, K. S., Min do, S., and Han, J. S. (2007) J Cell Biochem 101(1), 221-234
115. Ignelzi, M. A., Jr., Miller, D. R., Soriano, P., and Maness, P. F. (1994) Neuron 12(4), 873-884
116. Schmid, R. S., Pruitt, W. M., and Maness, P. F. (2000) J Neurosci 20(11), 4177-4188
117. Encinas, M., Tansey, M. G., Tsui-Pierchala, B. A., Comella, J. X., Milbrandt, J., and Johnson, E. M., Jr. (2001) J Neurosci 21(5), 1464-1472
118. Ren, R., Mayer, B. J., Cicchetti, P., and Baltimore, D. (1993) Science 259(5098), 1157-1161
119. Ramos-Morales, F., Romero, F., Schweighoffer, F., Bismuth, G., Camonis, J., Tortolero, M., and Fischer, S. (1995) Oncogene 11(8), 1665-1669
120. Jia, C. Y., Nie, J., Wu, C., Li, C., and Li, S. S. (2005) Mol Cell Proteomics 4(8), 1155-1166
121. Anafi, M., Rosen, M. K., Gish, G. D., Kay, L. E., and Pawson, T. (1996) J Biol Chem 271(35), 21365-21374

Part VII: Abbreviations

GPCR, G protein-coupled receptor; MOR, μ-opioid receptor; DOR, δ-opioid receptor; KOR, κ-opioid receptor; RPNI, ribophorin I; N2A, neuro2A neuroblastoma cell; ER, endoplasmic reticulum; DMEM, Dulbecco's modified Eagle's medium; G418, Geneticin; IP, Immunoprecipitation; IB, Immunoblot; MALDI-TOF, Matrix Assisted Laser Desorption /Ionization- Time Of Flight mass spectrometry; LC-MS/MS, Liquid chromatography-electrospray ionization tandem mass spectrometry; PBS, Phosphate-buffered saline; FACScan, fluorescence flow cytometry; PA, Ponasterone A; OST, Oligosaccharide transferase; MOR5ND, MOR with Asn^{9}, Asn^{31}, Asn^{38}. Asn^{46} and Asn^{53} residues at the N-terminus all mutated to Asp; C2, MOR with the ^{344}KFCTR^{348} sequence deleted; GRIN1, G protein-regulated inducer of neurite outgrowth 1; MOR, μ-opioid receptor; N2A, neuro2A neuroblastoma cell; DMEM, Dulbecco's modified Eagle's medium; G418, Geneticin; IP, Immunoprecipitation; IB, Immunoblot; MALDI-TOF, Matrix Assisted Laser Desorption /Ionization- Time Of Flight mass spectrometry.